SANDIA REPORT

SAND2017-10248
Unlimited Release
Printed August 2017

Optical nonlinearities of excitonic states in atomically thin 2D transition metal dichalcogenides

Daniel B. S. Soh

Prepared by
Sandia National Laboratories
Albuquerque, New Mexico 87185 and Livermore, California 94550

Sandia National Laboratories is a multimission laboratory managed and operated by National Technology and Engineering Solutions of Sandia, LLC., a wholly owned subsidiary of Honeywell International, Inc., for the U.S. Department of Energy's National Nuclear Security Administration under contract DE-NA0003525.

Sandia National Laboratories

Issued by Sandia National Laboratories, operated for the United States Department of Energy by National Technology and Engineering Solutions of Sandia, LLC.

Available to DOE and DOE contractors from
U.S. Department of Energy
Office of Scientific and Technical Information
P.O. Box 62
Oak Ridge, TN 37831

Telephone: (865) 576-8401
Facsimile: (865) 576-5728
E-Mail: reports@adonis.osti.gov
Online ordering: http://www.osti.gov/bridge

Available to the public from
U.S. Department of Commerce
National Technical Information Service
5285 Port Royal Rd
Springfield, VA 22161

Telephone: (800) 553-6847
Facsimile: (703) 605-6900
E-Mail: orders@ntis.fedworld.gov
Online ordering: http://www.ntis.gov/help/ordermethods.asp?loc=7-4-0#online

SAND2017-10248
Unlimited Release
Printed August 2017

Optical nonlinearities of excitonic states in atomically thin 2D transition metal dichalcogenides

Daniel B. S. Soh
Proliferation Signatures Discovery and Exploitation Department
Sandia National Laboratories
P.O. Box 969
Livermore, CA 94551-0969
dbsoh@sandia.gov

Abstract

We calculated the optical nonlinearities of the atomically thin monolayer transition metal dichalcogenide MoS_2, particularly for those linear and nonlinear transition processes that utilize the bound exciton states. We adopted the bound and the unbound exciton states as the basis for the Hilbert space, and derived all the dynamical density matrices that provides the induced current density, from which the nonlinear susceptibilities can be drawn order-by-order via perturbative calculations. We provide the nonlinear susceptibilities for the linear, the second-harmonic, the third-harmonic, and the kerr-type two-photon processes.

Acknowledgment

We thank Sandia's generous support of this work via Sandia's Special Degree Program at Stanford University.

Contents

List of Figures

List of Tables

1. Introduction

Atomically thin 2D materials are the ideal candidate for various on-chip functional devices, including the optical computing, laboratory on chip, on-chip cold atoms, on-chip cavity quantum electrodynamics, and qubit processors on chip. Recently the growth technologies for these 2D materials have greatly advanced so that any desired multi-layered atomically thin materials can be grown and deposited on top of the existing photonic circuits.

Recent studies on the 2D transient metal dichalcogenides (TMDC) materials including, MoS_2, $MoSe_2$, TSe_2, etc., revealed that such thin material provides a decent level of optical interaction, due to the reduction of dimensionality and, thus, the improved density of states. On top of that, the exciton states which accumulates all the available quantum states over the lattice Bloch states may further increase the optical responses so that one can utilize such material for making a strong interaction between the light and the material. In addition, optical nonlinearity can be used to realize important applications such as qubit operation via cavity quantum electrodynamics, optical transistor that controls the photonic signal flow through control optical signals (photons), and various frequency conversion operations.

We calculate the optical nonlinearities of a monolayer MoS_2 material, particularly when the input optical frequency is designed to utilize the optically highly active level of bound exciton states. For this we adopt the quantum description of the induced current, from which the optical susceptibility is deduced, in a perturbative manner. We then resolve the order-by-order optical responses from an external drive electromagnetic field.

This SAND report is composed of general theory that describes the interaction Hamiltonian of the 2D monolayer solids under the influence of the external field, the method to extract the susceptibility, and the perturbative calculation of the optical susceptibility up to the third order response. Then, the actual calculation of the physical parameters follow. Finally a summary and conclusion follows.

2. Theory for calculating perturbative optical susceptibilities

2.1 Assumptions

We assume zero temperature for simplicity. The coupling of exciton levels with the phonon levels are completely ignored. Thus, we count only the radiative transitions.

Our primary interest is the linear and the nonlinear optical processes that involves the bound exciton states of the monolayer MoS_2. We take the approach of second quantization for the unperturbed exciton bound states. We particularly assume a low density excitons so that we address only the regime of a single exciton over the sample. Therefore, we ignore the bosonic nature of the excitons nor the Bose-Einstein condensation of the excitons. We also ignore the exciton-exciton interaction. Consistently with the weakly exciting regime, we take the perturbative approach that naturally produces the first, the second, and the third-order nonlinear susceptibilities.

The MoS_2 monolayer exhibits the valley selection rule where only the circularly polarized photon excites a particular exciton levels for a given valley (either K or $K' = -K$). Without loss of generality, we assume therefore the incoming light has $\sigma+$ polarization, corresponding to the K valley. The case of $\sigma-$ polarization and the corresponding $-K$ valley is readily obtained by adjusting the energy gap via considering the difference in spin-orbit coupling energy.

For the band structure of the MoS_2, we assume the gapped Dirac cone model that was adopted in many of the theoretical works of the TMDS material calculations [25, 12, 17, 6, 16, 11, 19, 22, 23]. Our analytical calculation also includes the second-order perturbative solution for the unperturbed (without light interaction Hamiltonian) bound exciton states under the gapped Dirac cone approximation, in the hope of easy calculation of various dipole moment matrix elements, which however fails to address the required accuracy of the result. Therefore, we resorts to full numerical calculation for the evaluation of the nonlinear optical susceptibilities. While doing so, we adopt the higher-order correction of the gapped Dirac cone approximation [22, 23] that improves the accuracy of the level transition strengths.

2.2 Hamiltonian and exciton solutions

2.2.1 Unperturbed Hamiltonian of matter

Let us consider a semiconductor that has a direct nonzero bandgap. Let us define the second quantized electron and hole operators as

$$\alpha_{k,s} = a_{c,k,s}, \quad \beta^{\dagger}_{k,s} = a_{v,-k,s}, \tag{1}$$

where $a_{\lambda,k,s}$ is the fermionic annihilation operator for an electron at band $\lambda = c, v$ (conduction and valence bands, respectively) with the crystal momentum $\hbar k$ and spin s. Here, α and β are the annihilation operators of the electron (in the conduction band) and the hole (in the valence band).

From now on, the spin is implicit, combined to k. When we use the usual anti-commutator for the electrons:

$$\{a_{\lambda,k}, a_{\lambda',k'}\} = \{a^\dagger_{\lambda,k}, a^\dagger_{\lambda',k'}\} = 0, \quad \{a_{\lambda,k}, a^\dagger_{\lambda',k'}\} = \delta_{\lambda,\lambda'}\delta_{k,k'}, \tag{2}$$

one easily obtains the creation operator for an exciton (i.e., an electron-hole pair under the influence of Coulomb interaction between the two), moving with combined momentum as in $\hbar K$ [7]. For the details, see the Appendix B. The exciton creation operator is

$$B^\dagger_{\nu K} = \sum_k \psi_\nu \left(k - \frac{K}{2}\right) \alpha^\dagger_k \beta^\dagger_{K-k}, \tag{3}$$

where $\psi_\nu(k'')$ is the spatial Fourier transform (see the Appendix A) of the wave function $\psi_\nu(r)$ that satisfies the Wannier Schrödinger equation

$$\left[-\frac{\hbar^2\nabla_r^2}{2m_r} + V(r)\right] \psi_\nu(r) = E_\nu \psi_\nu(r), \tag{4}$$

with the reduced mass $m_r = (1/m_c + 1/|m_v|)^{-1}$ where $m_{c,v}$ are the effective mass of the conduction and valence band electrons, $V(r)$ the Coulomb potential between the electron and the hole. Rasmussen *et al.* [16] resolved the values $m_c = 0.55m_e$ and $m_v = -0.56m_e$ where m_e is the rest electron mass.

Here, the excitonic binding energy E_ν with the excitonic state quantum number $\nu = (n,l,m)$ is given as

$$E_\nu = E_n = \begin{cases} -E_0 \frac{1}{n^2}, & n = 1,2,3,\cdots, \quad \text{(3D)} \\ -E_0 \frac{1}{(n+1/2)^2}, & n = 0,1,2,\cdots, \quad \text{(2D)} \end{cases} \tag{5}$$

with

$$E_0 = \frac{e^4 m_r}{2(4\pi\varepsilon_0\varepsilon_r)^2\hbar^2} = \left(\frac{m_r}{m_e}\right)\left(\frac{1}{\varepsilon_r^2}\right) \text{Ry}, \tag{6}$$

with the electron charge $e = -|e| = -1.6 \times 10^{-19}$ C, and the vacuum and the relative material permittivity $\varepsilon_0, \varepsilon_r$, respectively. In addition, m_e is the electron mass and Ry = 13.6 eV is the hydrogen Rydberg energy. Note that the Rydberg of the exciton scales with respect to $(m_r/m_e)(1/\varepsilon_r^2)$. Typically the semiconductors have $\varepsilon_r \sim 10$. We will use $\varepsilon_r = 7$ through the manuscript. This value is nearly the optimal fit for the known range of the binding energy and the exciton radius. Hence, the typical exciton Rydberg energy E_0 is about $0.01 - 0.1$ eV range. The experimental result of the exciton binding energy for $n = 0$ in the monolayer MoS_2 is approximately $-0.5 \sim -0.3$ eV [26, 10, 8, 4, 18].

A physical intuition on the exciton creator given in equation (3) is that an exciton state is a superposition of all Bloch electron-hole pairs having the momentum $\hbar k$ and $\hbar(K-k)$, weighted by the orbital Fourier transform $\psi_\nu(k - K/2)$.

The solution to the Wannier equation is [7]:

$$\psi_{n,l,m}(r) = \begin{cases} -\sqrt{\left(\frac{2}{na_0}\right)\frac{(n-l-1)!}{2n[(n+l)!]^3}}\rho^l e^{-\rho/2} L_{n+1}^{2l+1}(\rho) Y_{l,m}(\theta,\phi), & \text{(3D)} \\ \sqrt{\frac{1}{\pi a_0^2 (n+1/2)^3}\frac{(n-|m|)!}{[(n+|m|)!]^3}}\rho^{|m|} e^{-\rho/2} L_{n+|m|}^{2|m|}(\rho) e^{im\phi}, & \text{(2D)} \end{cases} \tag{7}$$

where $V(A)$ is the quantizing volume (area), respectively, and $a_0 = 4\pi\hbar^2\varepsilon_0\varepsilon_r/(e^2 m_r)$, $\rho = 2r/((n+1/2)a_0)$, and $L_q^p(\rho)$ is the Laguerre polynomials defined by

$$L_q^p(\rho) = \sum_{\nu=0}^{q-p} (-1)^{\nu+p} \frac{(q!)^2 \rho^\nu}{(q-p-\nu)!(p+\nu)!\nu!}. \tag{8}$$

Recall the closure from equation (188):

$$\int_V d^3r\, |r\rangle\langle r| = \mathbf{1} \quad \text{(3D)}, \qquad \int_A d^2r\, |r\rangle\langle r| = \mathbf{1} \quad \text{(2D)}. \tag{9}$$

Then, the normalization condition is

$$\begin{aligned} \langle\psi|\psi\rangle &= \int_V d^3r \langle\psi|r\rangle\langle r|\psi\rangle = \int_V d^3r \psi^*_{n,l,m}(r)\psi_{n,l,m}(r) = 1, \quad \text{(3D)} \\ \langle\psi|\psi\rangle &= \int_A d^2r \langle\psi|r\rangle\langle r|\psi\rangle = \int_A d^2r \psi^*_{n,m}(r)\psi_{n,m}(r) = 1. \quad \text{(2D)} \end{aligned} \tag{10}$$

The solutions in equation (7) satisfy these normalization conditions.

Also one can consider the Fourier transform using the closure in equation (188) such that

$$\psi(r) = \frac{1}{\sqrt{A}}\sum_k \psi(k) e^{ik\cdot r}, \quad \psi(k) = \frac{1}{\sqrt{A}}\int_A d^2r \psi(r) e^{-ik\cdot r}. \tag{11}$$

Note that the the Fourier transform in actual calculation can be performed in the polar coordinate such that

$$\psi(k) = \frac{1}{\sqrt{A}}\int_0^{2\pi} d\phi \int_0^\infty dr \psi(r) e^{-ikr\cos(\theta-\phi)}, \tag{12}$$

where $r = (x,y) = (r\cos\phi, r\sin\phi)$ and $k = (k_x,k_y) = (k\cos\theta, k\sin\theta)$.

The possible indices for 3D are $n = 1,2,\cdots$, $l = 0,1,\cdots,n-1$, and $m = 0,\pm1,\cdots,\pm l$. Those for 2D are $n = 0,1,\cdots$ and $m = 0,\pm1,\cdots,\pm n$. The exciton radius is also experimetally resolved to approximately $6 \sim 10$ Å, at zero temperature [26]. The calculated wavefunctions and their Fourier transforms are shown in the table 1. The normalization of $\psi(k)$ is given by the closure (188):

$$1 = \langle\psi|\psi\rangle = \sum_k \langle\psi|k\rangle\langle k|\psi\rangle = \sum_k \psi^*(k)\psi(k) = A\int \frac{d^2k}{(2\pi)^2}\psi^*(k)\psi(k), \tag{13}$$

where we converted the sum into integral using the relation $d^2k = (2\pi)^2/A$. It is easily verifiable that all the Fourier transforms $\psi_\nu(k)$ appearing in the table 1 satisfy this normalization condition.

Table 1: 2D bound exciton wavefunctions and their Fourier transforms

n	m	$\psi_\nu(r)$	$\psi_\nu(k)$	E_n
0	**0**	$\frac{2\sqrt{2}}{a_0\sqrt{\pi}}e^{-\frac{2r}{a_0}}$	$\sqrt{\frac{2\pi}{A}}\frac{8a_0}{(4+a_0^2k^2)^{3/2}}$	$-4E_0$
1	**1**	$\sqrt{\frac{1}{3\pi}}\frac{8r}{9a_0^2}e^{-\frac{2r}{3a_0}}e^{i\phi}$	$\sqrt{\frac{3}{\pi A}}\int_0^{2\pi}d\phi\frac{16a_0e^{i\phi}}{(2+3ia_0k\cos(\theta-\phi))^3}$	$-\frac{4}{9}E_0$
1	**0**	$\sqrt{\frac{2}{3\pi}}\frac{2(3a_0-4r)}{9a_0^2}e^{-\frac{2r}{3a_0}}$	$\sqrt{\frac{6\pi}{A}}\frac{24a_0(9a_0^2k^2-4)}{(4+9a_0^2k^2)^{5/2}}$	$-\frac{4}{9}E_0$
1	**-1**	$\sqrt{\frac{1}{3\pi}}\frac{8r}{9a_0^2}e^{-\frac{2r}{3a_0}}e^{-i\phi}$	$\sqrt{\frac{3}{\pi A}}\int_0^{2\pi}d\phi\frac{16a_0e^{-i\phi}}{(2+3ia_0k\cos(\theta-\phi))^3}$	$-\frac{4}{9}E_0$
2	**-2**	$\sqrt{\frac{1}{15\pi}}\frac{16r^2}{125a_0^3}e^{-\frac{2r}{5a_0}}e^{-2i\phi}$	$\sqrt{\frac{15}{\pi A}}\int_0^{2\pi}d\phi\frac{32a_0e^{-2i\phi}}{(2i-5a_0k\cos(\theta-\phi))^4}$	$-\frac{4}{25}E_0$
2	**-1**	$-\sqrt{\frac{1}{15\pi}}\frac{8r(4r-15a_0)}{125a_0^3}e^{-\frac{2r}{5a_0}}e^{-i\phi}$	$\sqrt{\frac{15}{\pi A}}\int_0^{2\pi}d\phi\frac{16a_0(-2+5ia_0k\cos(\theta-\phi))e^{-i\phi}}{(2i-5a_0k\cos(\theta-\phi))^4}$	$-\frac{4}{25}E_0$
2	**0**	$\sqrt{\frac{2}{5\pi}}\frac{2(25a_0^2-40a_0r+8r^2)}{125a_0^3}e^{-\frac{2r}{5a_0}}$	$\sqrt{\frac{10\pi}{A}}\frac{40a_0(16-400a_0^2k^2+625a_0^4k^4)}{(4+25a_0^2k^2)^{7/2}}$	$-\frac{4}{25}E_0$
2	**1**	$-\sqrt{\frac{1}{15\pi}}\frac{8r(4r-15a_0)}{125a_0^3}e^{-\frac{2r}{5a_0}}e^{i\phi}$	$\sqrt{\frac{15}{\pi A}}\int_0^{2\pi}d\phi\frac{16a_0(-2+5ia_0k\cos(\theta-\phi))e^{i\phi}}{(2i-5a_0k\cos(\theta-\phi))^4}$	$-\frac{4}{25}E_0$
2	**2**	$\sqrt{\frac{1}{15\pi}}\frac{16r^2}{125a_0^3}e^{-\frac{2r}{5a_0}}e^{2i\phi}$	$\sqrt{\frac{15}{\pi A}}\int_0^{2\pi}d\phi\frac{32a_0e^{2i\phi}}{(2i-5a_0k\cos(\theta-\phi))^4}$	$-\frac{4}{25}E_0$
3	**0**	$\sqrt{\frac{2}{7\pi}}\frac{2(1029a_0^3-1764a_0^2r+504a_0r^2-32r^3)}{7203a_0^4}e^{-\frac{2r}{7a_0}}$	$\sqrt{\frac{14\pi}{A}}\frac{56a_0(49a_0^2k^2-4)(16-1568a_0^2k^2+2401a_0^4k^4)}{(4+49a_0^2k^2)^{9/2}}$	$-\frac{4}{49}E_0$
4	**0**	$\sqrt{\frac{2}{\pi}}\frac{2(19683a_0^4-34992a_0^3r+11664a_0^2r^2-1152a_0r^3+32r^4)}{631441a_0^5}e^{-\frac{2r}{9a_0}}$	$\sqrt{\frac{2\pi}{A}}\frac{216a_0(256-82944a_0^2k^2+3779136a_0^4k^4-34012224a_0^6k^6+43046721a_0^8k^8)}{(4+81a_0^2k^2)^{11/2}}$	$-\frac{4}{64}E_0$

We could obtain the completely analytical closed Fourier transform formulas for $\nu=(n,0)$, while we failed to obtain the closed form for $\nu=(n,m\neq 0)$, which we still successfully performed the radial integral, but left the angle integral as implicit forms. This angle integral can be obtained easily using numerical integrals.

It is also noteworthy that the expectation value of the exciton radius $\langle\psi_0|\,r\,|\psi_0\rangle = a_0/2$ for 2D case, and a_0 scales as [21]

$$a_0=\left(\frac{m_e}{m_r}\right)\left(\frac{\varepsilon_r}{1}\right)a_B, \tag{14}$$

where $a_B=4\pi\varepsilon_0\hbar^2/(m_e e^2)\sim 0.53$ Å.

The free Hamiltonian for the exciton system is then

$$\mathscr{H}_0 = \hbar \sum_{\nu,K} e_{\nu,K} B^\dagger_{\nu K} B_{\nu K}, \tag{15}$$

where the exciton energy eigenvalues are [21]

$$\hbar e_{\nu,K} = \begin{cases} E_g + E_\nu + \frac{\hbar^2 K^2}{2M}, & \text{(bound states)} \\ \hbar\omega_k + \frac{\hbar^2 K^2}{2M}, & \text{(unbound states).} \end{cases} \tag{16}$$

where E_g is the bandgap, $E_\nu = E_n$ as in equation (5), and the combined mass $M = m_e + |m_h|$, and the excitation energy $\hbar\omega_k$ for a single hole-pair with the momentum $\hbar k, -\hbar k$. Note that the above Hamiltonian includes both the bound and the unbound exciton states. For convenience, let us divide into two groups:

$$\mathscr{H}_0 = \hbar \sum_{\text{bound},\nu,K} e_{\nu,K} B^\dagger_{\nu K} B_{\nu K} + \hbar \sum_{\text{unbound},k,K} \omega_{k,K} C^\dagger_{k,K} C_{k,K}, \tag{17}$$

where $C^\dagger_{k,K}$ is the creator operator for the unbound exciton states with energy $\hbar\omega_{k,K} = \hbar\omega_k + \hbar^2 K^2/2M$ where $\hbar\omega_k$ is the energy of a single electron-hole pair with a crystal momentum $\hbar k, -\hbar k$.

Now, we consider the fact that the incoming photon has a negligibly small momentum, compared to the crystal momentum k. Hence, we are primarily interested in case where $K \approx 0$ as K must be compared to the magnitude of k. In this regime, the unperturbed exciton Hamiltonian is given as

$$\mathscr{H}_0 \approx \hbar \sum_{\text{bound},\nu} e_\nu B^\dagger_\nu B_\nu + \hbar \sum_{\text{unbound},k} \omega_k C^\dagger_k C_k, \tag{18}$$

where $B^\dagger_\nu$ and $C^\dagger_k$ are the bound and the unbound exciton states, respectively.

2.2.2 Interaction Hamiltonian

We consider the situation where a monochromatic external field given by

$$\widetilde{\mathscr{E}}(q,t) = \hat{\boldsymbol{\varepsilon}} \mathscr{E}(q) \mathrm{e}^{-i\omega_q t}, \tag{19}$$

with a polarization unit vector $\hat{\boldsymbol{\varepsilon}}$, interacts with the material. The nature of the interaction Hamiltonian between the classical external field and the exciton particle is the dipole interaction. This dipole interaction is captured by the following interaction Hamiltonian [7]:

$$\mathscr{H}_I = -\sum_k \left[d_{cv}(k) \alpha^\dagger_{\frac{1}{2}q+k} \beta^\dagger_{\frac{1}{2}q-k} \mathscr{E}(q) \mathrm{e}^{-i\omega_q t} + \text{h.c.} \right], \tag{20}$$

where the interband dipole moment is

$$d_{cv}(k) = \langle c(k) | e r \cdot \hat{\boldsymbol{\varepsilon}} | v(k) \rangle = e \langle c(k) | r \cdot \hat{\boldsymbol{\varepsilon}} | v(k) \rangle, \tag{21}$$

with the single particle states $|\lambda(k)\rangle$ with $\lambda = c, v$, the conduction and the valence band Bloch states with the momentum $\hbar k$.

One can second-quantize the external field by using

$$\mathscr{E}(q) = i\sqrt{\frac{\hbar\omega_q}{2V\varepsilon_0}}b_q. \tag{22}$$

where b_q is the boson annihilation operator for the photons and V is the quantizing volume. Then, the interaction Hamiltonian implies that an incoming photon with a momentum $\hbar q$ is annihilated, creating an electron-hole pair with the Bloch momentum $\hbar(q/2+k), \hbar(q/2-k)$, respectively, with the combined center of mass momentum $\hbar q$. Since k can be any, one must sum over all k. The interaction strength is proportional to $d_{cv}(k)$. Recall that the interband dipole is explicitly dependent on k.

Note that

$$\begin{aligned}\alpha^\dagger_{\frac{1}{2}q+k}\beta^\dagger_{\frac{1}{2}q-k} &= \sum_A \delta_{A,\frac{1}{2}q+k}\alpha^\dagger_A\beta^\dagger_{q-A} = \sum_A \delta_{k,A-\frac{1}{2}q}\alpha^\dagger_A\beta^\dagger_{q-A} \\ &= \sum_{A,\nu}\psi^*_\nu(k)\psi_\nu\left(A-\frac{1}{2}q\right)\alpha^\dagger_A\beta^\dagger_{q-A} \\ &= \sum_\nu \psi^*_\nu(k)B^\dagger_{\nu q},\end{aligned} \tag{23}$$

where the last equation follows from equation (3), and the third equation follows from

$$\delta_{k,k'} = \langle k|k'\rangle = \sum_\nu \langle k|\mathrm{x}_\nu\rangle\langle \mathrm{x}_\nu|k'\rangle = \sum_\nu \psi^*_\nu(k)\psi_\nu(k'). \tag{24}$$

Using equation (23), we obtain

$$\mathscr{H}_I = -\sum_\nu\left[\left(\sum_k d_{cv}(k)\psi^*_\nu(k)\right)B^\dagger_{\nu q}\mathscr{E}(q)\mathrm{e}^{-i\omega_q t} + \mathrm{h.c.}\right]. \tag{25}$$

Note that the photon momentum is negligibly small in the scale of the crystal momentum. Then, we can safely approximate $q/2 \pm k \approx \pm k$. Then, an exciton state ket is

$$\left|\mathrm{x}_{\nu,q}\right\rangle = B^\dagger_{\nu,q}|0\rangle \approx B^\dagger_\nu|0\rangle = \sum_k \psi_\nu(k)\alpha^\dagger_k\beta^\dagger_{-k}|0\rangle = \left|\mathrm{x}_{\nu,0}\right\rangle = |\mathrm{x}_\nu\rangle, \tag{26}$$

where we defined

$$B^\dagger_\nu = B^\dagger_{\nu,0} = \sum_k \psi_\nu(k)\alpha^\dagger_k\beta^\dagger_{-k}. \tag{27}$$

Let us set

$$g_\nu = \sum_k d_{cv}(k)\psi^*_\nu(k). \tag{28}$$

In Haug et al. [7], it is approximated to

$$\sum_k d_{cv}(k)\psi_v^*(k) \approx \sum_k d_{cv}(0)\psi_v^*(k) = \sqrt{A}d_{cv}(0)\psi_v^*(r=0), \tag{29}$$

where the following Fourier transform is used (see Appendix A):

$$\psi_v^*(r) = \frac{1}{\sqrt{A}}\sum_k \psi_v^*(k)\mathrm{e}^{-ik\cdot r}. \tag{30}$$

This is indeed a bold approximation where the interband dipole matrix element is approximated to be that of the band extrema (for a direct bandgap material). In this case, one obtains

$$g_v \approx \sqrt{A}d_{cv}(0)\psi_v^*(r=0). \tag{31}$$

Nevertheless, we are not going to use this approximation, but we will rather fully evaluate the numerical sum of g_v as in equation (28). Recall that the interaction Hamiltonian is from equations (25) and (28):

$$\mathscr{H}_I = -\sum_v \left[g_v B_v^\dagger \mathscr{E}(q)\mathrm{e}^{-i\omega_q t} + \mathrm{h.c.} \right]. \tag{32}$$

2.3 Susceptibility and induced current density

When an external field is present, an induced current is produced due to the dipole interaction as in the previous section. It is obtained as

$$J = 2\mathrm{Re}[\widetilde{J}] = \widetilde{J} + \widetilde{J}^* = eN_e\langle \mathrm{v}\rangle = eN_e\mathrm{tr}[\mathrm{v}\rho], \tag{33}$$

where $\widetilde{J}$ is the complex valued current, and N_e is the free carrier density, v is the velocity operator, and ρ is the density matrix, which follows the von Neumann equation:

$$\dot{\rho} = -\frac{i}{\hbar}[\mathscr{H}_0 + \mathscr{H}_I, \rho], \tag{34}$$

where the unperturbed Hamiltonian $\mathscr{H}_0$ is in equation (15) and the interaction Hamiltonian is in (32). Note that the above differential equation can be solved through a recursive relation:

$$\begin{aligned}
\rho(t) &= -\frac{i}{\hbar}\int_{-\infty}^{t} \mathrm{d}t'[\mathscr{H}_0 + \mathscr{H}_I, \rho(t')] \\
&= -\frac{i}{\hbar}\int_{-\infty}^{t} \mathrm{d}t'\left[\mathscr{H}_0 + \mathscr{H}_I, \left(-\frac{i}{\hbar}\int_{-\infty}^{t'} \mathrm{d}t''[\mathscr{H}_0 + \mathscr{H}_I, \rho(t'')]\right)\right] \\
&\qquad\qquad \vdots
\end{aligned} \tag{35}$$

Note that $\mathscr{H}_I \propto \mathscr{E}(q)$. Then, one can expand the perturbative order of ρ such that

$$\rho(t) = \rho^{(0)}(t) + \rho^{(1)}(t) + \rho^{(2)}(t) + \cdots, \tag{36}$$

where $\rho^{(n)}(t)$ involves only $\mathscr{O}(\mathscr{E}^n(q))$ terms. The result is the famous Dyson series, and one replaces the ordered solution of ρ into equation (33) to obtain the perturbative solution of the conductance σ through:

$$\widetilde{J} = \sigma\widetilde{E} = (\sigma^{(0)} + \sigma^{(1)} + \cdots)\widetilde{E}. \tag{37}$$

On the other hand, the polarization density P is related to the induced charge through

$$-Q_{\text{ind}} = \oint_{\partial V} \mathrm{d}A \cdot P, \tag{38}$$

where V is an infinitesimal volume and ∂V is the boundary (surface) of the volume, while the induced current density is related to the induced charge through the continuity:

$$-\dot{Q}_{\text{ind}} = \int_V \mathrm{d}V \nabla \cdot J = \oint_{\partial V} \mathrm{d}A \cdot J. \tag{39}$$

From these two, we obtain the relation between the induced current density and the induced polarization density as

$$J = \frac{\partial P}{\partial t} \tag{40}$$

Using the relation between the induced current and the external field

$$\widetilde{P} = \varepsilon_0 \chi \widetilde{E}, \tag{41}$$

and assuming the monochromatic field $\widetilde{E}(t) = \hat{\varepsilon}\mathscr{E}(q)\mathrm{e}^{-i\omega_q t}$, one obtains

$$\frac{\partial}{\partial t}\left(\varepsilon_0(\chi^{(1)} + \chi^{(2)} + \cdots)\widetilde{E}(t)\right) = (\sigma^{(1)} + \sigma^{(2)} + \cdots)\widetilde{E}(t). \tag{42}$$

Equating terms order by order from left to right establishes the relation between the susceptibility and the conductivity for each order.

2.4 Perturbative solution

We now solve the problem to obtain the induced current, order by order through the perturbative method. There are two plausible approaches to solve this problem. The first is to take the conventional single particle basis such as $|c(k)\rangle, |v(k)\rangle$ that are the single particle Bloch states with momentum $\hbar k$. This approach allows to use the conventionally known forms of operators such as the velocity operator relating to the Berry connection, etc., while it complicates the Schrödinger equation of ρ, due to the complex Coulomb potential. Although this method was successfully used to calculate the linear response [7], it is not certain whether the first method is tractable for the higher order calculations, due to the higher order Coulomb interaction in the perturbative approach.

Another approach is to take the many body basis $\{|0\rangle, |\mathrm{x}_{v=0,q}\rangle, |\mathrm{x}_{v=1,q}\rangle, \cdots\}$, which are anti-symmetrized Slater determinant states. This method incorporates the Coulomb potential in the

energy eigenvectors and eigenvalues of the excitonic states. Importantly the unperturbed Hamiltonian $\mathscr{H}_0$ that includes the Coulomb potential as in equation (15) is diagonal in this many body basis. This is already a great advantage over the first approach that does not diagonalize $\mathscr{H}_0$. Hence, solving the Schrödinger equation perturbatively is quite easy. However, one must represent the operators in these new many body kets and bras. If operators are successfully represented through the many body basis, the calculation is relatively straightforward.

We take the second approach to use the many body basis. Our first task is to calculate the velocity operator v in this new many body basis, which is critical in calculating the induced current in (33). In linear response theory where the incoming light frequency is close to a bound exciton state $|\psi_\nu\rangle$, our Hilbert space is two dimensional with the basis $\{|\mathrm{x}_\nu\rangle, |0\rangle\}$ where $|0\rangle$ is the ground state (Fermi sea). Consequently, the velocity operator and the density operator are now 2×2 matrices:

$$\mathrm{v} = \begin{pmatrix} \mathrm{v}_{\mathrm{ee}} & \mathrm{v}_{\mathrm{ef}} \\ \mathrm{v}_{\mathrm{fe}} & \mathrm{v}_{\mathrm{ff}} \end{pmatrix}, \quad \rho = \begin{pmatrix} \rho_{\mathrm{ee}} & \rho_{\mathrm{ef}} \\ \rho_{\mathrm{fe}} & \rho_{\mathrm{ff}} \end{pmatrix}, \tag{43}$$

where each element is such that, for example, $\mathrm{v}_{\mathrm{ef}} = \langle \mathrm{x}_\nu | \,\mathrm{v}\, | 0\rangle$. We calculate

$$\begin{aligned} \mathrm{v}_{\mathrm{fe}} &= \langle 0 | \,\dot{r}\, | \mathrm{x}_\nu\rangle = -\frac{i}{\hbar} \langle 0 | \,[r, \mathscr{H}_0 + \mathscr{H}_I]\, | \mathrm{x}_\nu\rangle = -\frac{i}{\hbar} \langle 0 | \,[r, \mathscr{H}_0]\, | \mathrm{x}_\nu\rangle \\ &= -\frac{i}{\hbar} \langle 0 | \,(r\mathscr{H}_0 - \mathscr{H}_0 r)\, | \mathrm{x}_\nu\rangle = -ie_\nu \langle 0 | \,r\, | \mathrm{x}_\nu\rangle . \end{aligned} \tag{44}$$

Here, we used the fact that $[r, \mathscr{H}_I] = 0$ since $\mathscr{H}_I \propto r$ since it involves the dipole moment element. Also we used that $\mathscr{H}_0 |\mathrm{x}_\nu\rangle = \hbar e_\nu |\mathrm{x}_\nu\rangle$ and $\langle 0 | \mathscr{H}_0 = 0$ (the energy of the Fermi sea is set to zero). It is also noteworthy that the diagonal terms of the velocity operator **v** are all zero according to the above derivation:

$$\langle \psi | \,\mathbf{v}\, | \psi\rangle = -\frac{i}{\hbar}(E_\psi - E_\psi) \langle \psi | \,r\, | \psi\rangle = 0. \tag{45}$$

Therefore, we need only the off-diagonal terms of the density matrix to calculate the induced current. Then, we have

$$J = \widetilde{J} + \widetilde{J^*} = eN_e(\mathrm{v}_{\mathrm{ef}}\rho_{\mathrm{fe}} + \mathrm{v}_{\mathrm{fe}}\rho_{\mathrm{ef}}). \tag{46}$$

Next, we calculate,

$$\begin{aligned} \langle 0 | \,\hat{\varepsilon}\cdot r\, | \mathrm{x}_\nu\rangle &= \sum_k \psi_\nu(k) \langle 0 | \,\hat{\varepsilon}\cdot r \alpha_k^\dagger \beta_{-k}^\dagger\, | 0\rangle = \sum_k \psi_\nu(k) \langle v(k) | \,\hat{\varepsilon}\cdot r\, | c(k)\rangle \\ &= \frac{1}{e}\sum_k \psi_\nu(k) d_{vc}(k) = \frac{g_\nu^*}{e}, \end{aligned} \tag{47}$$

where the last equation follows from equation (28). Here, we abbreviated such that $|c(k)\rangle = \sum_{\text{Slater perm}} \big|v(k')\big\rangle \otimes \cdots \otimes |v(k)''\rangle \otimes |c(k)\rangle \otimes \big|v(k''')\big\rangle \otimes \cdots$, which implies that $\alpha_k^\dagger \beta_{-k}^\dagger |0\rangle = |c(k)\rangle$ in the abbreviated notation. Then, we obtain, for an isotropic medium where the induced current direction coincides with the external field direction,

$$\mathrm{v}_{\mathrm{fe}} = \mathrm{v}_{\mathrm{ef}}^* = \frac{-ie_\nu g_\nu^*}{e}\hat{\varepsilon}, \tag{48}$$

where e_ν is given in equation (16).

Next, let us solve the Schrödinger equation for ρ. First, we calculate

$$\langle \mathrm{x}_\nu | \left[\mathscr{H}_0, \rho \right] | 0 \rangle = \hbar e_\nu \rho_{\mathrm{ef}}, \tag{49}$$

where we used the fact that the energy eigenvalue of the Fermi sea is zero. Using this, we establish a differential equation for ρ_{ef}:

$$\dot{\rho_{\mathrm{ef}}} = -ie_\nu \rho_{\mathrm{ef}} - \frac{i}{\hbar} \langle \mathrm{x}_\nu | \left[\mathscr{H}_I, \rho \right] | 0 \rangle . \tag{50}$$

Let us introduce the perturbative solution according to the perturbative orders:

$$\rho(t) = \rho^{(0)}(t) + \rho^{(1)}(t) + \rho^{(2)}(t) + \cdots . \tag{51}$$

We then carry out the bookkeeping for the differential equations on each order:

$$\begin{aligned}
\dot{\rho}^{(0)}_{\mathrm{ef}}(t) &= -ie_\nu \rho^{(0)}_{\mathrm{ef}}(t), \\
\dot{\rho}^{(1)}_{\mathrm{ef}}(t) &= -ie_\nu \rho^{(1)}_{\mathrm{ef}}(t) - \frac{i}{\hbar} \langle \mathrm{x}_\nu | \left[\mathscr{H}_I, \rho^{(0)} \right] | 0 \rangle , \\
\dot{\rho}^{(2)}_{\mathrm{ef}}(t) &= -ie_\nu \rho^{(2)}_{\mathrm{ef}}(t) - \frac{i}{\hbar} \langle \mathrm{x}_\nu | \left[\mathscr{H}_I, \rho^{(1)} \right] | 0 \rangle , \\
\dot{\rho}^{(3)}_{\mathrm{ef}}(t) &= -ie_\nu \rho^{(3)}_{\mathrm{ef}}(t) - \frac{i}{\hbar} \langle \mathrm{x}_\nu | \left[\mathscr{H}_I, \rho^{(2)} \right] | 0 \rangle ,
\end{aligned} \tag{52}$$

Other matrix elements for $\rho^{(n)}$ can be obtained in a similar manner.

2.4.1 Linear susceptibility

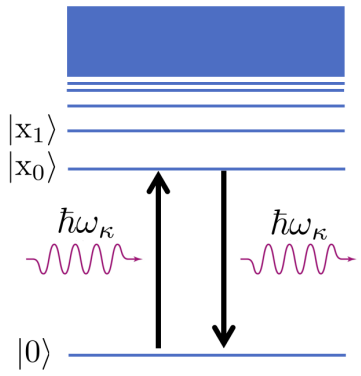

Figure 1: Transition involving the linear susceptibility. See the description of the state kets in the Appendix B.

The linear response involves the direct dipole absorption of the photon, matching the energy difference between the ground state (Fermi sea), and the exciton state. Figure 1 shows the relevant

transition. An incoming photon has an energy resonant with the exciton state energy, exciting the exciton state.

The first of equations (52) describes the dynamics of $\rho_{\rm ef}$ in the absence of any external perturbation. It is a free rotation. We then solve the second equation. For this, we calculate

$$\begin{aligned}
&\langle \mathrm{x}_\nu | \left[\mathscr{H}_I, \rho^{(0)}\right] | 0 \rangle \\
&= - \langle \mathrm{x}_\nu | \left(\sum_{\nu'} g_{\nu'} \left(B^\dagger_{\nu'} \rho^{(0)} - \rho^{(0)} B^\dagger_{\nu'} \right) \right) | 0 \rangle \, \mathscr{E}(q) \mathrm{e}^{-i\omega_q t} \\
&\quad - \langle \mathrm{x}_\nu | \left(\sum_{\nu'} g^*_{\nu'} \left(B_{\nu'} \rho^{(0)} - \rho^{(0)} B_{\nu'} \right) \right) | 0 \rangle \, \mathscr{E}^*(q) \mathrm{e}^{i\omega_q t} \\
&= -g_\nu \left(\langle \mathrm{x}_\nu | B^\dagger_\nu \rho^{(0)} | 0 \rangle - \langle \mathrm{x}_\nu | \rho^0 B^\dagger_\nu | 0 \rangle \right) \mathscr{E}(q) \mathrm{e}^{-i\omega_q t} \\
&= -g_\nu \left(\langle 0 | \rho^{(0)} | 0 \rangle - \langle \mathrm{x}_\nu | \rho^{(0)} | \mathrm{x}_\nu \rangle \right) \mathscr{E}(q) \mathrm{e}^{-i\omega_q t} \\
&= -g_\nu (\rho^{(0)}_{\rm ff} - \rho^{(0)}_{\rm ee}) \mathscr{E}(q) \mathrm{e}^{-i\omega_q t} \\
&= -g_\nu \mathscr{E}(q) \mathrm{e}^{-i\omega_q t},
\end{aligned} \tag{53}$$

where we used the fact that $B_\nu |0\rangle = 0$, $B^\dagger_{\nu'} |\mathrm{x}_\nu\rangle = 0$, and that $\rho^{(0)}_{\rm ff} = 1$ and $\rho^{(0)}_{\rm ee} = 0$ in the absence of the external field at zero temperature, that is, the state without the external field at zero temperature is the Fermi sea. From this, the first order differential equation is now

$$\dot{\rho}^{(1)}_{\rm ef}(t) = -ie_\nu \rho^{(1)}_{\rm ef}(t) + \frac{i}{\hbar} g_\nu \mathscr{E}(q) \mathrm{e}^{-i\omega_q t}. \tag{54}$$

Let us replace

$$\rho^{(1)}_{\rm ef}(t) = S^{(1)}(t) \mathrm{e}^{-ie_\nu t}. \tag{55}$$

Then, the differential equation for $S^{(1)}(t)$ is

$$\dot{S}^{(1)}(t) = \frac{i}{\hbar} g_\nu \mathscr{E}(q) \mathrm{e}^{i(e_\nu - \omega_q)t}. \tag{56}$$

Using the following

$$\int_{-\infty}^{t} \mathrm{d}t' \mathrm{e}^{i(e_\nu - \omega_q)t'} = \frac{\mathrm{e}^{i(e_\nu - \omega_q)t}}{i(e_\nu - \omega_q) + \varepsilon}, \tag{57}$$

where $\varepsilon > 0$ is the infinitesimal constant used to regulate the integral, we obtain

$$S^{(1)}(t) = \frac{g_\nu \mathscr{E}(q)}{\hbar} \frac{\mathrm{e}^{i(e_\nu - \omega_q)t}}{(e_\nu - \omega_q) - i\varepsilon}. \tag{58}$$

Hence, we obtain the first order solution

$$\rho^{(1)}_{\rm ef}(t) = \frac{g_\nu}{\hbar} \frac{1}{(e_\nu - \omega_q) - i\varepsilon} \mathscr{E}(q) \mathrm{e}^{-i\omega_q t}. \tag{59}$$

Let us also solve for $\rho_{\rm ee}^{(1)}(t)$ for later use. This calculation involves the following:

$$\langle \mathrm{x}_v | \left[\mathscr{H}_I, \rho^{(0)} \right] | \mathrm{x}_v \rangle = 0, \tag{60}$$

since $\mathscr{H}_I$ changes the state ket. Hence, $\dot{\rho}_{\rm ee}^{(1)}(t) = 0$. With the initial condition $\rho_{\rm ee}^{(1)}(-\infty) = 0$, we obtain $\rho_{\rm ee}^{(1)}(t) = 0$. Likewise, it easily follows that $\rho_{\rm ff}^{(1)}(t) = 0$.

According to the equations (46) and (48), we obtain

$$\widetilde{J}^{(1)} = eN_e \frac{-ie_v g_v^*}{e} \frac{g_v}{\hbar} \frac{1}{(e_v - \omega_q) - i\varepsilon} \hat{\varepsilon} \mathscr{E}(q) \mathrm{e}^{-i\omega_q t}. \tag{61}$$

From this, we obtain the linear conductivity

$$\sigma^{(1)} = -i \frac{e_v |g_v|^2 N_e}{\hbar} \frac{1}{(e_v - \omega_q) - i\varepsilon} \tag{62}$$

Using the relation in equation (42), one obtains the linear susceptibility. One more important aspect is that the atomic dipole moment element $d_{cv} = (-e) \langle c(k) | \hat{\varepsilon} \cdot r | v(k) \rangle$ depends on the relative orientation of the incoming light field with respect to the solid orientation. For a randomly polarized light, it is necessary to calculate the orientation-averaging such as

$$\langle |\hat{d}_{cv} \cdot \hat{\varepsilon}|^2 \rangle = \begin{cases} \frac{\int_0^\pi \sin\theta \mathrm{d}\theta \int_0^{2\pi} \mathrm{d}\phi \cos^2\theta}{\int_0^\pi \sin\theta \mathrm{d}\theta \int_0^{2\pi} \mathrm{d}\phi} = \frac{1}{3}, & (3D), \\ \frac{\int_0^{2\phi} \mathrm{d}\theta \cos^2\theta}{\int_0^{2\phi} \mathrm{d}\theta} = \frac{1}{2}, & (2D), \end{cases} \tag{63}$$

where $\hat{d}_{cv}$ is the unit vector in the direction of the random dipole moment and θ is the angle between $\hat{d}_{cv}$ and the field polarization direction $\hat{\varepsilon}$. Hence, for a randomly polarized light, the entire $\sigma^{(1)}$ must be divided by $D = d$ for $d-$dimensional problem. However, for other polarizations of the incoming photon, the value d_{cv} need to be calculated accordingly. For example, if $d_{cv} = d_{cv}^x \hat{x} + d_{cv}^y \hat{y}$, and the incoming light is a $\sigma+$ polarized light with $\hat{\varepsilon} = \frac{1}{\sqrt{2}}(\hat{x} + i\hat{y})$, the appropriate dipole moment is $d_{cv} = d_{cv} \cdot \hat{\varepsilon} = \frac{1}{\sqrt{2}} \left(d_{cv}^x + i d_{cv}^y \right)$.

We finally obtain the linear susceptibility of the exciton state:

$$\boxed{\chi^{(1)}(\omega_q) = \frac{e_v |g_v|^2 N_e}{\hbar \varepsilon_0 \omega_q} \frac{1}{(e_v - \omega_q) - i\varepsilon} = \frac{e_v |g_v|^2 N_e}{\hbar \varepsilon_0 \omega_q} \mathscr{P} \frac{1}{e_v - \omega_q} + i \frac{\pi e_v |g_v|^2 N_e}{\hbar \varepsilon_0 \omega_q} \delta(\varepsilon_v - \omega_q),} \tag{64}$$

where we used the Dirac identity

$$\lim_{\varepsilon \to 0} \frac{1}{r \mp i\varepsilon} = \mathscr{P} \frac{1}{r} \pm i\pi\delta(r), \tag{65}$$

with the Cauchy principal value symbol $\mathscr{P}$. From equation (31), one may approximate $g_v \approx \sqrt{A} d_{cv}(q=0) \psi_v^*(r=0)$ (see the table 1). Then, we obtain

$$\chi^{(1)}(\omega_q) = \left(\frac{\hbar e_v}{\hbar \omega_q} \right) \frac{AN_e}{\varepsilon_0} |d_{cv}(0)|^2 |\psi_v(r=0)|^2 \frac{1}{(\hbar e_n u - \hbar\omega_q) - i\hbar\varepsilon}. \tag{66}$$

We replace $N_e \to 2/(Ad_{\text{eff}})$ where $d_{\text{eff}} \approx 6.5$ Å [24, 15] is the effective monolayer thickness, assuming a weakly exciting situation at a single exciton (two charge carriers) level over the sample. Then, we obtain using $e_\nu \approx \omega_q$, for $\nu = 0$ the lowest exciton state:

$$\chi^{(1)}(\omega_q) \approx \frac{2|d_{cv}(0)|^2|\psi_{\nu=0}(r=0)|^2}{\varepsilon_0 d_{\text{eff}}} \frac{1}{(\hbar e_\nu - \hbar\omega_q) - i\hbar\varepsilon} = \frac{16|d_{cv}(0)|^2}{\pi a_0^2 d_{\text{eff}}\varepsilon_0} \frac{1}{(\hbar e_\nu - \hbar\omega_q) - i\hbar\varepsilon}. \quad (67)$$

Note that $\pi a_0^2 d_{\text{eff}}$ is the effective volume of the exciton. This formula exactly matches the results in Elliott's seminal paper [5] as well as the formula appearing in Haug, et al. [7] (see equation 10.103) and the formula appearing in Klingshirn [9] (see equation 27.52). The rationale to replace $N_e \to 2/Ad_{\text{eff}}$ is that the induced current density $J = \text{tr}[e(N_e\rho)\text{v}]$ in equation (33) captures the density of charge carriers and their movements. Particularly $N_e\rho = 2\rho/Ad_{\text{eff}}$ with the quantum mechanical density ρ (with the second quantized treatment, the maximum of the matrix element is unity) captures the density of the excited exciton. When the external field is near resonant with one of the exciton absorption line, the current density counts only the exciton charge carriers (an electron and a hole), and thus, it is correct to replace $N_e \to 2/Ad_{\text{eff}}$.

Using the relation between the refractive index and the susceptibility

$$n = \sqrt{1 + \chi^{(1)}}, \quad (68)$$

one obtains the absorption (fraction) given by αd_{eff} where d_{eff} is the effective thickness of the single layer 2D material. Using that the absorption coefficient is $\alpha = 2\text{Im}[n]\omega_q/c$, the total absorption is given by $\alpha d_{\text{eff}} = 2d_{\text{eff}}\text{Im}[\sqrt{1+\chi^{(1)}}]\omega_q/c$.

If we incorporate the phenomenological decay rate γ_ν of the exciton, the formula is

$$\text{Im}[\chi^{(1)}] = \frac{e_\nu |g_\nu|^2 N_e}{\hbar\varepsilon_0\omega_q} \frac{(\gamma_\nu/2)}{(e_\nu - \omega_q)^2 + (\gamma_\nu/2)^2}. \quad (69)$$

This is the usual Lorentzian lineshape with the line broadening factor γ_ν caused by the radiative decay (spontaneous emission).

Wang, et al.[23] calculated the radiative lifetime of the exciton at a temperature of 5 K to be $\sim$ 200 fs (see also the result of Selig, et al. in [19]), implying $\gamma_\nu \sim 5 \times 10^{12}$ rad/s. In addition, the real part is

$$\text{Re}[\chi^{(1)}] = \frac{e_\nu |g_\nu|^2 N_e}{\hbar\varepsilon_0\omega_q} \frac{e_\nu - \omega_q}{(e_\nu - \omega_q)^2 + (\gamma_\nu/2)^2}. \quad (70)$$

When the imaginary part is small, one obtains $\text{Re}[n] \approx \sqrt{1 + \text{Re}[\chi^{(1)}]}$.

A more precise value can be obtained if one sums over all the bound exciton levels such that

$$\begin{aligned} \text{Im}[\chi^{(1)}] &= \sum_\nu \frac{e_\nu |g_\nu|^2 N_e}{\hbar\varepsilon_0\omega_q} \frac{\gamma_\nu}{(e_\nu - \omega_q)^2 + (\gamma_\nu/2)^2}, \\ \text{Re}[\chi^{(1)}] &= \sum_\nu \frac{e_\nu |g_\nu|^2 N_e}{\hbar\varepsilon_0\omega_q} \frac{e_\nu - \omega_q}{(e_\nu - \omega_q)^2 + (\gamma_\nu/2)^2}. \end{aligned} \quad (71)$$

2.4.2 Second-order susceptibility

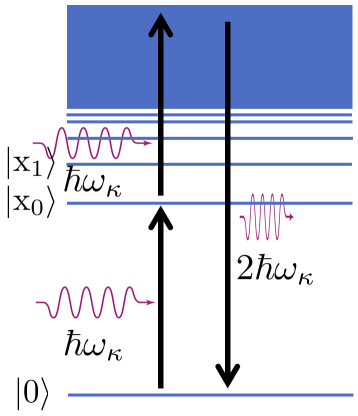

Figure 2: Transition involving the second-order susceptibility.

2.4.2.1 Second harmonic with input frequency resonant with exciton levels .

First, we consider the case where the external field frequency ω_q is near resonant with one of the bound exciton states. In the absence of another light with a different optical frequency, the primary second order effect is the second harmonic generation with the fundamental frequency of ω_q (see the figure 2). Given the exciton binding energy of TMDS materials, when the first transition is near resonant with the transition from the Fermi sea to one of the bound exciton states, the second transition must involve the transition from the bound exciton state to the free exciton state, which is a state of an electron in the conduction band, and a hole in the valence band, having the excitation energy $\hbar\omega_q$.

The interaction Hamiltonian for the second transition must be

$$\mathscr{H}_I' = -\sum_{k,\nu}\left[f_\nu(k)C_k^\dagger B_\nu \mathscr{E}(q)\mathrm{e}^{-i\omega_q t} + \mathrm{h.c.}\right], \tag{72}$$

where the new dipole transition element $f_\nu(k)$ is given as

$$\begin{aligned} f_\nu(k) &= e\langle C(k)|\,\hat{\varepsilon}\cdot r\,|\mathrm{x}_\nu\rangle = e\sum_{k'}\psi_\nu(k')\langle C(k)|\,\hat{\varepsilon}\cdot r\alpha_{k'}^\dagger\beta_{-k'}^\dagger\,|0\rangle \\ &= e\sum_{k'}\psi_\nu(k')\langle C(k)|\,\hat{\varepsilon}\cdot r\,|C(k')\rangle, \end{aligned} \tag{73}$$

where $|C(k)\rangle = C_k^\dagger|0\rangle$ is a free excitonic state of a single electron-hole pair having momentum $\hbar k, -\hbar k$ respectively, not bound by the Coulomb potential. The physical intuition is that this dipole moment is a superposition of all intraband dipole moment weighted by the (Fourier-transformed) exciton wavefunction.

From the equation (42), the second order susceptibility is obtained through

$$\frac{\partial}{\partial t}\varepsilon_0\chi^{(2)}(2\omega_q,\omega_q)\mathscr{E}^2(q)\mathrm{e}^{-i2\omega_q t} = \sigma^{(2)}\mathscr{E}^2(q)\mathrm{e}^{-i2\omega_q t}, \tag{74}$$

which relates

$$\chi^{(2)}(2\omega_q,\omega_q)=\frac{\sigma^{(2)}}{-i2\varepsilon_0\omega_q}. \tag{75}$$

The second order transition involves the three levels: $|0\rangle, |\mathrm{x}_\nu\rangle, |C(k)\rangle$ whose energy eigenvalues are 0, $\hbar e_\nu$, and $\hbar\omega_k(\approx 2\hbar\omega_q)$, respectively. In order to calculate the induced current, we need to calculate $\rho^{(2)}_{\mathrm{ef}}(t)=\langle \mathrm{x}_\nu|\rho^{(2)}(t)|0\rangle$, $\rho^{(2)}_{\mathrm{Cf},k}(t)=\langle C(k)|\rho^{(2)}(t)|0\rangle$, and $\rho^{(2)}_{\mathrm{Ce},k}(t)=\langle C(k)|\rho^{(2)}(t)|\mathrm{x}_\nu\rangle$.

We will show that the only substantial term is $\rho^{(2)}_{\mathrm{Cf},k}(t)$ among them. Let us first calculate $\rho^{(2)}_{\mathrm{ef}}(t)$, which is obtained through

$$\dot{\rho}^{(2)}_{\mathrm{ef}}(t)=-ie_\nu\rho^{(2)}_{\mathrm{ef}}(t)-\frac{i}{\hbar}\langle \mathrm{x}_\nu|\left[\mathscr{H}_I+\mathscr{H}_I',\rho^{(1)}\right]|0\rangle. \tag{76}$$

with the solution in equation (59), which is repeated here:

$$\rho^{(1)}_{\mathrm{ef}}(t)=\frac{g_\nu}{\hbar}\frac{1}{(e_\nu-\omega_q)-i\varepsilon}\mathscr{E}(q)\mathrm{e}^{-i\omega_q t}. \tag{77}$$

Note that

$$\langle \mathrm{x}_\nu|\left[\mathscr{H}_I,\rho^{(1)}\right]|0\rangle=-\langle \mathrm{x}_\nu|\left(\sum_{\nu'}g_{\nu'}\left(B^\dagger_{\nu'}\rho^{(1)}-\rho^{(1)}B^\dagger_{\nu'}\right)\right)|0\rangle\,\mathscr{E}(q)\mathrm{e}^{-i\omega_q t}. \tag{78}$$

Also note that the basis necessary to describe $\rho^{(1)}$ is only $\{|0\rangle, |\mathrm{x}_\nu\rangle\}$. Then, for $\rho^{(1)}$ we can use the following identity:

$$\begin{aligned}B^\dagger_\nu\rho^{(1)}&=B^\dagger_\nu\left(|0\rangle\langle 0|+|\mathrm{x}_\nu\rangle\langle \mathrm{x}_\nu|\right)\rho^{(1)},\\ \rho^{(1)}B^\dagger_\nu&=\rho^{(1)}\left(|0\rangle\langle 0|+|\mathrm{x}_\nu\rangle\langle \mathrm{x}_\nu|\right)B^\dagger_\nu.\end{aligned} \tag{79}$$

Using this and utilizing the fact that $\rho^{(1)}_{\mathrm{ff,ee}}(t)=0$ as we solved in the previous subsection, we obtain $\langle \mathrm{x}_\nu|\left[\mathscr{H}_I,\rho^{(1)}\right]|0\rangle=0$. This leads to

$$\dot{\rho}^{(2)}_{\mathrm{ef}}(t)=-ie_\nu\rho^{(2)}_{\mathrm{ef}}(t)-\frac{i}{\hbar}\langle \mathrm{x}_\nu|\left[\mathscr{H}_i',\rho^{(1)}\right]|0\rangle. \tag{80}$$

We calculate

$$\langle \mathrm{x}_\nu|\left[\mathscr{H}_I',\rho^{(1)}\right]|0\rangle=-\langle \mathrm{x}_\nu|\left(\sum_{k,\nu'}f_{\nu'}(k)\left(C^\dagger_k B_{\nu'}\rho^{(1)}-\rho^{(1)}C^\dagger_k B_{\nu'}\right)\mathscr{E}(q)\mathrm{e}^{-i\omega_q t}-\mathrm{h.c.}\right)|0\rangle. \tag{81}$$

Note that

$$\begin{aligned}\sum_{k,\nu'}f_{\nu'}(k)\langle \mathrm{x}_\nu|C^\dagger_k B_{\nu'}\rho^{(1)}|0\rangle&=\sum_{k,\nu'}f_{\nu'}(k)\langle \mathrm{x}_\nu|C^\dagger_k B_{\nu'}\left(|0\rangle\langle 0|+|\mathrm{x}_\nu\rangle\langle \mathrm{x}_\nu|\right)\rho^{(1)}|0\rangle\\ &=\sum_k f_\nu(k)\langle \mathrm{x}_\nu|C^\dagger_k|0\rangle\langle \mathrm{x}_\nu|\rho^{(1)}|0\rangle\\ &=\sum_k f_\nu(k)\langle \mathrm{x}_\nu|C(k)\rangle\langle \mathrm{x}_\nu|\rho^{(1)}|0\rangle\\ &=0,\end{aligned} \tag{82}$$

since $\langle \mathrm{x}_\nu | C(k) \rangle = 0$. Similarly it easily follows that

$$\begin{aligned}\sum_{k,\nu'} f_\nu^*(k) \langle \mathrm{x}_\nu | B_{\nu'}^\dagger C_k \rho^{(1)} |0\rangle &= \sum_{k,\nu'} f_\nu^*(k) \langle \mathrm{x}_\nu | B_{\nu'}^\dagger C_k \left(|0\rangle\langle 0| + |\mathrm{x}_\nu\rangle\langle \mathrm{x}_\nu| \right) \rho^{(1)} |0\rangle \\ &= \sum_k f_\nu^*(k) \langle 0 | C_k | \mathrm{x}_\nu \rangle \langle \mathrm{x}_\nu | \rho^{(1)} |0\rangle \\ &= \sum_k f_\nu^*(k) \langle C(k) | \mathrm{x}_\nu \rangle \langle \mathrm{x}_\nu | \rho^{(1)} |0\rangle \\ &= 0. \end{aligned} \tag{83}$$

In addition, we calculate

$$\sum_{k,\nu'} f_{\nu'}(k) \langle \mathrm{x}_\nu | \rho^{(1)} C_k^\dagger B_{\nu'} |0\rangle = 0 = \sum_{k,\nu'} f_{\nu'}^*(k) \langle \mathrm{x}_\nu | \rho^{(1)} B_{\nu'}^\dagger C_k |0\rangle . \tag{84}$$

Therefore, we obtain $\langle \mathrm{x}_\nu | [\mathscr{H}_i', \rho^{(1)}] |0\rangle = 0$. Since $\rho_{\mathrm{ef}}^{(2)}(-\infty) = 0$ and $\dot{\rho}_{\mathrm{ef}}^{(2)}(t) = -ie_\nu \rho_{\mathrm{ef}}^{(2)}(t)$, we obtain $\rho_{\mathrm{ef}}^{(2)}(t) = 0$.

Next, we solve the following to obtain $\rho_{Ce,k}(t)$:

$$\dot{\rho}_{\mathrm{Ce},k}^{(2)}(t) = -i(\omega_k - e_\nu)\rho_{\mathrm{Ce},k}^{(2)}(t) - \frac{i}{\hbar} \langle C(k) | [\mathscr{H}_i + \mathscr{H}_i', \rho^{(1)}] | \mathrm{x}_\nu \rangle . \tag{85}$$

First, we calculate

$$\begin{aligned}&\langle C(k) | [\mathscr{H}_I', \rho^{(1)}] | \mathrm{x}_\nu \rangle \\ &= -\langle C(k) | \left(\sum_{k,\nu'} f_\nu(k) \left(C_k^\dagger B_{\nu'} \rho^{(1)} - \rho^{(1)} C_k^\dagger B_{\nu'} \right) \mathscr{E}(q) \mathrm{e}^{-i\omega_q t} - \mathrm{h.c.} \right) | \mathrm{x}_\nu \rangle \\ &= -\left(\sum_{k,\nu'} f_\nu(k) \langle 0 | B_{\nu'} | \mathrm{x}_\nu \rangle \langle \mathrm{x}_\nu | \rho^{(1)} | \mathrm{x}_\nu \rangle - \sum_k \langle C(k) | \rho^{(1)} | C(k) \rangle \right) \mathscr{E}(q) \mathrm{e}^{-i\omega_q t} \\ &= 0. \end{aligned} \tag{86}$$

Also we calculate

$$\begin{aligned}\langle C(k) | [\mathscr{H}_I, \rho^{(1)}] | \mathrm{x}_\nu \rangle &= -\langle C(k) | \left(\sum_{\nu'} g_{\nu'} \left(B_{\nu'}^\dagger \rho^{(1)} - \rho^{(1)} B_{\nu'}^\dagger \right) \mathscr{E}(q) \mathrm{e}^{-i\omega_q t} + \mathrm{h.c.} \right) | \mathrm{x}_\nu \rangle \\ &= 0, \end{aligned} \tag{87}$$

since $B_\nu |C(k)\rangle = |0\rangle \langle \mathrm{x}_\nu | C(k) \rangle = 0$ and $B_{\nu'}^\dagger |\mathrm{x}_\nu\rangle = 0$. From the above two and the fact that $\rho_{\mathrm{Ce},k}^{(2)}(-\infty) = 0$, we obtain $\rho_{\mathrm{Ce},k}^{(2)}(t) = 0$.

Let us now calculate $\rho_{\mathrm{Cf},k}^{(2)}(t)$ using

$$\dot{\rho}_{\mathrm{Cf},k}^{(2)}(t) = -i\omega_k \rho_{\mathrm{Cf},k}^{(2)}(t) - \frac{i}{\hbar} \langle C(k) | [\mathscr{H}_I + \mathscr{H}_I', \rho^{(1)}] |0\rangle , \tag{88}$$

where $\hbar\omega_k$ is the energy eigenvalue of $|C(k)\rangle$. In this context, we can expand the basis to describe the matrix $\rho^{(1)}$ to $|C(k)\rangle, |\mathrm{ev}_\nu\rangle, |0\rangle$. In order to solve this equation, we need to know the matrix element $\rho^{(1)}_{\mathrm{Ce},k}(t)$ and $\rho^{(1)}_{\mathrm{ef}}(t)$, where the latter is obtained in (59). We also know that $\rho^{(1)}_{\mathrm{Cf},k}(t) = 0$ since the driving frequency ω_q is far from $\omega_k \approx 2\omega_q$. Let us calculate $\rho^{(1)}_{\mathrm{Ce},k}(t)$ through the differential equation

$$\dot{\rho}^{(1)}_{\mathrm{Ce},k}(t) = -ie_\nu \rho^{(1)}_{\mathrm{Ce},k}(t) - \frac{i}{\hbar}\langle C(k)|\left[\mathscr{H}_I + \mathscr{H}_I', \rho^{(0)}\right]|0\rangle. \tag{89}$$

We first calculate

$$\langle C(k)|\left[\mathscr{H}_I, \rho^{(0)}\right]|\mathrm{x}_\nu\rangle = 0, \tag{90}$$

since $\mathscr{H}_I$ involves $B^\dagger_\nu, B_\nu$ only. Next, we calculate

$$\begin{aligned}
&\langle C(k)|\left[\mathscr{H}_I', \rho^{(0)}\right]|\mathrm{x}_\nu\rangle \\
&= -\sum_{k',\nu'} f_\nu(k')\langle C(k)|C^\dagger_{k'}B_{\nu'}\rho^{(0)} - \rho^{(0)}C^\dagger_{k'}B_{\nu'}|\mathrm{x}_\nu\rangle \mathscr{E}(q)\mathrm{e}^{-i\omega_q t} \\
&= -f_\nu(k)\left(\langle 0|B_\nu|\mathrm{x}_\nu\rangle\langle \mathrm{x}_\nu|\rho^{(0)}|\mathrm{x}_\nu\rangle - \langle C(k)|\rho^{(0)}|C(k)\rangle\right)\mathscr{E}(q)\mathrm{e}^{-i\omega_q t} \\
&= -f_\nu(k)\left(\rho^{(0)}_{\mathrm{ee}} - \rho^{(0)}_{CC,k}\right)\mathscr{E}\mathrm{e}^{-i\omega_q t},
\end{aligned} \tag{91}$$

where we discarded the terms proportional to $\mathrm{e}^{i\omega_q t}$ as they produce zero results. Here, we also used the fact that $\rho^{(0)}$ has nonzero elements only on the diagonal terms. The quantities $\rho^{(0)}_{\mathrm{ee}}$ and $\rho^{(0)}_{CC}$ are negligibly small compared to $\rho^{(0)}_{\mathrm{ff}} \approx 1$. Therefore, we obtain that $\langle C(k)|\left[\mathscr{H}_I', \rho^{(0)}\right]|\mathrm{x}_\nu\rangle \approx 0$. Since the drive is zero, the differential equation (89) states that $\rho^{(1)}_{\mathrm{Ce},k}(t) = 0$ because $\rho^{(1)}_{\mathrm{Ce},k}(-\infty) = 0$.

Next, let us calculate the following:

$$\begin{aligned}
\langle C(k)|\left[\mathscr{H}_I, \rho^{(1)}\right]|0\rangle &= -\sum_{\nu'} g_{\nu'}\langle C(k)|B^\dagger_{\nu'}\rho^{(1)} - \rho^{(1)}B^\dagger_{\nu'}|0\rangle \mathscr{E}(q)\mathrm{e}^{-i\omega_q t} \\
&= \sum_{\nu'} g_{\nu'}\langle C(k)|\rho^{(1)}|\mathrm{x}_\nu\rangle \mathscr{E}(q)\mathrm{e}^{-i\omega_q t} \\
&= 0,
\end{aligned} \tag{92}$$

where we discarded the terms involving $\mathrm{e}^{i\omega_q t}$ as they produce zero results and used the fact that $\rho^{(1)}$ has only significant matrix element of $\rho^{(1)}_{\mathrm{ef}}(t)$. On the other hand, we calculate

$$\begin{aligned}
\langle C(k)|\left[\mathscr{H}_I', \rho^{(1)}\right]|0\rangle &= -\sum_{k',\nu'} f_\nu(k')\langle C(k)|C^\dagger_{k'}B_{\nu'}\rho^{(1)} - \rho^{(1)}C^\dagger_{k'}B_{\nu'}|0\rangle \mathscr{E}(q)\mathrm{e}^{-i\omega_q t} \\
&= -\sum_{\nu'} f_{\nu'}(k)\langle 0|B_{\nu'}|\mathrm{x}_\nu\rangle\langle \mathrm{x}_\nu|\rho^{(1)}|0\rangle \mathscr{E}(q)\mathrm{e}^{-i\omega_q t} \\
&= -\frac{f_\nu(k)g_\nu}{\hbar}\frac{1}{(e_\nu - \omega_q) - i\varepsilon}\mathscr{E}^2(q)\mathrm{e}^{-i2\omega_q t},
\end{aligned} \tag{93}$$

where we discarded the terms involving $e^{i\omega_q t}$, which produce zero results. We also used the fact that the only nonzero element of $\rho^{(1)}(t)$ is $\rho^{(1)}_{\rm ef}(t)$. Then, we obtain the following differential equation

$$\dot{\rho}^{(2)}_{{\rm Cf},k}(t) = -i\omega_k \rho^{(2)}_{{\rm Cf},k}(t) + i\frac{f_v(k)g_v}{\hbar^2}\frac{1}{(e_v-\omega_q)-i\varepsilon}\mathscr{E}^2(q)e^{-i2\omega_q t}. \tag{94}$$

Setting

$$\rho^{(2)}_{{\rm Cf},k}(t) = S'^{(2)}(t)e^{-i\omega_k t}, \tag{95}$$

the new differential equation for $S'^{(2)}(t)$ is now

$$\dot{S}'^{(2)}(t) = +i\frac{f_v(k)g_v}{\hbar^2}\frac{1}{(e_v-\omega_q)-i\varepsilon}\mathscr{E}^2(q)e^{i(\omega_k-2\omega_q)t}. \tag{96}$$

The solution is

$$\rho^{(2)}_{{\rm Cf},k}(t) = \frac{f_v(k)g_v}{\hbar^2}\frac{1}{\left((e_v-\omega_q)-i\varepsilon\right)\left((\omega_k-2\omega_q)-i\varepsilon'\right)}\mathscr{E}^2(q)e^{-i2\omega_q t}. \tag{97}$$

This quantity is substantial if ω_q is close to e_v and $\omega_k \approx 2e_v$. The only remaining quantity to calculate is the velocity element

$$v_{{\rm f}C,k} = \langle 0|\dot{r}|C(k)\rangle = -\frac{i}{\hbar}\langle 0|[r,\mathscr{H}_0]|C(k)\rangle \simeq -i\omega_{ck}\langle v(k)|r|c(k)\rangle. \tag{98}$$

This allows to obtain the induced current as

$$\begin{aligned} J^{(2)} &= eN_e{\rm tr}[v\rho^{(2)}] \approx \sum_k eN_e v_{{\rm f}C,k}\rho^{(2)}_{{\rm Cf},k} + {\rm h.c.} \\ &= -\sum_k i\frac{N_e f_v(k)g_v\omega_k d^*_{cv}(k)}{\hbar^2}\frac{1}{\left((e_v-\omega_q)-i\varepsilon\right)\left((\omega_k-2\omega_q)-i\varepsilon'\right)}\hat{\varepsilon}\mathscr{E}^2(q)e^{-i2\omega_q t} + {\rm h.c.} \end{aligned} \tag{99}$$

and, therefore, from $\widetilde{J}^{(2)} = \sigma^{(2)}\hat{\varepsilon}\mathscr{E}^2(q)e^{-i2\omega_q t}$, we obtain

$$\sigma^{(2)} = -i\sum_k \frac{N_e f_v(k)g_v\omega_{ck}d^*_{cv}(k)}{\hbar^2}\frac{1}{\left((e_v-\omega_q)-i\varepsilon\right)\left((\omega_k-2\omega_q)-i\varepsilon'\right)} \tag{100}$$

Then, from equation (75), we finally obtain

$$\boxed{\chi^{(2)}(\omega_q \sim e_v) = \frac{N_e g_v}{2\varepsilon_0\hbar^2\omega_q}\left(\frac{1}{(e_v-\omega_q)-i\varepsilon}\right)\left(\sum_k \frac{f_v(k)\omega_k d^*_{cv}(k)}{(\omega_k-2\omega_q)-i\varepsilon'}\right).} \tag{101}$$

This is the second-order nonlinear susceptibility relevant to the second harmonic generation from the fundamental frequency ω_q, which is close to e_v. With the phenomenological treatment of the decay rate of the transition $|0\rangle \leftrightarrow |x_v\rangle$, and $|x_v\rangle \leftrightarrow |C(k)\rangle$ with the decay rate γ_v, γ_k, respectively, we obtain

$$\chi^{(2)}(\omega_q \sim e_v) = \frac{N_e g_v}{2\varepsilon_0\hbar^2\omega_q}\left(\frac{1}{(e_v-\omega_q)-i(\gamma_v/2)}\right)\left(\sum_k \frac{f_v(k)\omega_k d^*_{cv}(k)}{(\omega_k-2\omega_q)-i(\gamma_k/2)}\right), \tag{102}$$

from which it is possible to extract the real and the imaginary values of $\chi^{(2)}$.

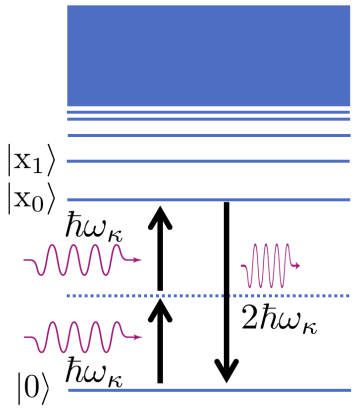

Figure 3: Second harmonic generation where the fundamental photon energy is half of the exciton energy. Dotted line represents a *virtual* energy level.

2.4.2.2 Low-frequency second harmonic In the next scenario, we consider the case where the incoming light energy is such that $\hbar\omega_q \sim \hbar e_\nu/2$. Unlike the previous scenario where $\hbar\omega_q \sim \hbar e_\nu$ that has inevitably a linear loss for the incoming light, this low frequency photon does not suffer from the linear loss for the fundamental frequency since the incoming photon is not directly resonant with any of the real energy levels.

The first transition from $|0\rangle$ by the external field $\mathscr{E}(q)\mathrm{e}^{-i\omega_q t}$ involves a *virtual* transition as shown in the figure 3. This virtual level is nothing other than the collective contribution from the higher order bound exciton states represented by the first order matrix elements in equation (59)

$$\rho^{(1)}_{\nu\mathrm{f}}(t) = \frac{g_\nu}{\hbar}\frac{1}{(e_\nu - \omega_q) - i\varepsilon_\nu}\mathscr{E}(q)\mathrm{e}^{-i\omega_q t}, \tag{103}$$

where ω_q is indeed not close to any of e_ν. Note that the previous solution to the case where $\omega_q \sim e_\nu$ was obtained by considering the first transition $|0\rangle \to |\mathrm{x}_\nu\rangle$, and the second transition $|\mathrm{x}_\nu\rangle \to |C_k\rangle$, and the most significant matrix element in $\rho^{(2)}$ was $\rho^{(2)}_{\mathrm{Cf},k}$. Then, in an analogy, we can obtain $\chi^{(2)}$ of the current low-frequency configuration by replacing the role as follows: the first transition is $|0\rangle \to |\mathrm{x}_\nu\rangle$, the second transition is $|\mathrm{x}_\nu\rangle \to |\mathrm{x}_0\rangle$, and the most significant matrix element of $\rho^{(2)}$ is $\rho^{(2)}_{0\mathrm{f}} = \langle \mathrm{x}_0|\,\rho^{(2)}\,|0\rangle$, since $2\omega_q \sim e_0$. Note that in this configuration, all ν may participate as the intermediate *virtual* level, except for $\nu = 0$ level, simply because the transition probability $|\mathrm{x}_0\rangle \to |\mathrm{x}_0\rangle$ through the external field is zero. Then, from equation (102), it easily follows that the correct solution for $\chi^{(2)}(\omega_q \sim e_0/2)$ is obtained as

$$\boxed{\chi^{(2)}(\omega_q \sim e_0/2) = \sum_{\nu\neq 0}\frac{e_\nu N_e g_\nu h_{\nu 0} g_0^*}{2\omega_q\varepsilon_0\hbar^2}\left(\frac{1}{\left(e_\nu - \omega_q - i(\gamma_\nu/2)\right)\left(e_0 - 2\omega_q - i(\gamma_0/2)\right)}\right),} \tag{104}$$

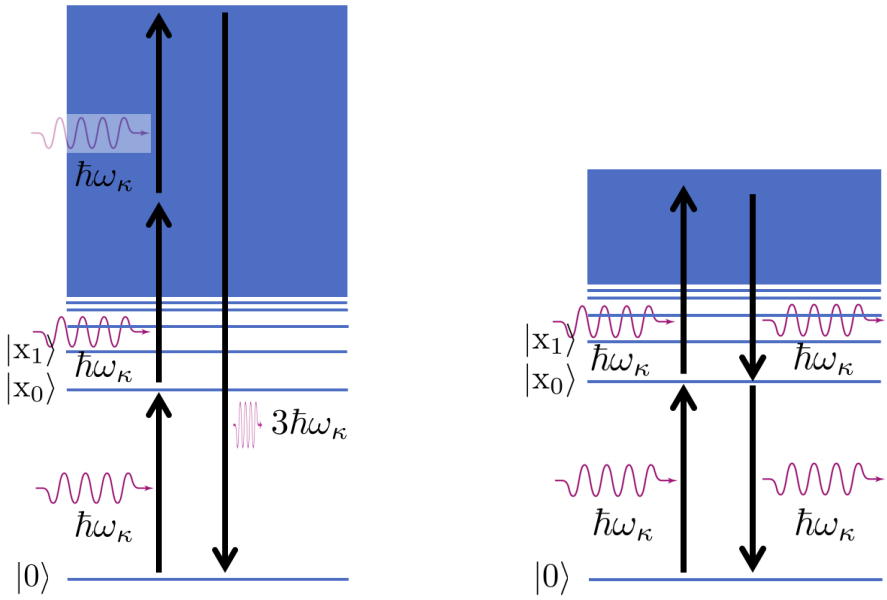

(a) Third harmonic generation

(b) Two photon transition

Figure 4: Two third-order nonlinear processes relevant to the case of a single external field that is resonant with the exciton energy.

where γ_ν is the radiative decay rate of $|x_\nu\rangle$ state and

$$\begin{aligned} g_0 &= \sum_k d_{cv}(k)\psi_0^*(k), \\ g_\nu &= \sum_k d_{cv}(k)\psi_\nu^*(k), \\ h_{\nu 0} &= e\langle x_\nu | r\cdot\hat{\varepsilon}\,|x_0\rangle\,. \end{aligned} \tag{105}$$

Note that using equation (204), we easily obtain

$$\langle x_\nu | r | x_0\rangle = \sum_{k,k'} \psi_\nu^*(k)\psi_0(k')\langle c(k)|\, r\,|c(k')\rangle\,, \tag{106}$$

and thus, using equation (73), we obtain

$$h_{\nu 0} = \sum_{k,k'} \psi_\nu^*(k)\psi_0(k')d_{cc}(k,k') = \sum_k \psi_\nu^*(k) f_0(k), \tag{107}$$

where $d_{cc}(k,k') = \langle c(k)|\, r\cdot\hat{\varepsilon}\,|c(k')\rangle$ is the *intraband* dipole moment matrix element for the conduction band.

2.4.3 Third-order susceptibility

2.4.3.1 High frequency third order processes We first consider the case where the driving external field is near resonant with the exciton level. The relevant third-order processes are twofolds:

(1) the third harmonic generation, and (2) the two-photon transition (i.e., Kerr nonlinearity and two-photon absorption) (see the figure 4).

We first calculate the third-harmonic generation process. This process involves the two interaction Hamiltonian $\mathscr{H}_I$ and $\mathscr{H}_I'$ in equations (32) and (72), respectively. It also involves additional transition from the upper level $|C(k)\rangle$ to a further up level in the continuum. Since the momentum must be preserved, it involves the following transition interaction Hamiltonian

$$\mathscr{H}_I'' = -\sum_{k,k'} \left[d_{c'c}(k',k) C_{k'}^{\prime\dagger} C_k \mathscr{E}(q) \mathrm{e}^{-i\omega_q t} + \mathrm{h.c.} \right], \tag{108}$$

where $d_{c'c}(k',k) = e \left\langle C'(k') \right| r \cdot \hat{\varepsilon} \left| C(k) \right\rangle$ is the dipole moment between the pair electron-hole state with k' and the pair electron-hole state with k.

Note that this process involves the four many body states $|0\rangle, |x_v\rangle, |C(k)\rangle, \left|C'(k')\right\rangle$. The only significant matrix element that involves the real transition is $\rho^{(3)}_{C'f,k} = \langle C'(k)| \rho^{(3)} |0\rangle$, which can be easily seen since all the other transition matrix elements involves some virtual levels whose transition strength is not as high as $\rho^{(3)}_{C'f,k}$. We can easily guess the form:

$$\begin{aligned}
&\rho^{(3)}_{C'f,k'}(t) \\
&= \sum_k \frac{f_v(k') d_{c'c}(k',k) g_v}{\hbar^3} \frac{1}{\left((e_v - \omega_q) - i\varepsilon\right)\left((\omega_{ck} - 2\omega_q) - i\varepsilon'\right)\left((\omega_{c'k} - 3\omega_q) - i\varepsilon''\right)} \mathscr{E}^3(q) \mathrm{e}^{-i3\omega_q t},
\end{aligned} \tag{109}$$

where $\hbar\omega_{ck}$ is the energy eigenvalue of $|C(k)\rangle$ and $\hbar\omega_{c'k}$ is that of $|C'(k)\rangle$. We also need the quantity

$$\mathrm{v}_{\mathrm{f}C',k'} = \langle 0| \dot{r} \left|C'(k')\right\rangle = -\frac{i}{\hbar} \langle 0| [r, \mathscr{H}_0] \left|C'(k')\right\rangle = -i\omega_{c'k'} \langle v(k)| r \left|c'(k')\right\rangle. \tag{110}$$

We then calculate the induced current for the third-harmonic generation:

$$\begin{aligned}
J^{(3)} &= eN_e \mathrm{tr}[\mathbf{v}\rho^{(3)}] \approx \sum_{k'} eN_e \mathbf{v}_{\mathrm{f}C',k'} \rho^{(3)}_{C'\mathrm{f},k'} + \mathrm{h.c.} \\
&= -i \sum_{k,k'} \left(\begin{array}{l} \frac{N_e f_v(k') d_{c'c}(k',k) g_v \omega_{c'k'} d^*_{c'v}(k')}{\hbar^3} \\ \times \frac{1}{\left((e_v - \omega_q) - i\varepsilon\right)\left((\omega_{ck} - 2\omega_q) - i\varepsilon'\right)\left((\omega_{c'k} - 3\omega_q) - i\varepsilon''\right)} \hat{\varepsilon} \mathscr{E}^3(q) \mathrm{e}^{-i3\omega_q t} \end{array} \right) + \mathrm{h.c.},
\end{aligned} \tag{111}$$

where $d_{c'v}(k') = e \left\langle c'(k') \right| r \cdot \hat{\varepsilon} \left| v(k') \right\rangle$. Then, from $\widetilde{J}^{(3)} = \sigma^{(3)} \hat{\varepsilon} \mathscr{E}^3(q) \mathrm{e}^{-i3\omega_q t}$, we obtain

$$\sigma^{(3)}_{TH} = -i \sum_{k,k'} \left(\begin{array}{l} \frac{N_e f_v(k') d_{c'c}(k',k) g_v \omega_{c'k'} d^*_{c'v}(k')}{\hbar^3} \\ \times \frac{1}{\left((e_v - \omega_q) - i\varepsilon\right)\left((\omega_{ck} - 2\omega_q) - i\varepsilon'\right)\left((\omega_{c'k} - 3\omega_q) - i\varepsilon''\right)} \end{array} \right). \tag{112}$$

The third-order susceptibility for the third-harmonic generation is obtained through

$$\frac{\partial}{\partial t} \varepsilon_0 \chi^{(3)}_{TH}(3\omega_q, \omega_q) \mathscr{E}^3(q) \mathrm{e}^{-i3\omega_q t} = \sigma^{(3)} \mathscr{E}^3(q) \mathrm{e}^{-i3\omega_q t}. \tag{113}$$

From this, we obtain

$$\chi^{(3)}_{TH}(3\omega_q,\omega_q)=\frac{\sigma^{(3)}}{-i3\varepsilon_0\omega_q}. \tag{114}$$

Finally, we obtain the third-order susceptibility for the third-harmonic generation as

$$\boxed{\chi^{(3)}_{TH}(\omega_q\sim e_\nu/3)=\sum_{k,k'}\left(\begin{array}{c}\frac{\omega_{c'k'}N_e f_\nu(k')d_{c'c}(k',k)g_\nu d^*_{c'\nu}(k')}{3\omega_q\varepsilon_0\hbar^3}\\ \times\frac{1}{\big((e_\nu-\omega_q)-i\varepsilon\big)\big((\omega_{ck}-2\omega_q)-i\varepsilon'\big)\big((\omega_{c'k}-3\omega_q)-i\varepsilon''\big)}\end{array}\right).} \tag{115}$$

Next, let us turn to the two-photon transition shown in figure 4. This process involves three levels, namely, $|0\rangle,|x_\nu\rangle,|C(k)\rangle$. Hence, $\rho^{(3)}$ has nine matrix elements, where only six are independent (Hermitian). The interaction Hamiltonians are $\mathscr{H}_I$ and $\mathscr{H}_I'$, which are repeated here for convenience:

$$\mathscr{H}_I=-\sum_\nu[g_\nu B^\dagger_\nu\mathscr{E}(q)\mathrm{e}^{-i\omega_q t}+\mathrm{h.c.}],$$
$$\mathscr{H}_I'=-\sum_{k,\nu}[f_\nu(k)C^\dagger_k B_\nu\mathscr{E}(q)\mathrm{e}^{-i\omega_q t}+\mathrm{h.c.}],$$

where

$$g_\nu=\sum_k\psi_\nu(k)d_{c\nu}(k),$$
$$f_\nu(k)=e\sum_{k'}\psi_\nu(k')\left\langle C(k)\right|\hat{\varepsilon}\cdot r\left|C(k')\right\rangle.$$

The third order perturbative solution $\rho^{(3)}$ for the two photon process is described through the three states $|0\rangle,|x_\nu\rangle,|C(k)\rangle$ as in the second-order calculation. In order to calculate the induced current density, we need the matrix elements of $\rho^{(3)}$. The matrix has nine elements, and six of them are independent. Since the diagonal terms of the velocity matrix are all zero as we have shown earlier, we are concerned with only the off-diagonal term (see equation (45) and the text around it). Then, we are concerned with only three terms $\rho^{(3)}_{\mathrm{Ce},k}$, $\rho^{(3)}_{\mathrm{Cf},k}$, $\rho^{(3)}_{\mathrm{ef}}$.

The differential equation for the third order involves the second order solution as in equations (52). Let us first calculate $\rho^{(3)}_{\mathrm{Ce},k}$ through

$$\dot{\rho}^{(3)}_{\mathrm{Ce},k}(t)=-i\omega_{cek}\rho^{(3)}_{\mathrm{Ce},k}(t)-\frac{i}{\hbar}\left\langle C(k)\right|\left[\mathscr{H}_I+\mathscr{H}_I',\rho^{(2)}\right]\left|\mathrm{x}_\nu\right\rangle, \tag{116}$$

where $\omega_{cek}=\omega_{ck}-e_\nu$. Let us first calculate

$$\begin{aligned}&\left\langle C(k)\right|\left[\mathscr{H}_I,\rho^{(2)}\right]\left|\mathrm{x}_\nu\right\rangle\\ &=-\sum_{\nu'}\left\langle C(k)\right|\left[\begin{array}{l}\left(g_{\nu'}B^\dagger_{\nu'}\mathscr{E}(q)\mathrm{e}^{-i\omega_q t}+g^*_{\nu'}B_{\nu'}\mathscr{E}^*(q)\mathrm{e}^{i\omega_q t}\right)\rho^{(2)}\\ -\rho^{(2)}\left(g_{\nu'}B^\dagger_{\nu'}\mathscr{E}(q)\mathrm{e}^{-i\omega_q t}+g^*_{\nu'}B_{\nu'}\mathscr{E}^*(q)\mathrm{e}^{i\omega_q t}\right)\end{array}\right]\left|\mathrm{x}_\nu\right\rangle\\ &=g^*_\nu\rho^{(2)}_{\mathrm{Cf},k}\mathscr{E}^*\mathrm{e}^{i\omega_q t}\\ &=\frac{f_\nu(k)|g_\nu|^2}{\hbar^2}\frac{1}{((e_\nu-\omega_q)-i\varepsilon)((\omega_{ck}-2\omega_q)-i\varepsilon')}|\mathscr{E}(q)|^2\mathscr{E}\mathrm{e}^{-i\omega_q t},\end{aligned} \tag{117}$$

where we used the fact that the only significant matrix element of $\rho^{(2)}$ is $\rho^{(2)}_{\mathrm{Cf},k}$, and the equation (97). Next, let us calculate

$$\begin{aligned}
&\langle C(k)|\,[\mathscr{H}_I',\rho^{(2)}]\,|\mathrm{x}_\nu\rangle \\
&= -\sum_{k',\nu'}\langle C(k)|\begin{bmatrix} \left(f_\nu(k')C^\dagger_{k'}B_{\nu'}\mathscr{E}(q)\mathrm{e}^{-i\omega_q t}+f^*_\nu(k')B^\dagger_{\nu'}C_{k'}\mathscr{E}^*(q)\mathrm{e}^{i\omega_q t}\right)\rho^{(2)} \\ -\rho^{(2)}\left(f_\nu(k')C^\dagger_{k}B_{\nu'}\mathscr{E}(q)\mathrm{e}^{-i\omega_q t}+f^*_\nu(k')B^\dagger_{\nu'}C_{k'}\mathscr{E}^*(q)\mathrm{e}^{i\omega_q t}\right)\end{bmatrix}|\mathrm{x}_\nu\rangle \\
&= 0,
\end{aligned} \tag{118}$$

where we again used the fact that the only significant term in $\rho^{(2)}$ is $\rho^{(2)}_{\mathrm{Cf},k}$. From these two, we obtain the differential equation

$$\dot\rho^{(3)}_{\mathrm{Ce},k}(t) = -i\omega_{cek}\rho^{(3)}_{\mathrm{Ce},k}(t) - i\frac{f_\nu(k)|g_\nu|^2}{\hbar^3}\frac{1}{((e_\nu-\omega_q)-i\varepsilon)((\omega_{ck}-2\omega_q)-i\varepsilon')}|\mathscr{E}(q)|^2\mathscr{E}\mathrm{e}^{-i\omega_q t}. \tag{119}$$

The solution is

$$\rho^{(3)}_{\mathrm{Ce},k}(t) = -\frac{f_\nu(k)|g_\nu|^2}{\hbar^3}\frac{1}{((e_\nu-\omega_q)-i\varepsilon)((\omega_{ck}-2\omega_q)-i\varepsilon')((\omega_{cek}-\omega_q)-i\varepsilon'')}|\mathscr{E}(q)|^2\mathscr{E}\mathrm{e}^{-i\omega_q t}. \tag{120}$$

Next, let us calculate $\rho^{(3)}_{\mathrm{Cf},k}$ through

$$\dot\rho^{(3)}_{\mathrm{Cf},k}(t) = -i\omega_{ck}\rho^{(3)}_{\mathrm{Cf},k}(t) - \frac{i}{\hbar}\langle C(k)|\,[\mathscr{H}_I+\mathscr{H}_I',\rho^{(2)}]\,|0\rangle\,. \tag{121}$$

Let us calculate

$$\begin{aligned}
&\langle C(k)|[\mathscr{H}_I,\rho^{(2)}]\,|0\rangle \\
&\quad= -\sum_{\nu'}\langle C(k)|\begin{bmatrix} \left(g_{\nu'}B^\dagger_{\nu'}\mathscr{E}(q)\mathrm{e}^{-i\omega_q t}+g^*_{\nu'}B_{\nu'}\mathscr{E}^*(q)\mathrm{e}^{i\omega_q t}\right)\rho^{(2)} \\ -\rho^{(2)}\left(g_{\nu'}B^\dagger_{\nu'}\mathscr{E}(q)\mathrm{e}^{-i\omega_q t}+g^*_{\nu'}B_{\nu'}\mathscr{E}^*(q)\mathrm{e}^{i\omega_q t}\right)\end{bmatrix}|0\rangle \\
&\quad= 0,
\end{aligned} \tag{122}$$

$$\begin{aligned}
&\langle C(k)|[\mathscr{H}_I',\rho^{(2)}]\,|0\rangle \\
&\quad= -\sum_{k',\nu'}\langle C(k)|\begin{bmatrix} \left(f_\nu(k')C^\dagger_{k'}B_{\nu'}\mathscr{E}(q)\mathrm{e}^{-i\omega_q t}+f^*_\nu(k')B^\dagger_{\nu'}C_{k'}\mathscr{E}^*(q)\mathrm{e}^{i\omega_q t}\right)\rho^{(2)} \\ -\rho^{(2)}\left(f_\nu(k')C^\dagger_{k'}B_{\nu'}\mathscr{E}(q)\mathrm{e}^{-i\omega_q t}+f^*_\nu(k')B^\dagger_{\nu'}C_{k'}\mathscr{E}^*(q)\mathrm{e}^{i\omega_q t}\right)\end{bmatrix}|0\rangle \\
&\quad= 0,
\end{aligned} \tag{123}$$

where we used the fact that the only significant term in $\rho^{(2)}$ is $\rho^{(2)}_{\mathrm{Cf},k}$. Then, we have only the free rotating term in the right hand side of equation (121). Since $\rho^{(3)}(t=-\infty)$ is zero, we obtain $\rho_{\mathrm{Cf},k}(t)=0$.

Next, let us calculate $\rho^{(3)}_{\mathrm{ef}}$ through

$$\dot\rho^{(3)}_{\mathrm{ef}}(t) = -ie_\nu\rho^{(3)}_{\mathrm{ef}}(t) - \frac{i}{\hbar}\langle \mathrm{x}_\nu|\,[\mathscr{H}_I+\mathscr{H}_I',\rho^{(2)}]\,|0\rangle\,. \tag{124}$$

Let us calculate

$$\begin{aligned}
&\langle \mathrm{x}_\nu|[\mathscr{H}_I,\rho^{(2)}]\,|0\rangle \\
&\quad=-\sum_{\nu'}\langle \mathrm{x}_\nu|\left[\begin{array}{l}\left(g_{\nu'}B^\dagger_{\nu'}\mathscr{E}(q)\mathrm{e}^{-i\omega_q t}+g^*_{\nu'}B_{\nu'}\mathscr{E}^*(q)\mathrm{e}^{i\omega_q t}\right)\rho^{(2)}\\ -\rho^{(2)}\left(g_{\nu'}B^\dagger_{\nu'}\mathscr{E}(q)\mathrm{e}^{-i\omega_q t}+g^*_{\nu'}B_{\nu'}\mathscr{E}^*(q)\mathrm{e}^{i\omega_q t}\right)\end{array}\right]|0\rangle \\
&\quad=0, \qquad (125)\\
&\langle \mathrm{x}_\nu|[\mathscr{H}'_I,\rho^{(2)}]\,|0\rangle \\
&\quad=-\sum_{k',\nu'}\langle \mathrm{x}_\nu|\left[\begin{array}{l}\left(f_\nu(k')C^\dagger_{k'}B_{\nu'}\mathscr{E}(q)\mathrm{e}^{-i\omega_q t}+f^*_\nu(k')B^\dagger_{\nu'}C_{k'}\mathscr{E}^*(q)\mathrm{e}^{i\omega_q t}\right)\rho^{(2)}\\ -\rho^{(2)}\left(f_\nu(k')C^\dagger_{k'}B_{\nu'}\mathscr{E}(q)\mathrm{e}^{-i\omega_q t}+f^*_\nu(k')B^\dagger_{\nu'}C_{k'}\mathscr{E}^*(q)\mathrm{e}^{i\omega_q t}\right)\end{array}\right]|0\rangle \\
&\quad=0, \qquad (126)
\end{aligned}$$

where we used the fact that the only significant term in $\rho^{(2)}$ is $\rho^{(2)}_{\mathrm{Cf},k}$. Hence, we obtain $\rho^{(3)}_{\mathrm{ef}}(t)=0$.

The two-photon induced current is

$$J^{(3)}=eN_e\mathrm{tr}[\mathbf{v}\rho^{(3)}]=\sum_k eN_e\mathbf{v}_{\mathrm{e}C,k}\rho^{(3)}_{\mathrm{Ce},k}+\mathrm{h.c.} \qquad (127)$$

Let us calculate

$$\begin{aligned}
\mathbf{v}_{\mathrm{e}C,k}&=\langle x_\nu|\,\dot{r}\,|C(k)\rangle=-\frac{i}{\hbar}\langle x_\nu|\,[r,\mathscr{H}_0]\,|C(k)\rangle=-i\omega_{cek}\langle \mathrm{x}_\nu|\,r\,|C(k)\rangle \\
&=-i\omega_{cek}\sum_{k'}\psi^*_\nu(k')\left\langle c(k')\right|r\,|c(k)\rangle\,. \qquad (128)
\end{aligned}$$

From this, we obtain

$$J^{(3)}=i\sum_k\left(\begin{array}{l}\frac{N_e\omega_{cek}|f_\nu(k)|^2|g_\nu|^2}{\hbar^3}\\ \times\frac{1}{((e_\nu-\omega_q)-i\varepsilon)((\omega_{ck}-2\omega_q)-i\varepsilon')((\omega_{cek}-\omega_q)-i\varepsilon'')}|\mathscr{E}(q)|^2\hat{\boldsymbol{\varepsilon}}\mathscr{E}\mathrm{e}^{-i\omega_q t}\end{array}\right)+\mathrm{h.c.}. \qquad (129)$$

Then, from $\widetilde{J}^{(3)}_{TP}=\sigma^{(3)}_{TP}|\mathscr{E}(q)|^2\hat{\boldsymbol{\varepsilon}}\mathscr{E}(q)\mathrm{e}^{-i\omega_q t}$, we obtain

$$\sigma^{(3)}_{TP}=i\sum_k\frac{N_e\omega_{cek}|f_\nu(k)|^2|g_\nu|^2}{\hbar^3}\frac{1}{((e_\nu-\omega_q)-i\varepsilon)((\omega_{ck}-2\omega_q)-i\varepsilon')((\omega_{cek}-\omega_q)-i\varepsilon'')}. \qquad (130)$$

The two-photon susceptibility is obtained through

$$\frac{\partial}{\partial t}\varepsilon_0\chi^{(3)}_{TP}(\omega_q)|\mathscr{E}(q)|^2\mathscr{E}(q)\mathrm{e}^{-i\omega_q t}=\sigma^{(3)}_{TP}|\mathscr{E}(q)|^2\mathscr{E}(q)\mathrm{e}^{-i\omega_q t}. \qquad (131)$$

Therefore, the relation is

$$\chi^{(3)}_{TP}(\omega_q)=\frac{\sigma^{(3)}_{TP}}{-i\varepsilon_0\omega_q}. \qquad (132)$$

From this, we finally obtain the two-photon susceptibility

$$\boxed{\chi^{(3)}_{TP}(\omega_q\sim e_\nu/2)=-\sum_k\frac{\omega_{cek}N_e|f_\nu(k)|^2|g_\nu|^2}{\omega_q\varepsilon_0\hbar^3}\frac{1}{((e_\nu-\omega_q)-i\varepsilon)((\omega_{ck}-2\omega_q)-i\varepsilon')((\omega_{cek}-\omega_q)-i\varepsilon'')}.} \qquad (133)$$

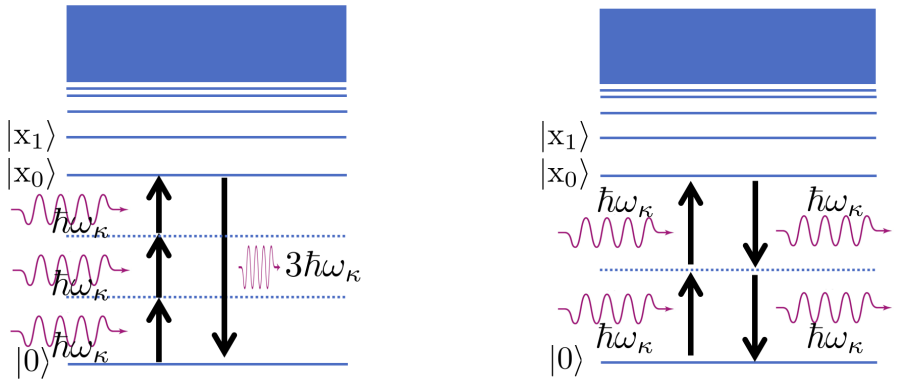

(a) Third harmonic (b) Two-photon

Figure 5: Third-order processes with low frequency input light. (a) Third harmonic generation where $3\omega_q \sim e_0$. (b) Two photon process where $2\omega_q \sim e_0$.

2.4.3.2 Low frequency third order processes We now consider the situation where $3\omega_q \sim e_\nu$, which is the third-harmonic generation process with a low frequency input field. Recall that the previous high-frequency third harmonic involved the cascaded process $|0\rangle \to |x_\nu\rangle \to |C(k)\rangle \to |C'(k)\rangle$. The low frequency third harmonic involves two virtual levels such that $|0\rangle \to |x_{\nu_1}\rangle \to |x_{\nu_2}\rangle \to |x_\nu\rangle$, where $\nu_1 \neq 0$ and $\nu_2 \neq \nu_1, \nu_2 \neq 0$. Hence, the dipole moments are analogous as $g_\nu \to g_{\nu_1}$, $f_\nu(k) \to h_{\nu_2\nu_1}$, $d_{c'c}(k) \to h_{\nu\nu_2}$, $d_{c'\nu}(k) \to g_\nu$. Then, analogous to equation (115), we easily obtain

$$\boxed{\chi^{(3)}_{TH}(\omega_q \sim e_\nu/3) = \sum_{\nu_1,\nu_2} \left(\frac{\frac{e_\nu N_e h_{\nu_2\nu_1} h_{\nu\nu_2} g_{\nu_1} g^*_\nu}{3\omega_q \varepsilon_0 \hbar^3}}{\big((e_{\nu_1} - \omega_q) - i\varepsilon_{\nu_1}\big)\big((e_{\nu_2} - 2\omega_q) - i\varepsilon_{\nu_2}\big)\big((e_\nu - 3\omega_q) - i\varepsilon_\nu\big)} \right),} \tag{134}$$

where for clarity

$$h_{\nu\nu'} = e\langle x_\nu | r\cdot\hat{\varepsilon}\,|x_{\nu'}\rangle = \sum_{k,k'} \psi^*_\nu(k)\psi_{\nu'}(k')d_{cc}(k,k') = \sum_k \psi^*_\nu(k) f_{\nu'}(k). \tag{135}$$

Lastly we calculate the two photon process for the low frequency input field. Let us generalize the case such that the upper level involved in the two-photon process is $|\psi_\nu\rangle$, instead of $|\psi_0\rangle$. Recall that the high-frequency two-photon process involved the transition $|0\rangle \to |x_\nu\rangle \to |C(k)\rangle \to |x_\nu\rangle \to |0\rangle$. The low-frequency two photon process involves the transition $|0\rangle \to |x_{\nu_1}\rangle \to |x_\nu\rangle \to |x_{\nu_2}\rangle \to |0\rangle$. Then, the role of dipole moments are related as $g_\nu \leftrightarrow g_{\nu_1}$, $f_\nu(k) \leftrightarrow h_{\nu\nu_1}$, $f^*_\nu(k) \leftrightarrow h^*_{\nu_2\nu}$, and $g^*_\nu \leftrightarrow g^*_{\nu_2}$. Therefore, we obtain

$$\boxed{\begin{aligned}&\chi^{(3)}_{TP}(\omega_q \sim e_\nu/2) \\ &= -\sum_{\nu_1,\nu_2} \left(\begin{array}{c} \frac{(e_\nu - e_{\nu_2}) N_e g_{\nu_1} h_{\nu\nu_1} h^*_{\nu\nu_2} g^*_{\nu_2}}{\omega_q \varepsilon_0 \hbar^3} \\ \times \frac{1}{\big((e_{\nu_1} - \omega_q) - i\varepsilon_{\nu_1}\big)\big((e_\nu - 2\omega_q) - i\varepsilon_\nu\big)\big((e_\nu - e_{\nu_2} - \omega_q) - i\varepsilon_{\nu_2}\big)} \end{array} \right).\end{aligned}} \tag{136}$$

$\chi^{(1)}(\omega)$	$\sum_\nu \frac{e_\nu \lvert g_\nu\rvert^2 N_e}{\hbar\varepsilon_0\omega_q}\frac{1}{(e_\nu-\omega_q)-i\varepsilon}$
$\chi^{(2)}(\omega_q\sim e_\nu)$	$\sum_\nu \frac{N_e g_\nu}{2\varepsilon_0\hbar^2\omega_q}\left(\frac{1}{(e_\nu-\omega_q)-i\varepsilon}\right)\left(\sum_k \frac{f_\nu(k)\omega_k d^*_{cv}(k)}{(\omega_k-2\omega_q)-i\varepsilon'}\right)$
$\chi^{(2)}(\omega_q\sim e_\nu/2)$	$\sum_{\nu'\neq\nu} \frac{e_\nu N_e g_{\nu'} h_{\nu\nu'} g^*_\nu}{2\omega_q\varepsilon_0\hbar^2}\left(\frac{1}{\big((e_{\nu'}-\omega_q)-i\varepsilon_{\nu'}\big)\big((e_\nu-2\omega_q)-i\varepsilon_\nu\big)}\right)$
$\chi^{(3)}_{TH}(\omega_q\sim e_\nu)$	$\sum_{k,k'\nu}\left(\begin{array}{l}\frac{\omega_{c'k}N_e f_\nu(k')d_{c'c}(k',k)g_\nu d^*_{c'\nu}(k')}{3\omega_q\varepsilon_0\hbar^3}\\ \times\frac{1}{\big((e_\nu-\omega_q)-i\varepsilon\big)\big((\omega_{ck}-2\omega_q)-i\varepsilon'\big)\big((\omega_{c'k'}-3\omega_q)-i\varepsilon''\big)}\end{array}\right)$
$\chi^{(3)}_{TH}(\omega_q\sim e_\nu/3)$	$\sum_{\nu,\nu_1,\nu_2}\left(\begin{array}{l}\frac{e_\nu N_e h_{\nu_2\nu_1}h_{\nu\nu_2}g_{\nu_1}g^*_\nu}{3\omega_q\varepsilon_0\hbar^3}\\ \frac{1}{\big((e_{\nu_1}-\omega_q)-i\varepsilon_{\nu_1}\big)\big((e_{\nu_2}-2\omega_q)-i\varepsilon_{\nu_2}\big)\big((e_\nu-3\omega_q)-i\varepsilon_\nu\big)}\end{array}\right)$
$\chi^{(3)}_{TP}(\omega_q\sim e_\nu)$	$-\sum_{k,\nu}\frac{\omega_{cek}N_e\lvert f_\nu(k)\rvert^2\lvert g_\nu\rvert^2}{\omega_q\varepsilon_0\hbar^3}\frac{1}{((e_\nu-\omega_q)-i\varepsilon)((\omega_{ck}-2\omega_q)-i\varepsilon')((\omega_{cek}-\omega_q)-i\varepsilon'')}$
$\chi^{(3)}_{TP}(\omega_q\sim e_\nu/2)$	$-\sum_{\nu,\nu_1,\nu_2}\left(\begin{array}{l}\frac{(e_\nu-e_{\nu_2})N_e g_{\nu_1}h_{\nu\nu_1}h^*_{\nu\nu_2}g^*_{\nu_2}}{\omega_q\varepsilon_0\hbar^3}\\ \times\frac{1}{\big((e_{\nu_1}-\omega_q)-i\varepsilon_{\nu_1}\big)\big((e_\nu-2\omega_q)-i\varepsilon_\nu\big)\big((e_\nu-e_{\nu_2}-\omega_q)-i\varepsilon_{\nu_2}\big)}\end{array}\right)$

Table 2: Summary of calculated exciton susceptibilities

2.5 Summary

We summarized the calculated susceptibilities in table 2. Note that we calculated the nonlinear susceptibilities for a fixed exciton order ν. For the actual spectra, however, we have to sum over all ν such that the form now become a general solution for any ω_q.

3. Calculation of various transition dipole moments

3.1 Massive Dirac cone approximation

The DFT calculation results show that the conduction band and the valence band around the $K, -K$ points are dominated by the atomic orbitals of the Mo atom [11]. Particularly, when we can write the Bloch state as

$$\psi_{k,\lambda}(r) = \mathrm{e}^{ik\cdot r} u_{k,\lambda}(r), \tag{137}$$

where $\lambda = c, v$ is the band index, and $uk, \lambda(r)$ is the Bloch function having the periodicity such that $u_{k,\lambda}(r+R) = u_{k,\lambda}(r)$ for any lattice vector R, one can approximate

$$u_{0,\lambda}(r) = \frac{1}{\sqrt{N}} \sum_m \mathrm{e}^{ik\cdot(R_m - r)} \phi_\lambda(r - R_m), \tag{138}$$

where

$$\phi_c(r) = \langle r|\phi_c\rangle = \left\langle r|d_{z^2}\right\rangle, \quad \phi_v(r) = \langle r|\phi_v\rangle = \frac{1}{\sqrt{2}}\left(\left\langle r|d_{x^2-y^2}\right\rangle + i\tau\left\langle r|d_{xy}\right\rangle\right), \tag{139}$$

with the valley index $\tau = \pm 1$ for $K, -K$ points, respectively. Here, $\left|d_{z^2}\right\rangle, \left|d_{x^2-y^2}\right\rangle, \left|d_{xy}\right\rangle$ are the 4d shell atomic orbitals of the Mo atom.

Using these two basis $\{\left|d_{z^2}\right\rangle, (1/\sqrt{2})(\left|d_{x^2-y^2}\right\rangle + i\tau\left|d_{xy}\right\rangle)\}$, one constructs the four tensor state basis $\{|\phi_c\rangle \otimes |\uparrow\rangle, |\phi_c\rangle \otimes |\downarrow\rangle, |\phi_v\rangle \otimes |\uparrow\rangle, |\phi_v\rangle \otimes |\downarrow\rangle\}$. Then, the Hamiltonian around the $K, -K$ points is approximately [25]:

$$H_\tau = \left(\hbar v(\tau q_x \sigma_x + q_y \sigma_y) + \frac{E_g}{2}\sigma_z\right) \otimes I_2 + \tau \frac{(1-\sigma_z)}{2} \otimes \frac{E_{\mathrm{soc}}}{2}\sigma_z, \tag{140}$$

where $(q_x, q_y) = k - (\pm K)$ is the differential crystal momentum around $\pm K$ points, E_g is the inter-band bandgap energy, and E_{soc} is the spin-orbit coupling split energy. Here, v is the Fermi velocity and, DFT calculation found $v \approx 5.8 \times 10^5$ m/s [17]. In matrix form,

$$H_\tau = \begin{pmatrix} E_g/2 & 0 & \hbar v(\tau q_x - i q_y) & 0 \\ 0 & E_g/2 & 0 & \hbar v(\tau q_x - i q_y) \\ \hbar v(\tau q_x + i q_y) & 0 & -E_g/2 + \tau E_{\mathrm{soc}}/2 & 0 \\ 0 & \hbar v(\tau q_x + i q_y) & 0 & -E_g/2 - \tau E_{\mathrm{soc}}/2 \end{pmatrix} \tag{141}$$

Let us focus on a particular valley τ. Also let us assume that our driving optical frequency is nearly at resonance with only one spin transition. Then, the state lives in the subspace spanned by $\{|\phi_c\rangle, |\phi_v\rangle\}$ with a particular spin. Let us also denote $\Delta = E_g + \tau E_{\mathrm{soc}}$ for the up spin and $\Delta = E_g - \tau E_{\mathrm{soc}}$ for the down spin, describing the bandgap energy between the valence and the conduction band for a particularly chosen spin. Then, the Hamiltonian in this subspace is

$$H = \begin{pmatrix} \Delta/2 & \hbar v(\tau q_x - i q_y) \\ \hbar v(\tau q_x + i q_y) & -\Delta/2 \end{pmatrix}. \tag{142}$$

According to the detailed DFT calculation [12], the numerical values are $\hbar v = 3.82$ eV Å(i.e., $v = 5.8 \times 10^5$ m/s), $E_g = 2.23$ eV (DFT-HSE06) [17] (and experimentally measured as 2.15 eV [27]), and $E_{\rm soc} \approx 146$ meV. Also it is noteworthy that the effective mass from the DFT band calculation is found to be $m^c_{\rm eff}/m_e = 0.48$ and $m^v_{\rm eff}/m_e = -0.62$ where m_e is the electron mass.

The eigenvalues of the Hamiltonian is easily obtained to be

$$E_\gamma(q) = \gamma\sqrt{\left(\frac{\Delta}{2}\right)^2 + \hbar^2 v^2 q^2}. \tag{143}$$

where $q = \sqrt{q_x^2 + q_y^2}$, and $\gamma = +1$ for the conduction band, and $\gamma = -1$ for the valence band. To calculate the eigenvectors, let us slightly modify such that

$$\hbar v(\tau q_x \mp i q_y) = \hbar v \tau (q_x \mp i\tau q_y) = \hbar v \tau q \mathrm{e}^{\mp i\tau\phi_q}, \tag{144}$$

where $\tan\phi_q = q_y/q_x$ is the phase of q. Let us set the eigenvector to be $(x,y)^T$. Then, the equation for the eigenvector is

$$\begin{pmatrix} \Delta/2 & \hbar v\tau q \mathrm{e}^{-i\tau\phi_q} \\ \hbar v\tau q \mathrm{e}^{+i\tau\phi_q} & -\Delta/2 \end{pmatrix} \begin{pmatrix} x \\ y \end{pmatrix} = \gamma\sqrt{\left(\frac{\Delta}{2}\right)^2 + \hbar^2 v^2 q^2} \begin{pmatrix} x \\ y \end{pmatrix}. \tag{145}$$

This equation is equivalent to

$$\begin{aligned} \frac{\Delta/2}{\sqrt{\left(\frac{\Delta}{2}\right)^2 + \hbar^2 v^2 q^2}} x + \frac{\hbar v\tau q \mathrm{e}^{-i\tau\phi_q}}{\sqrt{\left(\frac{\Delta}{2}\right)^2 + \hbar^2 v^2 q^2}} y &= \gamma x, \\ \frac{\hbar v\tau q \mathrm{e}^{i\tau\phi_q}}{\sqrt{\left(\frac{\Delta}{2}\right)^2 + \hbar^2 v^2 q^2}} x - \frac{\Delta/2}{\sqrt{\left(\frac{\Delta}{2}\right)^2 + \hbar^2 v^2 q^2}} y &= \gamma y. \end{aligned} \tag{146}$$

Multiplying γ on both sides of the second equation above, we obtain

$$\begin{aligned} \frac{\Delta/2}{\sqrt{\left(\frac{\Delta}{2}\right)^2 + \hbar^2 v^2 q^2}} x + \frac{\hbar v\tau q \mathrm{e}^{-i\tau\phi_q}}{\sqrt{\left(\frac{\Delta}{2}\right)^2 + \hbar^2 v^2 q^2}} y &= \gamma x, \\ \gamma\frac{\hbar v\tau q \mathrm{e}^{i\tau\phi_q}}{\sqrt{\left(\frac{\Delta}{2}\right)^2 + \hbar^2 v^2 q^2}} x - \gamma\frac{\Delta/2}{\sqrt{\left(\frac{\Delta}{2}\right)^2 + \hbar^2 v^2 q^2}} y &= y. \end{aligned} \tag{147}$$

Let us set

$$\cos\theta_{\gamma,q} = \gamma\frac{\Delta/2}{\sqrt{\left(\frac{\Delta}{2}\right)^2 + \hbar^2 v^2 q^2}}, \quad \sin\theta_{\gamma,q} = \frac{\hbar v q}{\sqrt{\left(\frac{\Delta}{2}\right)^2 + \hbar^2 v^2 q^2}}. \tag{148}$$

Then, the above equation is

$$\begin{aligned} \gamma x\cos\theta_{\gamma,q} + \tau y \mathrm{e}^{-i\tau\phi_q}\sin\theta_{\gamma,q} &= \gamma x, \\ \gamma\tau x \mathrm{e}^{+i\tau\phi_q}\sin\theta_{\gamma,q} - y\cos\theta_{\gamma,q} &= y. \end{aligned} \tag{149}$$

A slight modification to make the following:

$$\begin{aligned}\gamma x e^{+i\tau\phi_q/2}\cos\theta_{\gamma,q}+\tau y e^{-i\tau\phi_q/2}\sin\theta_{\gamma,q}&=\gamma x e^{+i\tau\phi_q/2},\\ \gamma x e^{+i\tau\phi_q/2}\sin\theta_{\gamma,q}-\tau y e^{-i\tau\phi_q/2}\cos\theta_{\gamma,q}&=\tau y e^{-i\tau\phi_q/2}.\end{aligned} \tag{150}$$

The above is solved by

$$\begin{pmatrix} x \\ y \end{pmatrix} = \begin{pmatrix} \gamma\cos(\theta_{\gamma,q}/2)e^{-i\tau\phi_q/2} \\ \tau\sin(\theta_{\gamma,q/2})e^{i\tau\phi_q/2} \end{pmatrix} \tag{151}$$

In summary, we obtained the energy eigenvalues and the energy eigenvectors as

$$\begin{aligned}E_\gamma(q)&=\gamma\sqrt{\left(\frac{\Delta}{2}\right)^2+\hbar^2v^2q^2},\\ |\lambda(q)\rangle&=\begin{pmatrix} \gamma\cos(\theta_{\gamma,q}/2)e^{-i\tau\phi_q/2} \\ \tau\sin(\theta_{\gamma,q}/2)e^{i\tau\phi_q/2} \end{pmatrix},\end{aligned} \tag{152}$$

where $\lambda = c, v$ is the band index, and $\gamma = 1$ for $\lambda = c$, and $\gamma = -1$ for $\lambda = v$.

Since $\psi_v(q)$ is significant only up to $1/a_0$ where $a_0/2 \sim 10$ Å is the Bohr radius of the exciton, it is expected that only a small portion of q in the FBZ will participate in the exciton formation. Then, one can assume that $\hbar vq \ll \Delta/2$, which allows for the perturbative expansion of the energy and the eigenvectors up to the second order:

$$E_\gamma(q) \approx \gamma\left(\frac{\Delta}{2}+\frac{\hbar^2v^2q^2}{\Delta}\right). \tag{153}$$

Then, the eigenvector equation is

$$\begin{aligned}\left(\frac{1}{2}(1-\gamma)-\gamma\frac{\hbar^2v^2q^2}{\Delta^2}\right)x+\frac{\hbar vq\tau}{\Delta}e^{-i\tau\phi_q}y&=0,\\ \frac{\hbar vq\tau}{\Delta}e^{+i\tau\phi_q}x-\left(\frac{1}{2}(1+\gamma)+\gamma\frac{\hbar^2v^2q^2}{\Delta^2}\right)y&=0.\end{aligned} \tag{154}$$

For $\gamma = 1$ (conduction band), we have

$$\begin{aligned}-\frac{\hbar^2v^2q^2}{\Delta^2}x+\frac{\hbar vq\tau}{\Delta}e^{-i\tau\phi_q}y&=0,\\ \frac{\hbar vq\tau}{\Delta}e^{+i\tau\phi_q}x-\left(1+\frac{\hbar^2v^2q^2}{\Delta^2}\right)y&=0.\end{aligned} \tag{155}$$

This has a solution that is correct up to the second order of q:

$$|u_{q,c}\rangle = \begin{pmatrix} x \\ y \end{pmatrix} = \begin{pmatrix} 1-\frac{\hbar^2v^2q^2}{\Delta^2} \\ \frac{\hbar vq\tau}{\Delta}e^{i\tau\phi_q} \end{pmatrix}. \tag{156}$$

For $\gamma = -1$ (valence band), we have

$$\left(1 + \frac{\hbar^2 v^2 q^2}{\Delta^2}\right) x + \frac{\hbar v q \tau}{\Delta} \mathrm{e}^{-i\tau\phi_q} y = 0,$$
$$\frac{\hbar v q \tau}{\Delta} \mathrm{e}^{i\tau\phi_q} x + \frac{\hbar^2 v^2 q^2}{\Delta^2} y = 0. \tag{157}$$

This has a solution that is correct up to the second order of q:

$$\left|u_{q,v}\right\rangle = \begin{pmatrix} x \\ y \end{pmatrix} = \begin{pmatrix} -\frac{\hbar v q \tau}{\Delta} \mathrm{e}^{-i\tau\phi_q} \\ 1 - \frac{\hbar^2 v^2 q^2}{\Delta^2} \end{pmatrix} \tag{158}$$

In summary, the approximate perturbative solution up to the second order of q is

$$\boxed{\begin{aligned} E_\gamma(q) &= \gamma\left(\frac{\Delta}{2} + \frac{\hbar^2 v^2 q^2}{\Delta}\right), \\ \left|u_{q,c}\right\rangle &= \left(1 - \frac{\hbar^2 v^2 q^2}{\Delta^2}\right)\left|u_{0,c}\right\rangle + \frac{\hbar v q \tau}{\Delta} \mathrm{e}^{i\tau\phi_q}\left|u_{0,v}\right\rangle, \\ \left|u_{q,v}\right\rangle &= -\frac{\hbar v q \tau}{\Delta} \mathrm{e}^{-i\tau\phi_q}\left|u_{0,c}\right\rangle + \left(1 - \frac{\hbar^2 v^2 q^2}{\Delta^2}\right)\left|u_{0,v}\right\rangle. \end{aligned}} \tag{159}$$

3.2 Higher order correction

There is a discrepancy between the DFT calculation results and the Dirac cone approximation in terms of effective mass and the actual band curvatures. Zhang et al. [26] and Kormanyos et al. [12] added a higher order correction to the Hamiltonian in equation (142) the following term:

$$\begin{pmatrix} \alpha q^2 & \kappa(q_x + i\tau q_y)^2 - \frac{\eta}{2} q^2 (q_x - i\tau q_y) \\ \kappa(q_x - i\tau q_y)^2 - \frac{\eta}{2} q^2 (q_x + i\tau q_y) & \beta q^2 \end{pmatrix}, \tag{160}$$

where the numerical values of the parameter based on the DFT calculations are $\alpha = 1.72$ eV Å^2, $\beta = -0.13$ eV Å^2, $\kappa = -1.02$ eV Å^2, and $\eta = 8.52$ eV Å^3.

Recall that we are mostly interested in the region around the Dirac cones where the direct bandgap occurs. Particularly we are interested within $|q| < 1$ rad/Å region where the exciton envelope wavefunction $\psi_\nu(q)$ is significant. Figure 6 shows some difference in the band structure between the second-order perturbative solution in equation (159) and the numerically calculated energy eigenvalues from the higher-order corrected Hamiltonian using equation (160). Certainly what is shown in the figure is that the higher-order corrected numerical solution has a larger valence band effective mass than the conduction band.

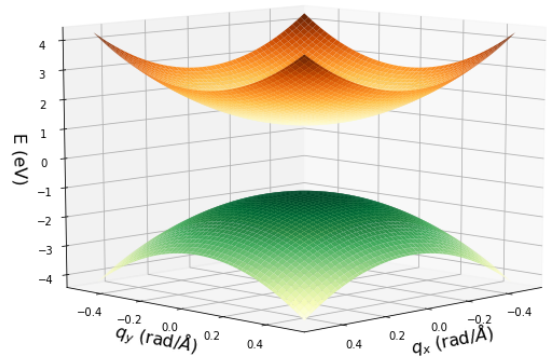

(a) Perturbative

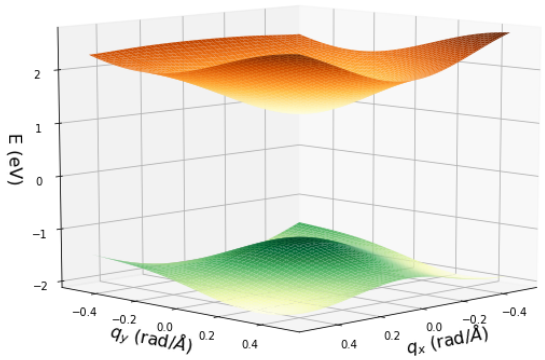

(b) HOC numerical

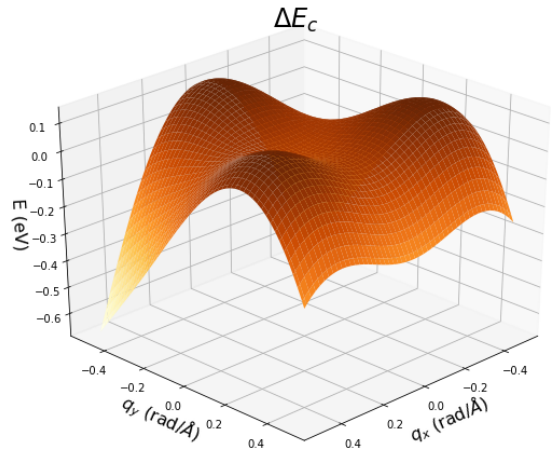

(c) $\Delta Ec(q)$

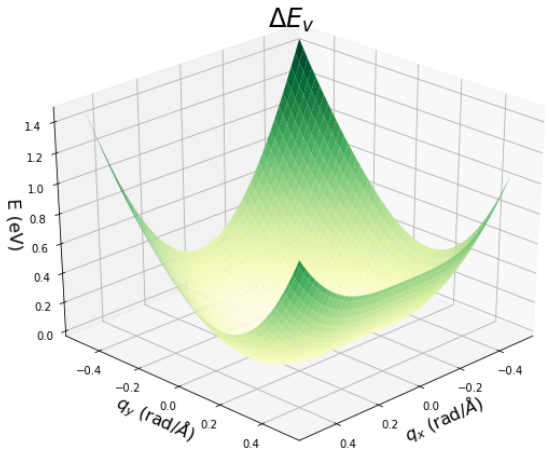

(d) $\Delta Ev(q)$

Figure 6: Comparison of band energy dispersion of (a) the perturbative analytical solution (159), (b) the higher-order corrected (HOC) numerical solution. Also shown are the differences between the two (c) the conduction band, and (d) the valence band.

3.3 Dipole moment calculation

3.3.1 Analytical solution and comparison with numerical solution

To calculate the dipole moment, we use the well known Blount formula [1]:

$$\left\langle \psi_{k,\lambda} \middle| r \middle| \psi_{k',\lambda'} \right\rangle = -i\nabla_k \left\langle \psi_{k,\lambda} \middle| \psi_{k',\lambda'} \right\rangle + i\delta_{k,k'} \left\langle u_{k,\lambda} \middle| \nabla_k \middle| u_{k,\lambda'} \right\rangle, \tag{161}$$

where the first term on the right hand side describes the contribution from the phase term in case $k = k', \lambda = \lambda'$. Unless there is discontinuity in $\left|\psi_{k,\lambda}\right\rangle$ with respect to k such as Riemann sheet

branch cuts, the first term is ignorable. Then, most of the cases we have

$$\left\langle \psi_{k,\lambda} \right| r \left| \psi_{k',\lambda'} \right\rangle = i\delta_{k,k'} \left\langle u_{k,\lambda} \right| \nabla_k \left| u_{k,\lambda'} \right\rangle. \tag{162}$$

Putting $k = k'$ and $\lambda = c, \lambda' = v$, we obtain

$$d_{cv}(q) = e\langle c(q)|r|v(q)\rangle = ie \left\langle u_{q,c} \right| \nabla_q \left| u_{q,v} \right\rangle \tag{163}$$

From equation (159),

$$\nabla_q \left| u_{q,v} \right\rangle = \hat{x} \left(-\frac{\hbar v \tau}{\Delta} \left| u_{0,c} \right\rangle - 2\frac{\hbar^2 v^2}{\Delta^2} q_x \left| u_{0,v} \right\rangle \right) + \hat{y} \left(i\frac{\hbar v}{\Delta} \left| u_{0,c} \right\rangle - 2\frac{\hbar^2 v^2}{\Delta^2} q_y \left| u_{0,v} \right\rangle \right). \tag{164}$$

Hence,

$$\begin{aligned} d_{cv}(q) =& ie\hat{x} \left(-\frac{\hbar v \tau}{\Delta} + \frac{\hbar^3 v^3 \tau q^2}{\Delta^3} - 2\frac{\hbar^3 v^3 q \tau}{\Delta^3} q_x \mathrm{e}^{-i\tau\phi_q} \right) \\ &+ ie\hat{y} \left(i\frac{\hbar v}{\Delta} - i\frac{\hbar^3 v^3 q^2}{\Delta^3} - 2\frac{\hbar^3 v^3 q \tau}{\Delta^3} q_y \mathrm{e}^{-i\tau\phi_q} \right). \end{aligned} \tag{165}$$

This is accurate up to the second order of q around the Dirac cone. if q approaches zero, the dipole moment is proportional to the ration $\hbar v/\Delta$. The parameter v is related to the hopping strength, and therefore, the oscillation strength is proportional to the hopping strength while inversely proportional to the bandgap.

If we calculate the dipole moment elements for the σ_+ light that has a polarization $\hat{\varepsilon} = \frac{1}{\sqrt{2}}(\hat{x} + i\hat{y})$, we obtain for $\tau = 1$:

$$\boxed{d_{cv}(q) = d_{cv}(q) \cdot \hat{\varepsilon} = -i\frac{\sqrt{2}e\hbar v}{\Delta}.} \tag{166}$$

This is a correct answer up to the second order of q. Note that the second-order perturbative solution is a constant imaginary value over the region of the Dirac cones.

Figure 7 shows the numerically evaluated $d_{cv}(q)$ according to the unperturbed full Dirac cone approximated eigenvectors of the Hamiltonian in equation (142), corrected by the higher-order correction term in equation (160). Compared to the analytical value of $d_{cv}(q) = -\sqrt{2}ie\hbar v/\Delta = -3.64i \times 10^{-29}$ (C-m), using the second order perturbation result in (166), the numerically evaluated Dirac cone approximated $d_{cv}(q)$ is not much different for the $|q| < 0.1$ rad/Å, which appears to be nearly constant. Nonetheless, the higher-order corrected numerical values exhibits non-zero real values and varying imaginary values of $d_{cv}(q)$ over the Diraction region.

We also calculate g_v according to equation (28):

$$g_v = \sum_k d_{cv}(q) \psi_v^*(q). \tag{167}$$

Using the second-order perturbative result in equation (166), we then obtain

$$g_v = \left(-i\frac{\sqrt{2}e\hbar v}{\Delta} \right) \sum_q \psi_v^*(q) = \left(-i\frac{\sqrt{2}e\hbar v}{\Delta} \right) \psi_v^*(r = 0). \tag{168}$$

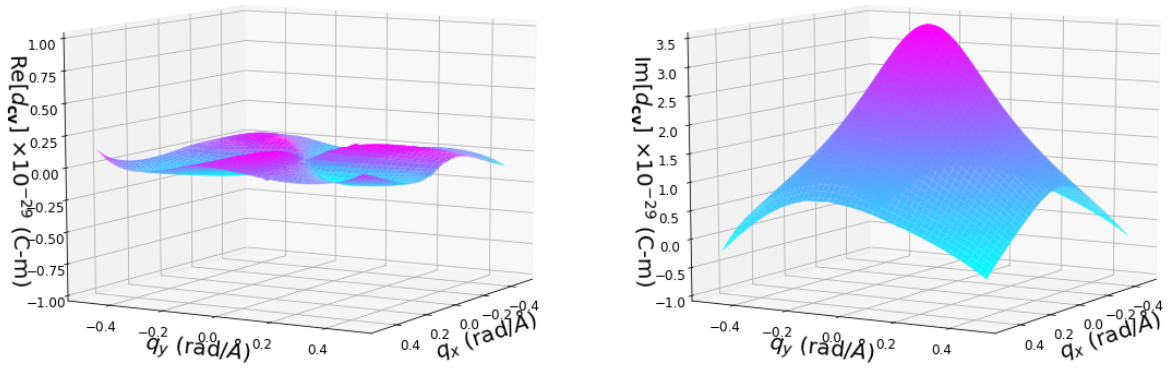

(a) Real

(b) Imaginary

Figure 7: Numerically evaluated $d_{cv}(q)$ for the σ_+ circularly polarized incoming photons, based on the second-order corrected Dirac cone approximation.

Using the result in table 1, one obtains $g_\nu = g_{n,m}$ as follows. The nonzero element occurs only for $m = 0$ since $\psi_\nu(r) \propto r$ for $m \neq 0$, and the first couple of nonzero g_ν are

$$g_{(0,0)} = -i\sqrt{\frac{A}{\pi}}\left(\frac{4e\hbar v}{a_0\Delta}\right), \quad g_{(1,0)} = -i\sqrt{\frac{A}{3\pi}}\left(\frac{4e\hbar v}{3a_0\Delta}\right), \quad g_{(2,0)} = -i\sqrt{\frac{A}{5\pi}}\left(\frac{4e\hbar v}{5\Delta a_0}\right). \tag{169}$$

It can be easily shown that

$$\boxed{g_{(n,0)} = -i\sqrt{\frac{A}{(2n+1)\pi}}\left(\frac{4e\hbar v}{(2n+1)a_0\Delta}\right).} \tag{170}$$

For the numerical evaluation based on the higher-order corrected Dirac cone approximation, we use the following conversion from sum to integral:

$$\sum_q \to \frac{A}{(2\pi)^2}\int \mathrm{d}^2 q \tag{171}$$

where we used the infinitesimal areal element $\mathrm{d}^2 q = (2\pi)^2/A$. Then, it follows that

$$g_\nu = \sum_k \psi_\nu^*(q) d_{cv}(q) = \frac{A}{(2\pi)^2}\int \mathrm{d}^2 q\ \psi_\nu^*(q) d_{cv}(q). \tag{172}$$

Table 3 shows the calculated g_ν based on the analytical solution in equation (170), on the numerical evaluation of the gapped Dirac cone Hamiltonian to obtain the eigenvectors, and on the numerical evaluation of the higher-order corrected gapped Dirac cone Hamiltonian to obtain the

ν	perturbative analytic g_ν	gapped Dirac cone g_ν	higher-order Dirac cone g_ν
$(0,0)$	$4.34i$	$2.43i$	$2.15i$
$(1,0)$	$0.84i$	$0.41i$	$0.33i$
$(2,0)$	$0.39i$	$0.19i$	$0.15i$
$(3,0)$	$0.23i$	$0.12i$	$0.10i$
$(4,0)$	$0.16i$	$0.02i$	$0.01i$

Table 3: Comparison of the calculated g_ν based on the second-order perturbative analytic solution, the numerical evaluation of the gapped Dirac cone approximation, and the higher-order corrected numerical evaluation of the gapped Dirac cone approximation. The unit is $10^{-20}/\sqrt{A}$(C-m).

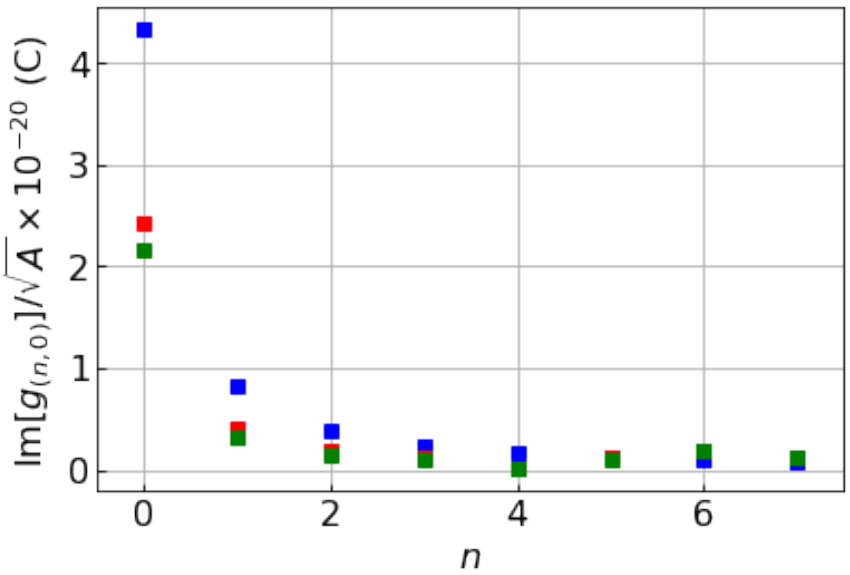

Figure 8: Comparison of the calculated g_ν for the perturbative analytic (blue), the gapped Dirac cone approximation (red), and the higher-order corrected gapped Dirac cone approximation (green).

eigenvectors. Since g_ν with $\nu = (n, m \neq 0)$ is negligible as expected since $\psi_\nu(r) \propto r$, we present only the results for $\nu = (n,0)$. It is easily seen that the perturbative analytic solution is not so accurate for the most important $\nu = (0,0)$ exciton state. In addition, the most accurate result of the numerically evaluated higher-order corrected gapped Dirac cone model shows the strong dominance of $g_{(0,0)}$ over all others. It is well expected that the exciton absorption spectra of MoS_2 would be dominated by the peak at $\omega_{(0,0)} = E_g - 4E_0/\hbar$.

Next, we calculate $f_\nu(k)$ which is given by

$$f_\nu(q) = e\sum_{q'} \psi_\nu(q') \langle c(q)| \hat{\varepsilon}\cdot r \left|c(q')\right\rangle . \tag{173}$$

Using the formula in equation (162), we calculate

$$\langle c(q)| r \left|c(q')\right\rangle = i\delta_{q,q'} \left\langle u_{q,c}\right| \nabla_q \left|u_{q,c}\right\rangle . \tag{174}$$

Let us calculate

$$\nabla_q \left|u_{q,c}\right\rangle = \hat{x}\left(-\frac{2\hbar^2 v^2 q_x}{\Delta^2}\left|u_{0,c}\right\rangle + \frac{\hbar v\tau}{\Delta}\left|u_{0,v}\right\rangle\right) + \hat{y}\left(-\frac{2\hbar^2 v^2 q_y}{\Delta^2}\left|u_{0,c}\right\rangle + i\frac{\hbar v}{\Delta}\left|u_{0,v}\right\rangle\right) \tag{175}$$

Then, we obtain

$$\begin{aligned}\left\langle u_{q,c}\right| \nabla_q \left|u_{q,c}\right\rangle &= \hat{x}\left(-\frac{2\hbar^2 v^2 q_x}{\Delta^2} + \frac{\hbar^2 v^2}{\Delta^2}(q_x - i\tau q_y)\right) + \hat{y}\left(-\frac{2\hbar^2 v^2 q_y}{\Delta^2} + i\frac{\hbar^2 v^2 \tau}{\Delta^2}(q_x - i\tau q_y)\right) \\ &= \hat{x}\left(-\frac{\hbar^2 v^2}{\Delta^2} q e^{i\tau\phi_q}\right) + \hat{y}\left(i\frac{\hbar^2 v^2 \tau}{\Delta^2} q e^{i\tau\phi_q}\right)\end{aligned} \tag{176}$$

Hence, we obtain

$$d_{cc}(q) = ie\hat{x}\left(-\frac{\hbar^2 v^2}{\Delta^2} q e^{i\tau\phi_q}\right) - e\hat{y}\left(\frac{\hbar^2 v^2 \tau}{\Delta^2} q e^{i\tau\phi_q}\right). \tag{177}$$

for σ_+ light with $\hat{\varepsilon} = \hat{x} + i\hat{y}$, we obtain

$$d_{cc}(q) = d_{cc}(q)\cdot\hat{\varepsilon} = -ie(1+\tau)\frac{\hbar^2 v^2}{\Delta^2} q e^{i\tau\phi_q}. \tag{178}$$

Therefore, we obtain

$$\boxed{f_v(q) = -ie\psi_v(q)(1+\tau)\frac{\hbar^2 v^2}{\Delta^2} q e^{i\tau\phi_q}.} \tag{179}$$

It is noteworthy that $f_v(q)$ and $d_{cc}(q)$ both exhibit the selection rule where $\sigma+$ light works for $\tau = 1$ valley and $\sigma-$ light works for $\tau = -1$ valley, but not cross.

Next, let us calculate h_{v0} which is given by

$$h_{v0} = e\left\langle \mathrm{x}_v\right| r\cdot\hat{\varepsilon}\left|\mathrm{x}_0\right\rangle. \tag{180}$$

Using the closure in equation (188), we calculate for the case of $\sigma+$ light with a circular polarization $\hat{\varepsilon} = \hat{x} + i\hat{y}$:

$$\begin{aligned}h_{v0} &= e\int \frac{\mathrm{d}^2 r}{A}\left\langle \mathrm{x}_v|r\right\rangle\left\langle r\right| r\cdot\hat{\varepsilon}\left|\mathrm{x}_0\right\rangle = e\int \frac{\mathrm{d}^2 r}{A}\psi_v^*(r)(r\cdot\hat{\varepsilon})\psi_0(r) \\ &= e\int \frac{\mathrm{d}x\mathrm{d}y}{A}\psi_v^*(x,y)(x+iy)\psi_0(x,y) \\ &= \frac{e}{A}\int_0^\infty r\mathrm{d}r\int_0^{2\pi}\mathrm{d}\phi\,\psi_v^*(r,\phi) r e^{i\phi}\psi_0(r,\phi).\end{aligned} \tag{181}$$

Note that this produces a natural selection rule that for $\sigma+$ light only the transition $\left|\mathrm{x}_{0,0}\right\rangle \leftrightarrow \left|\mathrm{x}_{n,1}\right\rangle$ is allowed due to the ϕ integral. We obtain h_{v0} using the wavefunction of the bound excitons in

table 1:

$$
\begin{aligned}
&h_{(1,1)(0,0)} = \frac{9}{32}\sqrt{\frac{3}{2}}|e|a_0, \quad h_{(1,0)(0,0)} = h_{(1,-1)(0,0)} = 0, \\
&h_{(2,1)(0,0)} = \frac{25}{162}\sqrt{\frac{5}{6}}|e|a_0, \quad h_{(2,-2)(0,0)} = h_{(2,-1)(0,0)} = h_{(2,0)(0,0)} = h_{(2,2)(0,0)} = 0, \\
&h_{(3,1)(0,0)} = \frac{147\sqrt{21}}{8192}|e|a_0, \quad h_{(4,1)(0,0)} = \frac{1944}{15625\sqrt{5}}|e|a_0, \quad h_{(5,1)(0,0)} = \frac{15125}{1119744}\sqrt{\frac{55}{6}}|e|a_0, \\
&h_{(6,1)(0,0)} = \frac{54756}{5764801}\sqrt{\frac{78}{7}}|e|a_0, \quad h_{(7,1)(0,0)} = \frac{3781575}{1073741824}\sqrt{\frac{105}{2}}|e|a_0, \quad \cdots
\end{aligned} \tag{182}
$$

so on. Note that $h_{\nu 0}$ keeps reducing as ν increases, and $h_{(6,1)(0,0)}$ is about ten times smaller than $h_{(1,1)(0,0)}$.

Finally, $h_{\nu_1\nu_2}$ for $\sigma+$ light, which is defined as

$$
h_{\nu_1\nu_2} = e\,\langle \mathrm{x}_{\nu_1}|\, r\cdot\hat{\varepsilon}\,|\mathrm{x}_{\nu_2}\rangle \tag{183}
$$

is similarly calculated:

$$
h_{\nu_1\nu_2} = \frac{e}{A}\int_0^\infty r\mathrm{d}r\int_0^{2\pi}\mathrm{d}\phi\,\psi^*_{\nu_1}(r,\phi)re^{i\phi}\psi_{\nu_2}(r,\phi). \tag{184}
$$

According to the selection rule due to ϕ integration, the first few that are not zero are:

$$
\begin{aligned}
&h_{(1,-1)(2,-2)} = \frac{10125\sqrt{5}}{8192}|e|a_0, \quad h_{(1,0)(2,-1)} = \frac{2025}{2048}\sqrt{\frac{5}{2}}|e|a_0, \quad h_{(1,1)(2,0)} = \frac{1125}{4096}\sqrt{\frac{15}{2}}|e|a_0, \\
&h_{(1,-1)(3,-2)} = \frac{27783}{31250}\sqrt{\frac{7}{5}}|e|a_0, \quad h_{(1,0)(3,-1)} = \frac{3969\sqrt{7}}{15625}|e|a_0, \quad h_{(1,1),(3,0)} = \frac{3087}{31250}\sqrt{\frac{21}{2}}|e|a_0, \\
&h_{(2,-2)(3,-3)} = \frac{7503125}{1119744}\sqrt{\frac{7}{6}}|e|a_0, \\
&h_{(2,-1)(3,-2)} = \frac{1071875\sqrt{7}}{559872}|e|a_0, \quad h_{(2,0)(3,-1)} = \frac{373625}{373248}\sqrt{\frac{35}{3}}|e|a_0, \\
&h_{(2,1)(3,0)} = \frac{248675}{279936}\sqrt{\frac{35}{6}}|e|a_0, \quad h_{(2,2)(3,1)} = \frac{300125}{1119744}\sqrt{\frac{35}{2}}|e|a_0,
\end{aligned} \tag{185}
$$

so on.

ν_1	ν_2	$h_{\nu_1\nu_2}$
$(1,-1)$	$(2,-2)$	2.76
$(1,-1)$	$(3,-2)$	1.05
$(1,0)$	$(2,-1)$	1.56
$(1,0)$	$(3,-1)$	0.67
$(1,1)$	$(2,0)$	0.75
$(1,1)$	$(3,0)$	0.32
$(2,-2)$	$(3,-3)$	7.24
$(2,-1)$	$(3,-2)$	5.07
$(2,0)$	$(3,-1)$	3.42
$(2,1)$	$(3,0)$	2.15
$(2,2)$	$(3,1)$	1.12

Table 4: Calculated $h_{\nu_1\nu_2}$. The unit is ea_0 (C-m). For MoS_2, $a_0 = 6.0$ Å.

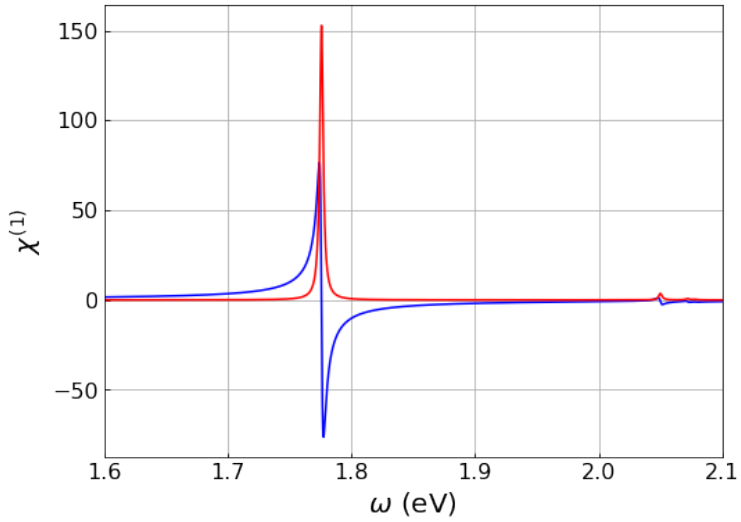

Figure 9: Numerically evaluated $\chi^{(1)}$ based on the higher-order corrected Dirac cone approximation. Real value of $\chi^{(1)}$ in blue and imaginary value of $chi^{(1)}$ in red.

4. Numerical evaluation of susceptibilities

In this section, we apply the numerically evaluated various dipole moments calculated in the previous section to the fomula for the linear and the nonlinear susceptibilities in the table 2. Since we saw some significant discrepancies in the dipole moments among the various approaches, namely (1) the second-order perturbative Dirac cone, (2) the numerical Dirac cone, and (3) higher-order corrected Dirac cone, we will exclusive use the dipole moments based on the higher-order corrected Dirac cone.

4.1 Linear susceptibility

We calculated $\chi^{(1)}$, which is shown in figure 9. Both the real and the imaginary values are shown in the graph. Five exciton resonances are prominent, which corresponds to $\left|\psi_{(0,0)}\right\rangle, \left|\psi_{(1,0)}\right\rangle, \left|\psi_{(2,0)}\right\rangle, \left|\psi_{(3,0)}\right\rangle$, and $\left|\psi_{(4,0)}\right\rangle$, corresponding to 1.776, 2.050, 2.072, 2.078, 2.080 eV, respectively. For the broadening factor, we used $\gamma_\nu = \gamma_0$ uniformly. The line broadening is due to the radiative transition, for which we used 200 fs as the lifetime.

We then calculate the absorption as $\alpha d_{\text{eff}} = 2d_{\text{eff}}\text{Im}[\sqrt{1+\chi^{(1)}}]\omega_q/c$ where we used $d_{\text{eff}} =$ 6.5 Å. The absorption leaves a long tail beyond the first resonance frequency. The peak absorption is estimated to be approximately 23 % at the resonance frequency 1.776 eV of $\left|\psi_{(0,0)}\right\rangle$. Compared to the experimental values of $10 \sim 15\%$, our predicted value is approximately double. This discrepancy is due to (1) the 2D treatment of the problem and (2) the gapped Dirac Hamiltonian approximation. To compensate for this discrepancy, we introduce a fitting parameter ξ such that we replace $g_\nu \to \xi g_\nu$. We chose $\xi = 0.5$, resulting in the maximum absorption at the resonance to be 11.6%.

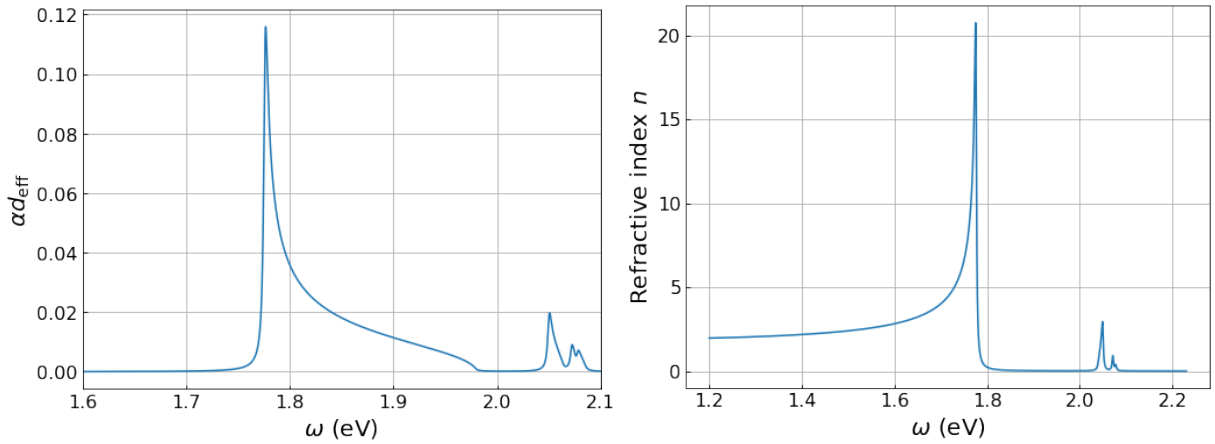

(a) Absorption

(b) Refractive index

Figure 10: The deduced absorption of the monolayer MoS_2 material and the refractive index spectra.

We also calculated the refractive index through $n = \text{Re}[\sqrt{1+\chi^{(1)}}]$. The refractive index has a long tail below the first exciton state resonance.

4.2 Second-order susceptibility

We then calculate the second-order susceptibility. We are primarily interested in the low-frequency second-harmonic generation in the figure 3, where the input light has a frequency $\omega_q \approx e_0/2$. For the $\chi^{(2)}(\omega_q \sim e_0/2)$, one needs to use $g_\nu, h_{\nu 0}, g_0$ as is shown in the table 2, which are all calculated and listed in the previous section. While performing the summation over ν, we summed up to $\nu = (n,0) = (7,0)$. The difference of the maximum $|\chi^{(2)}|$ between summing up to $n = 7$ and up to $n = 6$ is only 0.7 %. Hence, we concluded summing up to $n = 7$ is sufficient.

As we described in the appendix E, the intensity of the second harmonic at the exciton resonant frequency e_0 depends on the absolute value $|\chi^{(2)}|$ whereas the phase of $\chi^{(2)}$ explains the phase delay of the second harmonic light. The estimated maximum value of $|\chi^{(2)}|$ at frequency $e_0/2$ is approximately 8×10^{-8} m/V. The order or magnitude of this result matches the experimental result found in Kumar, et al. of $\sim 10^{-7}$ m/V [13] and the experimental result found in Malard, et al., of $\sim 10^{-7}$ m/V [14].

Compared to the typical $\chi^{(2)}$ value 20 pm/V of lithium niobate, which is the common material for the second harmonic generation, the $\chi^{(2)}$ of MoS_2 monolayer exciton is about four orders of magnitude larger.

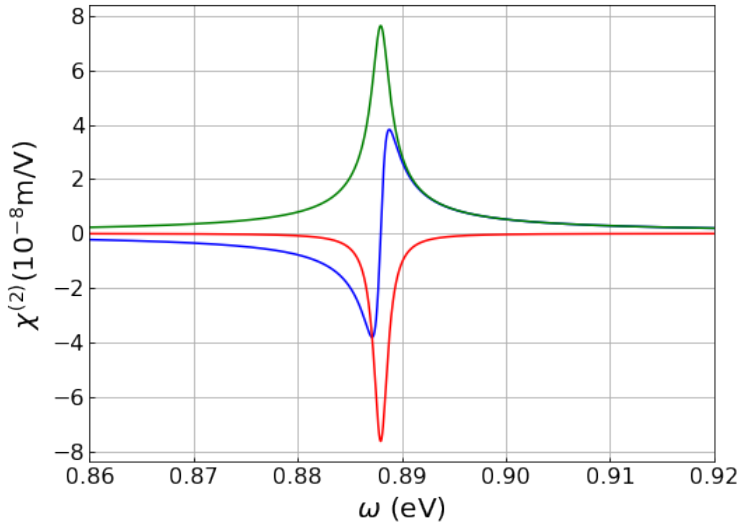

Figure 11: Numerically evaluated $\chi^{(2)}$ based on the higher-order corrected Dirac cone approximation. The real value (blue), the imaginary value (red), and the absolute value (green) of $\chi^{(2)}$ are shown.

4.3 Third-order susceptibility

4.3.1 Third harmonic generation

We are primarily interested in the case where the fundamental frequency is one third of the lowest exciton resonance frequency: $\omega_q \sim e_0/3$ (see figure 5 (a)). The formula of $\chi^{(3)}(\omega_q \sim e_0/3)$ involves the dipole moment $h_{\nu_2\nu_1}$ multiplied by $h_{0\nu_2}$. Note that $h_{0\nu_2}$ has nonzero element for $\sigma+$ incoming photons, only when $\nu_2 = (n_2, m_2)$ with $m_2 = -1$. Hence, we are only concerned with $h_{\nu_2\nu_1}$ in the case where $\nu_1 = (n_1, m_1)$ with $m_1 = -2$. These are the coefficients such as $h_{(1,-1)(2,-2)}$, $h_{(1,-1)(3,-2)}$, $h_{(2,-1)(3,-2)}$, $h_{(2,-1)(4,-2)}$, and so on. Table 5 shows the useful values of both $h_{0\nu_2}$ and $h_{\nu_2\nu_1}$ for calculating the susceptibility relevant to the third-harmonic generation process.

Using the values in the table 5, we evaluated the third-harmonic generation $\chi^{(3)}_{TH}(\omega_q \sim e_0/3)$. The maximum $|\chi^{(3)}|$ is found to be 5.5×10^{-17} m^2/V^2.

4.3.2 Two photon process

We also primarily focus on the case where the upper level of the two photon process involves the lowest exciton bound state $|\psi_0\rangle$, as shown in the figure 5 (b). Let us recall that the relevant susceptibility calculated is given in equation (136). If we set $|\psi_\nu\rangle \to |\psi_0\rangle$ in the equation, we

ν_2	ν_1	$h_{0\nu_2}$	$h_{\nu_2\nu_1}$
$(1,-1)$	$(2,-2)$	0.344	2.76
	$(3,-2)$		1.05
	$(4,-2)$		0.61
	$(5,-2)$		0.42
	$(6,-2)$		0.31
	$(7,-2)$		0.25
$(2,-1)$	$(3,-2)$	0.141	5.07
	$(4,-2)$		2.05
	$(5,-2)$		1.22
	$(6,-2)$		0.85
	$(7,-2)$		0.64
$(3,-1)$	$(4,-2)$	0.082	8.01
	$(5,-2)$		3.25
	$(6,-2)$		1.94
	$(7,-2)$		1.35
$(4,-1)$	$(5,-2)$	0.056	11.6
	$(6,-2)$		4.65
	$(7,-2)$		2.76
$(5,-1)$	$(6,-2)$	0.041	15.8
	$(7,-2)$		6.27
$(6,-1)$	$(7,-2)$	0.032	20.7

Table 5: Calculated $h_{\nu_1\nu_2}$ that is useful to calculate $\chi^{(3)}_{TH}(3\omega_q \sim e_0, \omega_q)$. The unit is ea_0 (C-m). For MoS_2, $a_0 = 13.4$ Å.

obtain

$$\chi^{(3)}_{TP}(\omega_q \sim e_0/2) = -\sum_{\nu_1,\nu_2} \left(\begin{array}{c} \frac{(e_0-e_{\nu_2})N_e g_{\nu_1} h_{0\nu_1} h^*_{0\nu_2} g^*_{\nu_2}}{\omega_q \varepsilon_0 \hbar^3} \\ \times \frac{1}{\left((e_{\nu_1}-\omega_q)-i\varepsilon_{\nu_1}\right)\left((e_0-2\omega_q)-i\varepsilon_0\right)\left((e_0-e_{\nu_2}-\omega_q)-i\varepsilon_{\nu_2}\right)} \end{array} \right). \tag{186}$$

For $\sigma+$ light having the polarization vector $\hat{\varepsilon} = (1/\sqrt{2})(\hat{x}+i\hat{y})$, we showed that $g_{\nu'} \approx \psi_\nu(r=0)d_{cv}(0)$ is nonzero only for $\nu' = (n,m)$ with $m = 0$, due to the multiplication by r^m in $\psi_\nu(r)$ as shown in the table 1. Then, the nonzero contribution occurs only if $\nu_1 = (n_1,m_1), \nu_2 = (n_2,m_2)$ have both $m_1 = m_2 = 0$. In addition, we also showed that for $\sigma+$ light, the nonzero value $h_{\nu'0}$ occurs only if $\nu' = (n',m')$ with $m' = 1$ (see the equation (182)). Therefore, for $\sigma+$ light, the two photon process does not occur since $g_{\nu_1}h_{0\nu_1} = 0$ for any ν_1. Then, for $\sigma+$ light, $\chi^{(3)}_{TP}(\omega_q \sim e_0/2)$ is nonzero only if we include the unbound exciton states and sum over them for the virtual levels whose contribution is diminished, due to a large values of the frequency difference in the

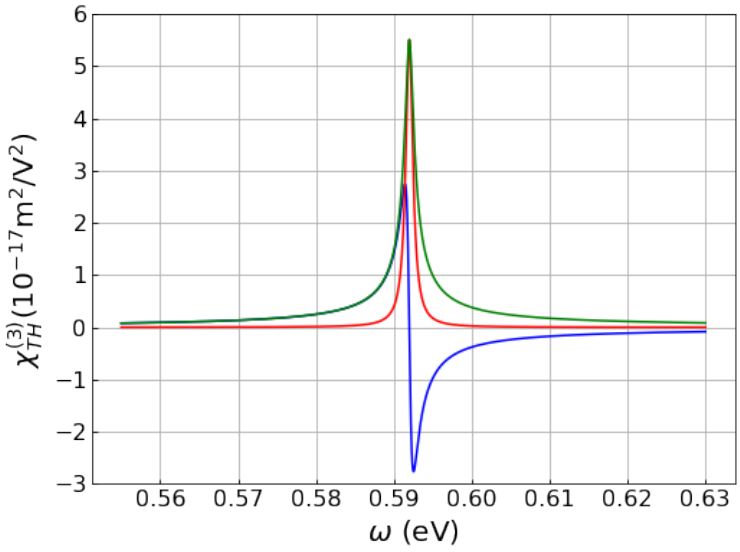

Figure 12: Numerically evaluated $\chi^{(3)}(\omega_q \sim e_0/3)$ based on the higher-order corrected Dirac cone approximation. This process corresponds to the figure 5 (a) where the input light frequency is approximately one third of the lowest exciton resonant frequency e_0. The real value (blue), the imaginary value (red), and the absolute value (green) of $\chi^{(2)}$ are shown.

denominator. Thus, it is expected that $\chi^{(3)}_{TP}(\omega_q \sim e_0/2)$ will be very small for $\sigma+$ light photons. Instead, the two photon process involving $|\psi_\nu\rangle \to |\psi_{(1,-1)}\rangle$ with the corresponding $\chi^{(3)}_{TP}(\omega_q \sim e_{(1,-1)}/2)$ will be more significant as it involves the quantities such as $g_{(n,0)} \neq 0$ and $h_{(n,0)(1,-1)} \neq 0$. The two-photon susceptibility is for $\nu = (1,1)$:

$$\begin{aligned}
&\chi^{(3)}_{TP}(\omega_q \sim e_{(1,1)}/2) \\
&= -\sum_{\nu_1,\nu_2} \left(\frac{(e_{(1,1)} - e_{\nu_2}) N_e g_{\nu_1} h_{(1,1)\nu_1} h^*_{(1,1)\nu_2} g^*_{\nu_2}}{\omega_q \varepsilon_0 \hbar^3} \right. \\
&\qquad \left. \times \frac{1}{\big((e_{\nu_1} - \omega_q) - i\varepsilon_{\nu_1}\big)\big((e_{(1,1)} - 2\omega_q) - i\varepsilon_{(1,1)}\big)\big((e_{(1,1)} - e_{\nu_2} - \omega_q) - i\varepsilon_{\nu_2}\big)} \right).
\end{aligned} \tag{187}$$

The useful dipole moments $h_{(1,1)\nu_1}$ with ν_1 such that g_{ν_1} is nonzero are shown in table 6.

The numerically evaluated $\chi^{(3)}_{TP}(\omega_q \sim e_{(1,1)}/2)$ is shown in figure 13. As we stated in the Appendix E, the imaginary value is real two-photon absorption and the real value is related to the Kerr effect where the refractive index changes proportionally to the intensity of light. The maximum of the real value of $\chi^{(3)}_{TP}$ is shown to be approximately 1×10^{-18} m^2/V^2. The maximum of the imaginary is shown to be approximately 2×10^{-18} m^2/V^2.

For the Kerr nonlinearity applications, one wants that the photon changes the refractive index of the material while not suffering from the incoherent effect of the two-photon absorption. Therefore, the ratio between the real and the imaginary values of $\chi^{(3)}_{TP}$ is important. The ratio reaches quite large values of > 50 while the absolute value of the real $\chi^{(3)}_{TP}$ is still large. The negative sign appearing in equation (13) is significant: the fact that $h_{(1,1)(1,0)}$ is both dominant and negative is

ν_1	$h_{(1,1)\nu_1}$
$(0,0)$	0.344
$(1,0)$	-3.18
$(2,0)$	0.752
$(3,0)$	0.320
$(4,0)$	0.194
$(5,0)$	0.135
$(6,0)$	0.102
$(7,0)$	0.080

Table 6: Calculated $h_{(1,1)\nu_1}$ that is useful to calculate $\chi^{(3)}_{TP}(2\omega_q \sim e_{(1,1)}, \omega_q)$. The unit is ea_0 (C-m). For MoS_2, $a_0 = 13.4$ Å.

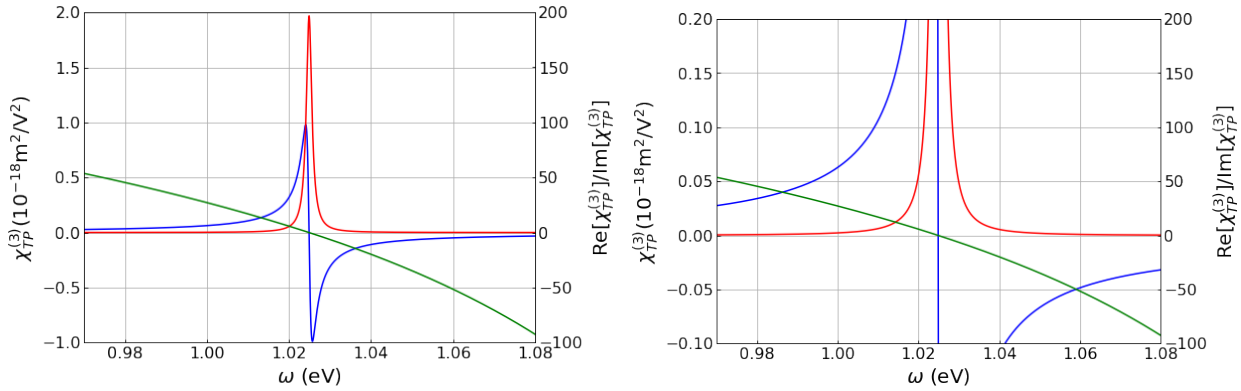

(a) Larger scale

(b) Zoomed in

Figure 13: Numerically evaluated $\chi^{(3)}_{TP}(\omega_q \sim e_{(1,1)}/2)$ based on the higher-order corrected Dirac cone approximation. This process corresponds to the figure 5 (b) where the input light frequency is approximately one half of the $|\psi_{(1,1)}\rangle$ exciton resonant frequency $e_{(1,1)}$. The real value (blue) and the imaginary value (red) $\chi^{(2)}$ are shown. Also shown is the ratio between the real and the imaginary values of $\chi^{(3)}_{TP}$ (green).

combined with the negative sign to produce a positive imaginary value, which nicely explains the two photon absorption.

5. Conclusion

We have calculated the optical nonlinear susceptibilities of the monolayer MoS_2, based on the second-order corrected gapped Dirac cone approximation around K points. The calculated optical nonlinearities are impressively large compared to other 3D bulk materials. Particularly the Kerr optical nonlinearity of the monolayer MoS_2 is quite large in the spectral region where the two-photon absorption is negligibly small, which indeed is a promising result to use the MoS_2 material for the cavity QED configuration to operate the qubits on a semiconductor platform. Although graphenes also exhibits a large third-order susceptibility [20], graphene suffers from the linear loss for all incoming light's frequencies, due to the gapless Dirac cone dispersion. Unlike graphene, MoS_2's Kerr effect does not suffer from the linear absorption and one can expect a sufficiently coherent operation utilizing a strong Kerr nonlinearity in the monolayer MoS_2 platform. Combined with the newly developed CVD capabilities to deposit sheet-by-sheet on the existing photonic circuits, our results indicate that MoS_2 is indeed a good candidate for chip-scale qubit operator as well as low energy optical transitors on chip.

We found that our result is within an order of magnitude compared with a few existing experimental results for the second and the third harmonic generation from the excitonic levels of the monolayer MoS_2. This indeed is a good agreement as a nonlinearity calculation. We did not include the sophisticated higher order effect such AC stark shift or self-coupling as in [20], which however are expected to be a small correction compared to the two-photon absorption or direct Kerr effect.

Appendices

A. Fourier transforms

In this section, we clarify the normalization constants for the state kets. For this, we will clearly define the Fourier transforms with appropriate normalization constants. We begin with two important closures (completeness of the Hilbert spaces):

$$\begin{aligned}\int_V \mathrm{d}^3 r\, |r\rangle\langle r| &= \mathbf{1},\\ \sum_k |k\rangle\langle k| &= \mathbf{1},\end{aligned} \tag{188}$$

where V is the quantizing volume. We treat r as the continuous eigenvalues of the operator $\hat{r}$, while we treat k as the discrete eigenvalues of the operator $\hat{k}$. Note that the definition of this closure is consistent with the interpretation that $|\psi(r)|^2 = \langle\psi|r\rangle\langle r|\psi\rangle$ is the probability density for a particle to be found at r since, putting the above closure into a normalized state $|\psi\rangle$:

$$\langle\psi|\psi\rangle = 1 = \int_V \mathrm{d}^3 r\, \langle\psi|r\rangle\langle r|\psi\rangle = \int_V \mathrm{d}^3 r |\psi(r)|^2. \tag{189}$$

This ensures that the integration of the probability density must be unity.

We know that the wavefunction in the position basis for a particle of a state $|k\rangle$ is $\langle r|k\rangle \propto \mathrm{e}^{ik\cdot r}$. The way to calculate the normalization constant is to set $\langle r|k\rangle = C\mathrm{e}^{ik\cdot r}$ and use the following normalization condition:

$$\langle k|k'\rangle = \delta_{k,k'} = \int_V \mathrm{d}^3 r\, \langle k|r\rangle\langle r|k'\rangle = |C|^2 \int_V \mathrm{d}^3 r \mathrm{e}^{i(k'-k)\cdot r} = \begin{cases} |C|^2 V, & \text{if } k = k', \\ 0, & \text{if } k \neq k'. \end{cases} \tag{190}$$

The above holds because k, k' are discrete quantities such that $k\cdot a_l = 2m\pi, k'\cdot a_l = 2m'\pi$ where m, m' are integers and a_l is the lattice constant. Therefore,

$$\int_V \frac{\mathrm{d}^3 r}{V}\, \mathrm{e}^{i(k-k')\cdot r} = \left\{ \begin{array}{ll} 1, & \text{if } k = k', \\ 0, & \text{if } k \neq k' \end{array} \right\} = \delta_{k,k'}. \tag{191}$$

Then, we obtain $C = 1/\sqrt{V}$ and consequently

$$\langle r|k\rangle = \frac{1}{\sqrt{V}}\mathrm{e}^{ik\cdot r}. \tag{192}$$

Then, the Fourier transform of a wave function is clearly defined as

$$\begin{aligned}\psi(r) = \langle r|\psi\rangle &= \sum_k \langle r|k\rangle\langle k|\psi\rangle = \frac{1}{\sqrt{V}}\sum_k \psi(k)\mathrm{e}^{ik\cdot r},\\ \psi(k) = \langle k|\psi\rangle &= \int_V \mathrm{d}^3 r\, \langle k|r\rangle\langle r|\psi\rangle = \frac{1}{\sqrt{V}}\int_V \mathrm{d}^3 r \psi(r)\mathrm{e}^{-ik\cdot r}.\end{aligned} \tag{193}$$

Extending to the two particle wavefunctions follows easily: using the closures

$$\begin{aligned}\int_V \mathrm{d}^3 r \mathrm{d}^3 r' \left|r, r'\right\rangle\left\langle r, r'\right| &= \mathbf{1},\\ \sum_{k,k'} \left|k, k'\right\rangle\left\langle k, k'\right| &= \mathbf{1},\end{aligned} \tag{194}$$

one obtains the normalized wavefunction:

$$\left\langle r,r'|k,k'\right\rangle = \frac{1}{V}\mathrm{e}^{ik\cdot r+ik'\cdot r'}, \tag{195}$$

which leads to the Fourier transforms:

$$\begin{aligned}
\psi(r,r') &= \left\langle r,r'|\psi\right\rangle = \sum_{k,k'}\left\langle r,r'|k,k'\right\rangle\left\langle k,k'|\psi\right\rangle = \frac{1}{V}\sum_{k,k'}\psi(k,k')\mathrm{e}^{ik\cdot r+ik'\cdot r'}, \\
\psi(k,k') &= \left\langle k,k'|\psi\right\rangle = \int_V \mathrm{d}^3r\mathrm{d}^3r'\left\langle k,k'|r,r'\right\rangle\left\langle r,r'|\psi\right\rangle = \frac{1}{V}\int_V \mathrm{d}^3r\mathrm{d}^3r'\psi(r,r')\mathrm{e}^{-ik\cdot r-ik'\cdot r'}.
\end{aligned} \tag{196}$$

B. Exciton creation operator

According to the anticommutation relation of the electron operators in (2), we obtain the following anticommutators for the lowering and raising operators of the electrons and holes:

$$\begin{aligned}
&\{\alpha_k, \alpha_{k'}\} = \left\{\alpha_k, \beta_{k'}^\dagger\right\} = \{\alpha_k, \beta_{k'}\} = \{\beta_k, \beta_{k'}\} = 0, \\
&\left\{\alpha_k^\dagger, \alpha_{k'}^\dagger\right\} = \left\{\alpha_k^\dagger, \beta_{k'}\right\} = \left\{\alpha_k^\dagger, \beta_{k'}^\dagger\right\} = \left\{\beta_k^\dagger, \beta_{k'}^\dagger\right\} = 0, \\
&\left\{\alpha_k, \alpha_{k'}^\dagger\right\} = \delta_{k,k'}, \quad \left\{\beta_k, \beta_{k'}^\dagger\right\} = \delta_{k,k'}.
\end{aligned} \tag{197}$$

We treat the bound exciton in a second quantized context. Let us now derive the creation operator for the exciton state. If we denote the exciton state as $|\nu K\rangle$ where $\nu = (n,l,m)$ is the exciton state index and K is the total momentum vector of the exciton, one can express the exciton creation operator using the Dirac notation as

$$B_{\nu,K}^\dagger = |\nu K\rangle \langle 0|, \tag{198}$$

where $|0\rangle$ represents the ground state where all valence band states are filled and all conduction band states are empty (i.e., the Fermi sea), with zero energy eigenvalue.

Note that the exciton state $|\nu K\rangle$ is a dual-particle state where there is one electron-hole pair. One can use a single electron-hole pair basis $|k,-k\rangle$ that represents a free electron (in the conduction band) with the momentum $\hbar k$, and a free hole (in the valence band) with the momentum $-\hbar k$. Any single electron-hole pair then lives in a Hilbert space that is spanned by basis $\{|k,-k\rangle\}$. In this subspace, the closure relation is

$$\sum_{k,k'} \left|k,-k'\right\rangle \left\langle k,-k'\right| = \mathbf{1}. \tag{199}$$

Then, we obtain

$$\begin{aligned}
B_{\nu K}^\dagger &= \sum_{k,k'} \left|k,-k'\right\rangle \left\langle k,-k'|\nu K\right\rangle \langle 0| \\
&= \sum_{k,k'} \left\langle k,-k'|\nu K\right\rangle \left|k,-k'\right\rangle \langle 0| \\
&= \sum_{k,k'} \left\langle k,-k'|\nu K\right\rangle \alpha_k^\dagger \beta_{-k'}^\dagger,
\end{aligned} \tag{200}$$

where $\alpha_k^\dagger, \beta_{-k'}^\dagger$ are the creation operators for the free electron and the free hole, respectively. We calculate the following using the closure $\int \mathrm{d}^3r\mathrm{d}^3r' \,|r,r'\rangle\langle r,r'| = \mathbf{1}$ and the equation (195):

$$\begin{aligned}
\left\langle k,-k'|\nu K\right\rangle &= \int_V \mathrm{d}^3r\mathrm{d}^3r' \left\langle k,-k'|r,r'\right\rangle \left\langle r,r'|\nu K\right\rangle \\
&\approx \int \mathrm{d}^3r\mathrm{d}^3r' \frac{1}{V} \mathrm{e}^{-ik\cdot r} \mathrm{e}^{ik'\cdot r'} \psi_\nu(r-r') \frac{1}{\sqrt{V}} \mathrm{e}^{iK\cdot\frac{r+r'}{2}},
\end{aligned} \tag{201}$$

where $\psi_\nu(r'')$ is the solution to the exciton Schrödinger equation in equation (4), with the quantum number $\nu = (n,l,m)$, and we approximated the electron and the hole pair states as the free electron and free hole states. Then, we Fourier-transform ψ_ν by using equation (193) to obtain

$$\begin{aligned}
&\langle k,-k'|\nu K\rangle \\
&= \frac{1}{V^2}\sum_{k''}\int \mathrm{d}^3 r \mathrm{d}^3 r' \exp\left[i\left(K\cdot\frac{r+r'}{2} - k\cdot r + k'\cdot r' + k''\cdot(r-r')\right)\right]\psi_\nu(k'') \\
&= \frac{1}{V^2}\sum_{k''}\int \mathrm{d}^3 r \mathrm{d}^3 r' \exp\left[i\left(r\cdot\left(\frac{K}{2} - k + k''\right) + r'\cdot\left(\frac{K}{2} + k' - k''\right)\right)\right]\psi_\nu(k'')
\end{aligned} \tag{202}$$

Using the equation (191), we finally obtain

$$\langle k,-k'|\nu K\rangle = \delta_{K,(k-k')}\psi_\nu\left(\frac{k+k'}{2}\right). \tag{203}$$

Hence, we obtain

$$\begin{aligned}
B^\dagger_{\nu K} &= \sum_{k,k'}\delta_{K,(k-k')}\psi_\nu\left(\frac{k+k'}{2}\right)\alpha^\dagger_k\beta^\dagger_{-k'} \\
&= \sum_k \psi_\nu\left(k-\frac{K}{2}\right)\alpha^\dagger_k\beta^\dagger_{K-k}.
\end{aligned} \tag{204}$$

This coincides with those appearing in the references [23, 22].

One can calculate the boson commutator for the lowest order $\nu = 0$ exciton operator as follows:

$$\begin{aligned}
[B_{0,0}, B^\dagger_{0,0}] &= \sum_{k,k'}\psi_0(k)\psi_0(k')[\beta_{-k}\alpha_k, \alpha^\dagger_{k'}\beta^\dagger_{-k'}] \\
&= \sum_k |\psi_0(k)|^2(1-\alpha^\dagger_k\alpha_k - \beta^\dagger_{-k}\beta_{-k}) \\
&= 1 - \mathscr{O}(na_0^d),
\end{aligned} \tag{205}$$

where n is the density of the excitons, $a_0 = \hbar^2\varepsilon_0/e^2 m_r$ is the Bohr radius of the exciton, and $d = 2,3$ is the dimension. Hence, in the limit of a vanishing number of excitons ($na_0^d \to 0$), we obtain the boson commutator for the excitons. Hence, the excitons are approximately bosons when the exciton density is sufficiently small.

If we assume that $K \approx 0$, viewed in the scale of the crystal momentum since the incoming photon's momentum is negligibly small, we interchangeably use the notation $|\nu 0\rangle = |\mathrm{x}_\nu\rangle$. Then, from the definition of the exciton creation operator and the derived result of equation (204), we obtain

$$B^\dagger_\nu = |\mathrm{x}_\nu\rangle\langle 0| = \sum_k \psi_\nu(k)\alpha^\dagger_k\beta^\dagger_{-k}. \tag{206}$$

From this, the following is obvious:

$$B^\dagger_\nu|0\rangle = |\mathrm{x}_\nu\rangle, \quad B^\dagger_\nu|\mathrm{x}_\nu\rangle = 0. \tag{207}$$

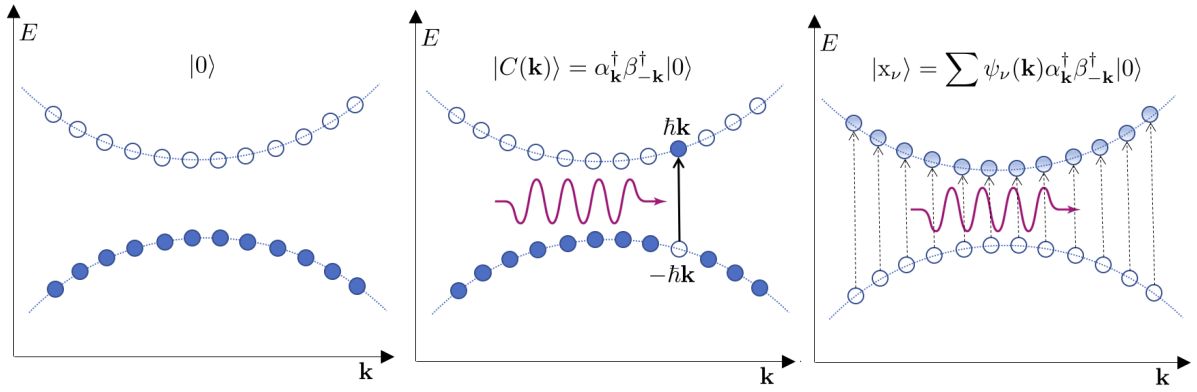

(a) Fermi sea (b) Single electron-hole pair (c) Exciton

Figure 14: Band representation of many body states for the Fermi sea ($|0\rangle$), the single electron-hole pair excitation (not bounded by the Coulomb interaction) ($|C(k)\rangle = |k,-k\rangle$), and the exciton state ($|x_\nu\rangle$)

We can obtain the reverse relation to express $\alpha^\dagger_k\beta^\dagger_{-k}$ using $B^\dagger_\nu$ as follows. Note that

$$\delta_{k,k'} = \langle k|k'\rangle = \sum_\nu \langle k|\nu\rangle\langle\nu|k'\rangle = \sum_\nu \psi^*_\nu(k)\psi_\nu(k'). \tag{208}$$

We multiply $\psi^*_\nu(k')$ on the left of both sides in equation 206 and sum over ν:

$$\sum_\nu \psi^*_\nu(k')B^\dagger_\nu = \sum_{k,\nu} \psi^*_\nu(k')\psi_\nu(k)\alpha^\dagger_k\beta^\dagger_{-k} = \sum_k \delta_{k,k'}\alpha^\dagger_k\beta^\dagger_{-k} = \alpha^\dagger_{k'}\beta^\dagger_{-k'}. \tag{209}$$

Hence, we obtain the reverse relation:

$$\alpha^\dagger_k\beta^\dagger_{-k} = \sum_\nu \psi^*_\nu(k)B^\dagger_\nu. \tag{210}$$

Also note that, explicitly, the Fourier transformed $\psi_0(k)$ for the lowest exciton state is given by [7]

$$\psi_0(k) = \begin{cases} 8\sqrt{\frac{\pi a_0^3}{V}}\frac{1}{(1+(ka_0)^2)^2}, & \text{(3D)} \\ \sqrt{\frac{2\pi}{A}}a_0\frac{1}{(1+(ka_0/2)^2)^{3/2}}, & \text{(2D).} \end{cases}, \tag{211}$$

where V,A are the volume and the area of the sample, respectively. These are relatively flat for $0 < k < 1/a_0$ and rapidly decreasing for $k > 1/a_0$. Therefore, the exciton size a_0 determines what portion of k points in the FBZ would participate in creating the exciton significantly. For example, MoS_2 has a unit cell size of 3.2 Å[16], while it has the lowest exciton radius a_0 of 10.5 Å. Since the size of the FBZ is $2\pi/a_l$ where a_l is the lattice constant, it implies that about 10 % of FBZ k points strongly participating in building an exciton state.

Figure 14 shows the many body state represented by the band structure of a solid. The Fermi sea state has a fully occupied valence band and a fully empty conduction band. The single electron-hole pair state is not bounded by the Coulomb potential (i.e., above the Coulomb bounded state

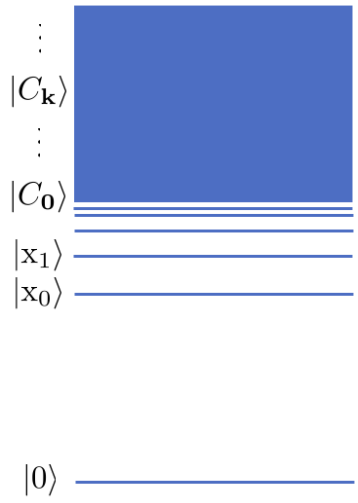

Figure 15: Energy levels of various many body states.

- excitons). The exciton state is a superposition of the single electron-hole pairs for all possible k, with a weight $\psi_\nu(k)$. This is somewhat a remarkable physical insight for an exciton, which is originally a bound electron-hole pair state by the Coulomb potential, which turns out to be a superposition state of all possible k, with the Fourier-transformed exciton wave function $\psi_\nu(k)$ as the superposing weight.

Figure 15 shows the energy levels of the various many body states. We regard the Fermi sea state energy to be zero. The first excited state is the lowest exciton state $|\mathrm{x}_0\rangle$, and the next levels are the exciton states $|\mathrm{x}_1\rangle, |\mathrm{x}_2\rangle \cdots$ which are bound state according to the Coulomb potential. Then, the unbounded states $C(k)$ starts, which is more or less like a continuum of an energy band.

C. Optical selection rule for $\pm K$ valleys

The result in section 3.3.1 also nicely explains the selection rule. Let us consider the $\sigma\pm$ light that has the polarization $\hat{\varepsilon}_\pm \propto \hat{x} \pm i\hat{y}$. Then, the dipole moment at the band extrema is proportional to $d^x_{cv}(0) \pm i d^y_{cv}(0)$ where $d^{x,y}_{cv}(0)$ is the x, y component of the dipole moment in equation (165). For K valley, we set $\tau = 1$:

$$d^+_{cv,K} = [d^x_{cv}(0) + i d^y_{cv}(0)]_{\tau=+1} = ie\left(-\frac{\hbar v}{\Delta} - \frac{\hbar v}{\Delta}\right) = -2ie\frac{\hbar v}{\Delta}. \tag{212}$$

However, we calculate

$$d^-_{cv,K} = [d^x_{cv}(0) - i d^y_{cv}(0)]_{\tau=+1} = ie\left(-\frac{\hbar v}{\Delta} + \frac{\hbar v}{\Delta}\right) = 0. \tag{213}$$

Therefore, at K valleys, only $\sigma+$ light is absorbed. At $-K$ valleys, one can show that

$$\begin{aligned} d^+_{cv,-K} &= [d^x_{cv}(0) + i d^y_{cv}(0)]_{\tau=-1} = ie\left(\frac{\hbar v}{\Delta} - \frac{\hbar v}{\Delta}\right) = 0, \\ d^-_{cv,-K} &= [d^x_{cv}(0) - i d^y_{cv}(0)]_{\tau=-1} = ie\left(\frac{\hbar v}{\Delta} + \frac{\hbar v}{\Delta}\right) = 2ie\frac{\hbar v}{\Delta}. \end{aligned} \tag{214}$$

Therefore, at $-K$ valleys, only $\sigma-$ light is absorbed. Hence, by adjusting the light polarization, one can selectively excite either K valleys or $-K$ valleys.

According to (165), the optical selection rule starts deviating from the above result for the cases $q_x \neq q_y$. However, note that the deviation from the valley selection rule is a second-order effect.

D. Lifetime of an electron hole pair

When an electron-hole pair is excited, the recombination takes place either through a radiative or a non-radiative process. The radiative process is the spontaneous emission while the non-radiative process is the scattering involving phonons. At zero temperature, the dominant process is the radiative process due to the lack of phonon excitations.

According to the Fermi's golden rule (first order perturbation theory), the differential transition rate $\mathrm{d}W_{fi}$ from an initial state $|i\rangle$ to a final state $|f\rangle$ subject to a perturbation from an interaction Hamiltonian $\mathscr{H}_I$ is given by [3]

$$\mathrm{d}W_{fi} = \frac{2\pi}{\hbar} |\langle f|\mathscr{H}_I|i\rangle|^2 \rho_f(E)\delta(E-\hbar\omega)\mathrm{d}E, \tag{215}$$

In our case, the interaction Hamiltonian is given by

$$\mathscr{H}_I = -\sum_k \left[d_{cv}\alpha_k^\dagger \beta_{-k}^\dagger i\sqrt{\frac{\hbar\omega_q}{2V\varepsilon_0}} b_q - d_{cv}^* i\sqrt{\frac{\hbar\omega_q}{2V\varepsilon_0}} b_q^\dagger \alpha_k \beta_{-k} \right], \tag{216}$$

where $\alpha_k^\dagger, \beta_k^\dagger$ are the raising operators for the electron and hole, respectively, and $b_q^\dagger$ is the photon creation operator.

Note that the states are tensor states $|i\rangle = |0_q\rangle \otimes |k,-k\rangle = \alpha_k^\dagger \beta_{-k}^\dagger |0_q\rangle \otimes |0\rangle$, describing the state where the number of photons is zero and an electron hole pair is excited, and $|f\rangle = |1_q\rangle \otimes |0\rangle = b_q^\dagger |0_q\rangle \otimes |0\rangle$ where one photon state is excited and the solid is in the ground state (Fermi sea). Hence, we find

$$\begin{aligned}
\langle f|\mathscr{H}_I|i\rangle &= +d_{cv}^* i\sqrt{\frac{\hbar\omega_q}{2V\varepsilon_0}} \langle 0_q| \otimes \langle 0| b_q b_q^\dagger |0_q\rangle \otimes |0\rangle \\
&= d_{cv}^* i\sqrt{\frac{\hbar\omega_q}{2V\varepsilon_0}} \langle 0_q| (b_q^\dagger b_q + 1) |0_q\rangle \\
&= d_{cv}^* i\sqrt{\frac{\hbar\omega_q}{2V\varepsilon_0}}.
\end{aligned} \tag{217}$$

The photon energy is given through

$$E_q = \hbar\omega_q = \hbar c q, \quad q = \frac{E_q}{\hbar c}, \tag{218}$$

and the count of states

$$N_q = 2\frac{V}{(2\pi)^3}\frac{4\pi}{3}q^3, \quad \mathrm{d}N_q = 2\frac{V}{(2\pi)^3}4\pi q^2 \mathrm{d}q = 2\frac{V}{(2\pi)^3}4\pi\frac{E_q^2}{\hbar^2 c^2}\frac{\mathrm{d}E_q}{\hbar c}, \tag{219}$$

where we put extra factor 2 for counting two possible polarization. Hence, the density of states is

$$\rho_q(E_q) = \frac{\mathrm{d}N_q}{\mathrm{d}E_q} = \frac{VE_q^2}{\pi^2\hbar^3c^3} = \frac{V\omega_q^2}{\pi^2\hbar c^3}. \tag{220}$$

On the other hand, the solid state band energy is given through

$$E(k) = E_g + \frac{\hbar^2k^2}{2m_r}, \quad k\mathrm{d}k = \mathrm{d}E(k)\frac{m_r}{\hbar^2} \tag{221}$$

The count of states is

$$N = \frac{A}{(2\pi)^2}\pi k^2, \quad \mathrm{d}N = \frac{A}{(2\pi)^2}2\pi k\mathrm{d}k = \frac{A}{4\pi^2}2\pi\frac{m_r}{\hbar^2}\mathrm{d}E(k) = \frac{Am_r}{2\pi\hbar^2}\mathrm{d}E(k). \tag{222}$$

Hence, the density of states is

$$\rho(E(k)) = \frac{\mathrm{d}N}{\mathrm{d}E(k)} = \frac{Am_r}{2\pi\hbar^2} \tag{223}$$

Then, we obtain the total spontaneous emission rate

$$W = \int \mathrm{d}W_{fi} = \frac{2\pi}{\hbar}\frac{|d_{cv}|^2}{2}\frac{\hbar\omega_q}{2V\varepsilon_0}\frac{V\omega_q^2}{\pi^2\hbar c^3} = \frac{\omega_q^3}{2\pi\varepsilon_0\hbar c^3}|d_{cv}|^2 = \frac{1}{\tau}, \tag{224}$$

where τ is the lifetime. Here, we put the extra factor $1/2$ to average out $|d_{cv}|^2$ for all possible polarization (2D). Putting the parameters of the MoS_2, we obtain $\tau \sim 5$ ns.

E. Nonlinear propagation of light

We briefly remind of the nonlinear propagation of light at harmonic frequencies affected by the nonlinear optical susceptibilities. We follow the treatment in Boyd [2]. We start with the Maxwell equations:

$$\begin{aligned} \nabla \cdot D &= \rho, \\ \nabla \cdot B &= 0, \\ \nabla \times E &= -\frac{\partial B}{\partial t}, \\ \nabla \times H &= \frac{\partial D}{\partial t} + J, \end{aligned} \tag{225}$$

which is supplemented by the materials without free charges or currents:

$$\rho = 0, \quad J = 0, \tag{226}$$

but, having the polarization

$$D = \varepsilon_0 E + P. \tag{227}$$

The material is assumed to be non-magnetic:

$$B = \mu_0 H, \tag{228}$$

where μ_0 is the vacuum permeability. Then, differentiating the Maxwell equation, we obtain

$$\nabla^2 E - \frac{1}{c^2}\frac{\partial^2}{\partial t^2}E = \frac{1}{\varepsilon_0 c^2}\frac{\partial^2 P}{\partial t^2}, \tag{229}$$

where $\mu_0\varepsilon_0 = 1/c^2$ is used, and $\nabla \cdot E$ is assumed to be negligibly small even for the non-isotropic medium (P varies over space). By splitting the linear and the nonlinear parts of polarization such that $P = P^{\mathrm{L}} + P^{\mathrm{NL}}$ with $P^{\mathrm{L}} = \varepsilon_0 \chi^{(1)} E$, we obtain

$$\nabla^2 E - \frac{\varepsilon^{(1)}}{c}\frac{\partial^2 E}{\partial t^2} = \frac{1}{\varepsilon_0 c^2}\frac{\partial^2 P^{\mathrm{NL}}}{\partial t^2}, \tag{230}$$

where $\varepsilon^{(1)} = 1 + \chi^{(1)}$. Assuming a plane wave and using the complex tilde envelopes such that, for example,

$$E(r,t) = \widetilde{E}(r)\mathrm{e}^{-i\omega_n t} + c.c., \tag{231}$$

we obtain

$$\nabla^2 \widetilde{E} + \frac{\omega_q^2}{c^2}\varepsilon^{(1)}(\omega_q)\widetilde{E} = -\frac{\omega_q^2}{\varepsilon_0 c^2}\widetilde{P}^{\mathrm{NL}}. \tag{232}$$

For the second harmonic generation,

$$\widetilde{P}^{(2)}(\omega_q) = \varepsilon_0 \chi^{(2)}(\omega_q/2)\widetilde{E}^2(\omega_q/2). \tag{233}$$

Let us use the plane wave approximation $\widetilde{E} = \hat{\varepsilon}A(z)e^{ikz}$, and calculate only for the envelope $A(z)$, while applying the slowly varying envelope approximation where

$$\left|\frac{d^2A(z)}{dz^2}\right| \ll \left|k\frac{dA(z)}{dz}\right|, \tag{234}$$

where $k = n\omega_q/c$ with the refractive index n at ω_q, the differential equation for the z propagating plane wave at ω_q is givenas

$$2ik\frac{dA(\omega_q)}{dz} \simeq -\frac{\chi^{(2)}\omega_q^2}{c^2}A^2(\omega_q/2)e^{i\Delta kz}, \tag{235}$$

where $\Delta k = 2k(\omega_q/2) - k(\omega_q)$ is the phase mismatch term. This leads to

$$\frac{dA(\omega_q)}{dz} = i\frac{\chi^{(2)}\omega_q}{2cn}A^2(\omega_q/2)e^{i\Delta kz}, \tag{236}$$

The solution after propagating distance of L is

$$A(\omega_q;L) = i\frac{\chi^{(2)}\omega_q}{2cn}A^2(\omega_q/2)\int_0^L dz\, e^{i\Delta kz} = i\frac{\chi^{(2)}\omega_q}{2cn}A^2(\omega_q/2)\frac{e^{i\Delta kL}-1}{i\Delta k}. \tag{237}$$

The intensity is given as

$$I = 2n\varepsilon_0 c|A|^2. \tag{238}$$

Hence, we find

$$I(\omega_q) = \frac{\varepsilon_0\omega_q^2|\chi^{(2)}(\omega_q/2)|^2}{2cn}L^2\frac{\sin^2(\Delta kL/2)}{(\Delta kL/2)^2}. \tag{239}$$

From this, we see that, for the intensity of the second harmonic, the absolute value $|\chi^{(2)}|$ at the fundamental frequency $\omega_q/2$ matters, and the phase of $\chi^{(2)}$ enters in equation (237) to describe the phase lag of the second harmonic envelope.

Third harmonic is similarly calculated, and what matters for the intensity of the third harmonic is the absolute value $|\chi^{(3)}|$ at the fundamental frequency $\omega_q/3$, and the phase of $\chi^{(3)}$ enters to describe the phase lag of the third harmonic envelope.

The two photon process is somewhat different since the nonlinearity is given as

$$\widetilde{P}^{NL}(\omega_q) = 3\varepsilon_0\chi^{(3)}_{TP}(\omega_q = \omega_q + \omega_q - \omega_q)|\widetilde{E}(\omega_q)|^2\widetilde{E}(\omega_q) \tag{240}$$

Hence, the total polarization (excluding the second order) is given as

$$\widetilde{P}(\omega_q) = \varepsilon_0\chi^{(1)}\widetilde{E}(\omega_q) + 3\varepsilon_0\chi^{(3)}_{TP}(\omega_q)|\widetilde{E}(\omega_q)|^2\widetilde{E}(\omega_q). \tag{241}$$

Therefore, the effective susceptibility is

$$\chi_{\text{eff}} = \chi^{(1)} + 3\chi^{(3)}_{TP}|\widetilde{E}(\omega_q)|^2. \tag{242}$$

Recall that the complex refractive index n is given as

$$n^2 = 1 + \chi_{\text{eff}}. \tag{243}$$

Hence, the real value of $\chi^{(3)}_{TP}$ serves as the self phase modulation (modifying the refractive index depending on the intensity $\propto |A(\omega_q)|^2$), while the imaginary value of $\chi^{(3)}_{TP}$ is indeed a loss term, describing the two photon absorption, which is also intensity dependent.

F. Derivation of Blount formula

In this section, we study the Blount formula given in equation (161), which is repeated here:

$$\left\langle \psi_{k,\lambda} \middle| r \middle| \psi_{k',\lambda'} \right\rangle = -i\nabla_{k'} \left\langle \psi_{k,\lambda} | \psi_{k',\lambda'} \right\rangle + i\delta_{k,k'} \left\langle u_{k,\lambda} \middle| \nabla_k \middle| u_{k,\lambda'} \right\rangle. \tag{244}$$

Let us consider the Bloch theorem:

$$\left\langle r | \psi_{k,\lambda} \right\rangle = \mathrm{e}^{ik\cdot r} \left\langle r | u_{k,\lambda} \right\rangle. \tag{245}$$

Then, we calculate

$$\begin{aligned}
\nabla_{k'} \left\langle \psi_{k,\lambda} | \psi_{k',\lambda'} \right\rangle &= \nabla_{k'} \int \mathrm{d}^3 r \left\langle u_{k,\lambda} | r \right\rangle \mathrm{e}^{-ik\cdot r} \mathrm{e}^{ik'\cdot r} \left\langle r | u_{k',\lambda'} \right\rangle \\
&= i \int \mathrm{d}^3 r \left\langle \psi_{k,\lambda} | r \right\rangle r \left\langle r | \psi_{k',\lambda'} \right\rangle + \int \mathrm{d}^3 r \left\langle u_{k,\lambda} | r \right\rangle \mathrm{e}^{-ik\cdot r} \mathrm{e}^{ik'\cdot r} \left\langle r \middle| \nabla_{k'} \middle| u_{k',\lambda'} \right\rangle \\
&= i \left\langle \psi_{k,\lambda} \middle| r \middle| \psi_{k',\lambda'} \right\rangle + \left\langle u_{k,\lambda} \right| \left(\int \mathrm{d}^3 r |r\rangle\langle r| \, \mathrm{e}^{i(k'-k)\cdot r} \right) \nabla_{k'} \left| u_{k',\lambda'} \right\rangle.
\end{aligned} \tag{246}$$

Note that, for any normalized state kets $|\phi\rangle, |\phi'\rangle$:

$$\langle \phi | \left(\int \mathrm{d}^3 r |r\rangle\langle r| \, \mathrm{e}^{i(k'-k)\cdot r} \right) |\phi'\rangle = \int \mathrm{d}^3 r \phi^*(r) \phi'(r) \mathrm{e}^{i(k'-k)\cdot r}. \tag{247}$$

If $k' = k$, the right hand side is equal to $\langle \phi | \phi' \rangle$. Otherwise, the phase rapidly changes for large r, and the net contribution must become zero. Hence, we conclude

$$\int \mathrm{d}^3 r |r\rangle\langle r| \, \mathrm{e}^{i(k'-k)\cdot r} = \delta_{k,k'} \mathbf{1}. \tag{248}$$

From this, we obtain

$$\nabla_{k'} \left\langle \psi_{k,\lambda} | \psi_{k',\lambda'} \right\rangle = i \left\langle \psi_{k,\lambda} \middle| r \middle| \psi_{k',\lambda'} \right\rangle + \delta_{k,k'} \left\langle u_{k,\lambda} \middle| \nabla_{k'} \middle| u_{k',\lambda'} \right\rangle. \tag{249}$$

This is equivalent to the Blount formula in equation (244).

Things become complicated when $k' \to k$. Taking this limit on the left, we obtain

$$\left\langle \psi_{k,\lambda} \middle| r \middle| \psi_{k,\lambda'} \right\rangle = -i \lim_{k' \to k} \nabla_{k'} \left\langle \psi_{k,\lambda} | \psi_{k',\lambda'} \right\rangle + i \left\langle u_{k,\lambda} \middle| \nabla_k \middle| u_{k,\lambda'} \right\rangle. \tag{250}$$

We know that $\left\langle \psi_{k,\lambda} | \psi_{k,\lambda'} \right\rangle = \delta_{\lambda,\lambda'}$ since $\left| \psi_{k,\lambda} \right\rangle$ and $\left| \psi_{k,\lambda'} \right\rangle$ are the eigenvectors of the Hamiltonian, which is a Hermitian operator. The real question is whether we can bring the limit inside the derivative $\nabla_{k'}$. This in general is not possible, due to, for example, the dependence of the phase of $\left| \psi_{k,\lambda'} \right\rangle$ on k'. Unless the phase is discontinuous as in the Riemann branch cuts, indeed the function value of $\nabla_{k'} \left\langle \psi_{k,\lambda} | \psi_{k',\lambda'} \right\rangle$ must be continuous as k' passes through k. Hence, as Blount stated in his paper [1], the first term is in most cases $\delta_k \delta_{\lambda,\lambda'} = 0$.

In case of the monolayer MoS_2, there is no reason to believe that the phase of $\left|\psi_{k,\lambda}\right\rangle$ becomes discontinuous at any point of k around $\pm K$ points. Hence, we obtain

$$\left\langle \psi_{k,\lambda}\right| r \left|\psi_{k,\lambda'}\right\rangle = i\left\langle u_{k,\lambda}\right| \nabla_k \left|u_{k,\lambda'}\right\rangle . \tag{251}$$

Next, we show that the well known formula of the velocity operator

$$\mathrm{v} = \frac{1}{\hbar}\nabla_k \mathscr{H}, \tag{252}$$

where $\mathscr{H}$ is a Hamiltonian, is consistent with the above result. For this, let us consider

$$\langle c|\,\mathrm{v}\,|v\rangle = \langle c|\,\dot{r}\,|v\rangle = \frac{1}{i\hbar}\langle c|\,[r,\mathscr{H}]\,|v\rangle = i(\omega_c-\omega_v)\langle c|\,r\,|v\rangle , \tag{253}$$

where $|c,v\rangle$ are the kets of the conduction and the valence band states, and $\hbar\omega_{c,v}$ is the energy of the conduction and the valence band, respectively. Hence, we obtain

$$\langle c|\,r\,|v\rangle = \frac{i}{\hbar(\omega_v-\omega_c)}\langle c|\,\nabla_k\mathscr{H}\,|v\rangle . \tag{254}$$

Note that

$$\nabla_k\left(\mathscr{H}\,|v\rangle\right) = \left(\nabla_k\mathscr{H}\right)|v\rangle + \mathscr{H}\nabla_k\,|v\rangle . \tag{255}$$

On the other hand, since $\mathscr{H}\,|v\rangle = \hbar\omega_v\,|v\rangle$, we have

$$\nabla_k\left(\mathscr{H}\,|v\rangle\right) = \left(\nabla_k\hbar\omega_v\right)|v\rangle + \hbar\omega_v\nabla_k\,|v\rangle . \tag{256}$$

From these two, we obtain

$$\left(\nabla_k\mathscr{H}\right)|v\rangle = \left(\nabla_k\hbar\omega_v\right)|v\rangle + \hbar\omega_v\nabla_k\,|v\rangle - \mathscr{H}\nabla_k\,|v\rangle . \tag{257}$$

We take bra on left:

$$\begin{aligned}\langle c|\left(\nabla_k\mathscr{H}\right)|v\rangle &= \left(\nabla_k\hbar\omega_v\right)\langle c|v\rangle + \hbar\omega_v\langle c|\,\nabla_k\,|v\rangle - \hbar\omega_c\langle c|\,\nabla_k\,|v\rangle \\ &= \hbar(\omega_v-\omega_c)\langle c|\,\nabla_k\,|v\rangle .\end{aligned} \tag{258}$$

From equations (254) and (258), we obtain

$$\langle c|\,r\,|v\rangle = i\langle c|\,\nabla_k\,|v\rangle . \tag{259}$$

On the other hand, we calculate

$$\begin{aligned}\langle c|\,\nabla_k\,|v\rangle &= \int \mathrm{d}^3 r\,\langle u_c|r\rangle\,\mathrm{e}^{-ik\cdot r}\,\langle r|\,\nabla_k\left(\mathrm{e}^{ik\cdot r}\,|u_v\rangle\right) \\ &= \int \mathrm{d}^3 r\,[(ir)\,\langle u_c|r\rangle\,\langle r|u_v\rangle + \langle u_c|r\rangle\,\langle r|\,\nabla_k\,|u_v\rangle] \\ &= ir\,\langle u_c|u_v\rangle + \langle u_c|\,\nabla_k\,|u_v\rangle \\ &= \langle u_c|\,\nabla_k\,|u_v\rangle .\end{aligned} \tag{260}$$

From these two equations (259) and (260), we finally obtain

$$\langle c|\,r\,|v\rangle = i\langle u_c|\,\nabla_k\,|u_v\rangle , \tag{261}$$

which exactly matches the Blount formula in equation (251). Therefore, we verified that the well known formula of the velocity operator in equation (252) is consistent with the Blount formula in equation (251).

References

[1] EI Blount. Formalisms of band theory. *Solid state physics*, 13:305–373, 1962.

[2] Robert W Boyd. *Nonlinear optics*. Academic press, 2003.

[3] Dmitry Budker, Derek F Kimball, and David P DeMille. *Atomic physics: an exploration through problems and solutions*. Oxford University Press, USA, 2004.

[4] Ming-Hui Chiu, Chendong Zhang, Hung-Wei Shiu, Chih-Piao Chuu, Chang-Hsiao Chen, Chih-Yuan S Chang, Chia-Hao Chen, Mei-Yin Chou, Chih-Kang Shih, and Lain-Jong Li. Determination of band alignment in the single-layer mos2/wse2 heterojunction. *Nature communications*, 6, 2015.

[5] RJ Elliott. Intensity of optical absorption by excitons. *Physical Review*, 108(6):1384, 1957.

[6] Shiang Fang, Rodrick Kuate Defo, Sharmila N Shirodkar, Simon Lieu, Georgios A Tritsaris, and Efthimios Kaxiras. Ab initio tight-binding hamiltonian for transition metal dichalcogenides. *Physical Review B*, 92(20):205108, 2015.

[7] Hartmut Haug and Stephan W Koch. *Quantum theory of the optical and electronic properties of semiconductors*. World Scientific Publishing Co Inc, 2009.

[8] Heather M Hill, Albert F Rigosi, Cyrielle Roquelet, Alexey Chernikov, Timothy C Berkelbach, David R Reichman, Mark S Hybertsen, Louis E Brus, and Tony F Heinz. Observation of excitonic rydberg states in monolayer mos2 and ws2 by photoluminescence excitation spectroscopy. *Nano letters*, 15(5):2992–2997, 2015.

[9] Claus F Klingshirn. *Semiconductor optics*. Springer, 2012.

[10] AR Klots, AKM Newaz, Bin Wang, D Prasai, H Krzyzanowska, Junhao Lin, D Caudel, NJ Ghimire, J Yan, BL Ivanov, et al. Probing excitonic states in suspended two-dimensional semiconductors by photocurrent spectroscopy. *Scientific reports*, 4:6608, 2014.

[11] Andor Kormányos, Guido Burkard, Martin Gmitra, Jaroslav Fabian, Viktor Zólyomi, Neil D Drummond, and Vladimir Fal'ko. k· p theory for two-dimensional transition metal dichalcogenide semiconductors. *2D Materials*, 2(2):022001, 2015.

[12] Andor Kormányos, Viktor Zólyomi, Neil D Drummond, Péter Rakyta, Guido Burkard, and Vladimir I Fal'ko. Monolayer mos 2: Trigonal warping, the γ valley, and spin-orbit coupling effects. *Physical review b*, 88(4):045416, 2013.

[13] Nardeep Kumar, Sina Najmaei, Qiannan Cui, Frank Ceballos, Pulickel M Ajayan, Jun Lou, and Hui Zhao. Second harmonic microscopy of monolayer mos 2. *Physical Review B*, 87(16):161403, 2013.

[14] Leandro M Malard, Thonimar V Alencar, Ana Paula M Barboza, Kin Fai Mak, and Ana M de Paula. Observation of intense second harmonic generation from mos 2 atomic crystals. *Physical Review B*, 87(20):201401, 2013.

[15] Branimir Radisavljevic, Aleksandra Radenovic, Jacopo Brivio, i V Giacometti, and A Kis. Single-layer mos2 transistors. *Nature nanotechnology*, 6(3):147–150, 2011.

[16] Filip A Rasmussen and Kristian S Thygesen. Computational 2d materials database: electronic structure of transition-metal dichalcogenides and oxides. *The Journal of Physical Chemistry C*, 119(23):13169–13183, 2015.

[17] Emilia Ridolfi, Duy Le, TS Rahman, ER Mucciolo, and CH Lewenkopf. A tight-binding model for mos2 monolayers. *Journal of Physics: Condensed Matter*, 27(36):365501, 2015.

[18] Albert F Rigosi, Heather M Hill, Kwang Taeg Rim, George W Flynn, and Tony F Heinz. Electronic band gaps and exciton binding energies in monolayer m o x w 1- x s 2 transition metal dichalcogenide alloys probed by scanning tunneling and optical spectroscopy. *Physical Review B*, 94(7):075440, 2016.

[19] Malte Selig, Gunnar Berghäuser, Archana Raja, Philipp Nagler, Christian Schüller, Tony F Heinz, Tobias Korn, Alexey Chernikov, Ermin Malic, and Andreas Knorr. Excitonic linewidth and coherence lifetime in monolayer transition metal dichalcogenides. *Nature communications*, 7:13279, 2016.

[20] Daniel BS Soh, Ryan Hamerly, and Hideo Mabuchi. Comprehensive analysis of the optical kerr coefficient of graphene. *Physical Review A*, 94(2):023845, 2016.

[21] Yutaka Toyozawa. *Optical processes in solids*. Cambridge University Press, 2003.

[22] Haining Wang, Jared H Strait, Changjian Zhang, Weimin Chan, Christina Manolatou, Sandip Tiwari, and Farhan Rana. Fast exciton annihilation by capture of electrons or holes by defects via auger scattering in monolayer metal dichalcogenides. *Physical Review B*, 91(16):165411, 2015.

[23] Haining Wang, Changjian Zhang, Weimin Chan, Christina Manolatou, Sandip Tiwari, and Farhan Rana. Radiative lifetimes of excitons and trions in monolayers of the metal dichalcogenide mos 2. *Physical Review B*, 93(4):045407, 2016.

[24] Qing Hua Wang, Kourosh Kalantar-Zadeh, Andras Kis, Jonathan N Coleman, and Michael S Strano. Electronics and optoelectronics of two-dimensional transition metal dichalcogenides. *Nature nanotechnology*, 7(11):699–712, 2012.

[25] Di Xiao, Gui-Bin Liu, Wanxiang Feng, Xiaodong Xu, and Wang Yao. Coupled spin and valley physics in monolayers of mos 2 and other group-vi dichalcogenides. *Physical Review Letters*, 108(19):196802, 2012.

[26] Changjian Zhang, Haining Wang, Weimin Chan, Christina Manolatou, and Farhan Rana. Absorption of light by excitons and trions in monolayers of metal dichalcogenide mo s 2: Experiments and theory. *Physical Review B*, 89(20):205436, 2014.

[27] Chendong Zhang, Amber Johnson, Chang-Lung Hsu, Lain-Jong Li, and Chih-Kang Shih. Direct imaging of band profile in single layer mos2 on graphite: quasiparticle energy gap, metallic edge states, and edge band bending. *Nano letters*, 14(5):2443–2447, 2014.

DISTRIBUTION:

1	MS 9033	David Reyna, 08648
1	MS 9033	Daniel Soh, 08648
1	MS 0899	Technical Library, 9536 (electronic copy)


Sandia National Laboratories